Role of the trunk sensorimotor cortex in supporting rehabilitation assisted functional improvement in locomotion after spinal contusion injury

By

Bharadwaj Nandakumar
Dissertation

Submitted in partial satisfaction of the requirements for the degree of

Doctor of Philosophy

in

Biomedical Engineering

in the

OFFICE OF GRADUATE STUDIES

of the

UNIVERSITY OF CALIFORNIA

DAVIS

Approved:

Karen Moxon, Chair

Carolynn Patten

Leah Krubitzer

Committee in Charge

2021

Acknowledgments

This Journey of mine couldn't have been possible if not for the support of my family, friends and the Moxon lab. The pursuit and curiosity to understand the inner workings of the world have always inspired me to become a scientist. Today, I am very glad to accomplish the first step in that direction.

Thank you Appa and Amma and Sowmyah. Without your encouragement, care, nurture and sacrifice I couldn't have made it this far. Thanks for introducing me to this world of science, by identifying and nurturing my curiosity with popular science books. I love you and cannot wait to see you all soon.

I would like to first acknowledge my advisor Dr. Karen Moxon for providing me all the resources necessary to conduct research, your passion and hard work and diligence in pursuing science has always been inspiring. Thank you for introducing me to the fascinating world of ephys, spikes and neural encoding. Thanks for all the constructive feedback, scientific discussions, mentoring to communicate science better.

I acknowledge my committee members Dr. Carolynn Patten and Dr. Leah Krubitzer, research collaborators Dr. John Bethea, Dr. Valerie Ricard and Dr. Jerome Ricard for mentoring and providing constructive feedback throughout the duration of my thesis.

I would like to thank my colleague, Gary Blumenthal for being part of this journey throughout. We have done a lot of problem-solving, troubleshooting, and doing some fascinating experiments together. The Adventure with electrical stimulation, Von-Frey hairs, laminar recordings, and a lot of code writing was indeed a lot of fun. Thank you for teaching me all the skills that were helpful to conduct research. You showed me the ropes to perform neurosurgery, perfusion, contusion and everything there is about animal care. I am grateful for that. Our collaboration on improving the understanding of the trunk sensorimotor system is a highlight in our scientific career. We have a lot more work to do together. I hope we continue to find ways to collaborate in our next and future scientific adventures. It has been a real pleasure working with you, Gary.

I thank Dr. Francois Pauzin, for all the fascinating scientific discussions and exciting opto-ephys experiments, and all the fun times, dart session, fun at Delta of Venus and Sophia's with the people of Davis. I am glad we met, had a wonderful time in Davis and did fascinating science together. Merci baku Francois.

I acknowledge the contribution of Moxon lab past alumni, and present students. Thanks Jonathan Garcia and Nathaniel Bridges. Research days at Drexel university wouldn't have been fun if not for the both of you. I acknowledge the contribution of Ashley Schneider for helping me with surgeries, lab management and animal behavior. I thank the undergraduate research team Zexi Zang, Vanessa, Miranda, Shanon Lamb for their contribution in data analysis and animal behavior.

I thank my best friends Vignesh Ravikumar, Harini Harinarayanan for putting up with me throughout the entire journey, thanks for all the pampering I got when visiting the bay area. Thanks

for hearing my rants, keeping my mental health in shape and helping me cope during tough times. I do not know what I would do without the both of you by my side. I love you both.

I have also been lucky to form good friendships during my years in Davis. Special thanks to Sridhar Majety, I will miss all our quantum physics and neuroscience discussion, fun times at Sophia's, backyard discussion, dart games with Francois, delta days. Thanks for being an amazing housemate, friend and family in Davis. Thanks for being there for me during tough times amidst the pandemic and during good ones as well.

Special thanks to Subha, Sridhar for all the fun times, wonderful memories with toffy at 117C street Davis. I cannot thank you enough and deeply grateful for helping me recover from surgery and getting back to doing experiments.

Special thanks to friends from Philly (Guruprasad Krishnamoorthy, Arun Gowtham, Sowbhagya, Abilash, Thyagesh, Prabhu Shankar, Aarthi, Maarinath, Ajay, Sanjay) for supporting me in this Endeavor and helping me with the transition from Philadelphia to Davis. Those memorable 'aatam paatam kondaaatam' sessions in philly with all of you are memorable experiences that I will carry for life

Lastly, I acknowledge the contribution of my past teachers (Ravishankar Sir, Madhumohan Sir and Prof Richard Feynman) to have shaped me and encouraged me to be critical and ask questions. Sri Gurubhyo Namah to all of you.

Abstract

Spinal cord injury (SCI) is a debilitating condition often resulting in motor deficits and loss of tactile sensation below the injury. The brain needs to relearn strategies to regain motor control after SCI. This ability of the brain to adapt after injury/rehabilitation is defined as neuroplasticity. Neuroplasticity in motor cortex (M1) required to gain cortical control of trunk muscles below the injury level is not well understood after a clinically relevant incomplete mid-thoracic spinal contusion injury. After an incomplete SCI, there is a substantial spontaneous recovery of function that can be further facilitated by physical rehabilitation. The difference in cortical neuroplasticity associated with the rehabilitation-assisted recovery and spontaneous recovery of function is unknown. This thesis aimed to understand whether neuroplasticity in trunk M1 after rehabilitation is a mere enhancement of the learning strategy adopted by the cortex during spontaneous recovery or whether they represent a different strategy to regain control of muscle groups below the level of the lesion. Regions within trunk M1 that control lower thoracic trunk muscle (LTM1) were specialized in the neuronal encoding of posture in intact animals. After an incomplete mid-thoracic spinal contusion injury, the network and cellular neuroplasticity in trunk M1 differed between animals that received physical rehabilitation and animals that spontaneously recovered. In animals that received the therapy, the lower thoracic trunk motor cortex (LTM1) maintained some control of trunk muscles below the injury, in addition to recruiting trunk muscles at/above the level of injury. Exercise therapy also prevented the degradation of neuronal responsiveness in the reorganized cortex to unexpected postural perturbation as well as during treadmill locomotion.

This knowledge can help design activity-based therapy paradigms that improve cortical plasticity in the LTM1, relevant for postural control.

Table of Contents

Table of Figures

List of Tables

Aims and Significance

Role of the trunk sensorimotor cortex in supporting rehabilitation assisted functional improvement in locomotion after spinal contusion injury.

Spinal cord injury (SCI) is a debilitating condition often resulting in motor deficits and loss of tactile sensation below the injury level. Incomplete SCI Injury is the most common in humans (1). Most studies have utilized hemisection injury model in rodents to examine therapy mediated functional improvements after incomplete SCI (2–4). While the injury is less variable, the approach is not in line with pathophysiologies encountered in SCI patients (5). On the contrary contusion injuries in the rodent model are variable, but constitute a clinincally relevant model of incomplete SCI (6, 7) For example, incomplete mid thoracic spinal cord injury results in motor control deficits in the lower limbs including maintaining posture, interlimb co-ordination and reduction in weight supported stepping. Current understanding of the impact of therapeutic interventions such as physical rehabilitation after SCI, suggests functional improvement relies on plasticity along the entire neural axis(8–16). Moreover, neuroplasticity in M1 is required to maintain these therapy induced functional improvements after SCI (9, 11, 17, 18). Control of lower limbs involves dynamic interactions of several body segments, especially the trunk musculature. Hence, regaining control of trunk musculature is critical to the recovery of locomotor function (19–23). Neuroplasticity in M1 required to gain cortical control of trunk muscles below the injury level is not well understood. Some details have emerged from recent studies evaluating therapy dependent plasticity in complete spinal cord injury models, with no scope for recovery without therapy (11, 24). However especially after more bilateral moderate contusive injuries, spontaneous recovery is substantial and can be further enhanced by physical rehabilitation. Despite advances

in our understanding of physical rehabilitation's role in modulating plasticity in cortex to enhance functional recovery, the difference in cortical neuroplasticity associated with rehabilitation assisted recovery, and spontaneous recovery of function after SCI is unknown.

The long-term goal of this project is to develop optimal treatment strategies to maximize functional outcome after SCI. The brain needs to relearn strategies to regain motor control after SCI. This ability of the brain to adapt after injury/ rehabilitation is termed neuroplasticity. The goal of this work was to understand whether changes in M1 after rehabilitation are a mere enhancement of the strategy adopted by the cortex during spontaneous recovery or whether they represent a different strategy to regain control of muscle groups below the level of the lesion. This knowledge is important to optimize physical therapy and perhaps aid in identifying possible target sites/ strategies for neuromodulation-based therapies in the future. This thesis' **central hypothesis** is that *improved functional outcome in response to physical rehabilitation is accompanied by novel cellular and network plasticity changes that are distinctly different from the plasticity associated with spontaneous recovery of function*. This hypothesis is based on our preliminary data that 1) support previous studies showing rehabilitation induces neuroplasticity in M1 required to optimize functional locomotor outcome after complete SCI 2) suggest that neuroplasticity is related to differences in how sensory input is integrated with motor output in the motor cortex to regain control of trunk muscles below the level of the lesion in animals that receive physical therapy compared to those that do not.

To address this hypothesis, I will first examine the organization of somatosensory input and motor output and assess sensorimotor integration in trunk M1 in intact rodent animal model, since

surprisingly, little is known about this (Aim 1). Aim1 will provide a framework against which plasticity can be better understood after spinal cord injury. Then I will compare M1 reorganization associated with spontaneous recovery to that associated with rehabilitation assisted recovery of function using a clinically relevant moderate, incomplete bilateral midthoracic spinal cord contusion model (Aim2) in both anesthetized and awake behaving conditions. In the anesthetized state, I assess motor output by performing motor mapping studies of M1 using intracortical microstimulation (ICMS) and assess somatosensory input in M1 by recording neuronal responses in response to electrical stimulation of trunk and extremities. In the awake state, I will assess sensorimotor integration in S1 and M1 by recording single neuron activity in two relevant tasks in the same group of animals before and in the weeks after SCI. In the first, animals work to maintain posture on a tilt platform (tilt task) in response to unexpected perturbations in the lateral plane (tilt task). In the second, animals walk on a treadmill (treadmill task). For both, I will assess phase modulated changes in single neuron activity in trunk sensorimotor cortex to understand the impact of exercise therapy. The central hypothesis will be addressed with the following specific aims.

Aim1: Assess the integration of sensory input and motor output in the trunk motor cortex in intact animals.

Aim1a: Examine organization of sensory and motor information within trunk motor cortex to gain insight into the control of muscles at, above and below the level of the proposed lesion.

Aim 1b: Examine the functional relevance of sensorimotor integration involved in postural control.

Hypothesis 1: There is extensive integration of hindlimb somatosensory input that influences both trunk sensory and motor cortices. This network encodes information about postural perturbations.

Aim 2: Identify differences in M1 reorganization both at cellular and network level between animals that undergo physical rehabilitation and those that do not after spinal cord contusion injury.

Aim 2a: Identify the effect of physical rehabilitation on M1 reorganization.

Aim 2b: Examine the functional relevance of this reorganization in postural control and neural encoding of posture and weight supported stepping on a treadmill.

Chapter 1 will provide background and context for understanding cortical organization, cortical plasticity associated with spinal cord injury with some historical perspectives, current advances in the therapeutic strategies to recover from injury and the role of cortex in supporting these functional improvements.

Chapter 2 will address aim 1a, 1b focusing on the understanding the organization of trunk M1 and sensorimotor integration in trunk M1 in intact animals.

Chapter 3 will address aim 2a focusing on understanding the network level changes between rehabilitation assisted recovery and animals that spontaneously recover using 2 contusion injury models with varying severity.

Chapter 4 will address aim2b focusing on the functional relevance of therapy mediated reorganization in neuronal encoding of posture after injury as well as weight supported stepping on a treadmill and will lend insight into changes in reorganization during the early as well as late phase of exercise therapy.

Significance

My work demonstrated that, in the intact animal, hindlimb somatosensory information influences both trunk sensory and motor cortices to support trunk stabilization, especially regarding the lower thoracic trunk motor cortex preferentially encoding for changes in posture. After SCI, while physical rehabilitation facilitated spontaneous recovery of function, the cortex's neuromuscular control strategies after rehabilitation were neither similar nor merely enhanced compared to spontaneous recovery. Rather the trunk muscle recruitment strategy differed between animals that received physical therapy compared to animals that did not, with the latter relying mainly on trunk

control at/above level of the injury. In animals that received rehabilitation, M1 maintained some exclusive control of trunk muscles below injury previously identified in intact animals, in addition to recruiting trunk muscles at/above level of injury. Rehabilitation independent spontaneous recovery to regain weight supported stepping was associated with expansion of trunk M1 into de-efferent HLM1. Rehabilitation dependent enhancement of spontaneous recovery was associated with reorganization of putative lower thoracic trunk M1, re-establishing cortical control of lower thoracic trunk muscles below injury level. Exercise therapy also prevented the degradation of neuronal responsiveness to unexpected tilts as well as weight supported stepping on a treadmill.

This knowledge can help design activity-based therapy paradigms that improve cortical plasticity in the lower thoracic trunk M1, relevant for postural control. Additionally, the outcomes suggest the design of strategies to recruit trunk muscles below the injury, instead of focusing on compensatory strategies, relying on trunk muscles above injury level.

Chapter 1: Background

Spinal cord injury (SCI) is a debilitating condition with far-reaching physical, emotional and economic consequences for patients, families, and societies at large (9, 10), with the highest prevalence of SCI in the United States affecting 54 people per million, or about 17810 new SCI cases in the US alone (10). Most SCI injuries are anatomically incomplete (1, 11), caused by trauma resulting from vehicle accidents, falls, and violence (1). While cardiovascular (12) and autonomic (13) dysregulation are other problems associated with SCI, motor paralysis and loss of tactile sensation below the injury level is a major challenge. In this thesis, we would focus on approaches aimed at improving functional recovery of locomotion after an incomplete spinal cord injury.

Spinal cord injury disrupts sensory perception/motor control

Paralysis is due to the disruption in the transmission of descending motor commands between supraspinal and spinal circuits below the injury level involved in locomotion. Targeting isolated spinal circuits below the injury with varying sensory, electrical / pharmacological stimulation can initiate stereo typical locomotor stepping (14–17). However, weight bearing ability, inter-limb co-ordination, postural control and volitional movement are more complex that require descending commands from supraspinal circuits (7, 18–21). In addition to paralysis, after SCI, there is loss of tactile sensation and haptic proprioception due to the disruption of ascending sensory information from below the level of injury to supraspinal centers such as the sensory and motor cortex. The role of the motor cortex is to utilize this sensory information (tactile, proprioception, visual) for planning and execute volitional locomotion by sending descending commands to the spinal cord. This transformation of sensory input in the cortex, necessary to produce goal directed behavior is called sensorimotor integration. Despite the injury, the supraspinal circuits such as sensorimotor cortex has the capacity to re-organize and learn new strategies for motor control. This ability of the central nervous system (CNS) to reorganize/'rewire' and adapt to compensate for sensorimotor loss is termed as plasticity.

Improving Functional recovery after SCI

Current research in the field has paved way to three main types of approaches to efficiently route descending commands from the supraspinal circuits to the spinal cord below level of lesion. The first approach is focused on promoting spinal cord repair /axonal regeneration of damaged pathways across lesion site (22–24) however, the functional efficacy of regenerated axons is rather limited (25). The second approach is to exploit a brain machine interface that could bypass the

lesion site and restore volitional control by controlling either an external device such as prosthetic limb (26, 27) or exoskeleton (28–30), reinnervating spared muscles below injury site or by sending electrical impulses to spinal cord below the injury to re-enable volitional control of gait (15, 17, 31–33). The third approach is utilizing rehabilitation to enhance recovery of function after SCI. Rehabilitation strategies that reinforced sensory experience associated with motor practice, particularly through exercise therapy were shown substantially to improve sensorimotor recovery after SCI (34–41). Rehabilitation therapy is currently a ubiquitous clinical approach to SCI that is not only essential for neurological recovery and improvement in function, but also maintenance of musculoskeletal system and cardiovascular health (42–45). It is likely that BMI or regenerative approaches will be combined with physical rehabilitation. Hence in this thesis, we focus on understanding the impact of quadrupedal treadmill rehabilitation in enhancing recovery of locomotion after incomplete spinal cord injury,

Rehabilitation induced Plasticity in the CNS.

Improvement in functional outcome after exercise therapy is considered to be the result of plasticity in response to increased activation of spared neuronal networks that bypass the lesion site after incomplete SCI (46–49). In case of spinal cord injury, these strategies have primarily focused on modulating plasticity below the lesion (50–53). Recent studies from our research group (7, 46, 54–57) and others (18, 20, 58–63) have pointed out that rehabilitation affects multiple levels of the nervous system spanning the entire neuroaxis that includes remodeling of supraspinal networks such as sensorimotor cortex as well as spinal circuits below the lesion. Recent studies showed that plasticity in the sensorimotor cortex is in fact necessary to maintain rehabilitation assisted improvement in weight supported stepping after SCI both in neonatally spinalized (20) as

well as adult rats (7). In this thesis, I examined plasticity in the trunk sensorimotor cortex associated with rehabilitation assisted recovery of function after incomplete spinal cord injury.

Plasticity associated with Spontaneous recovery of function

On the other hand, spontaneous recovery of function occurs even without any rehabilitation, especially if the injury is incomplete, in patients as well as in animal models (62, 64–70). However, the spontaneous recovery is often limited, and the time course of recovery can range from months to years after injury (15, 64, 71, 72). In fact, previous studies have shown a correlation between plasticity in the sensorimotor cortex and spontaneous recovery of function in humans (73, 74)) as well as in animal models (65, 69, 75, 76). This relationship between cortical plasticity and spontaneous functional recovery has also been observed in stroke patients (77–80). Therefore, we selected a moderate contusion model where there is significant spontaneous recovery, and we could work towards understanding the effect of therapy in addition to the spontaneous recovery.

Somatotopic organization of motor cortex, A historical perspective

To understand cortical plasticity after spinal cord injury, it is important to examine the organization of sensory and motor cortices. Fortunately, there is a very clear organization of the sensory and motor cortices with a rich history of how we came to understand what is considered the putative motor cortex. In the 4th century BC, Greek philosopher Aristotle considered the brain to be a secondary organ that served as cooling for the heart and a place where ‘spirits’ came together as *sensus communis* or ‘common sense’. By first century AD Roman physician Galen, concluded that the mental activity occurred in the brain rather the heart, and it was thought the spirits resided in the ventricles rather. The beginning of the 16th century saw developments in neuroanatomy with extensive dissections by Leonardo DaVinci, and investigation by English Physician Thomas Willis

in his treatise published in 1664, that led the foundation for modern neuroanatomy of the brain (81). It was long thought, the cortex was reserved for executive functions and not involved in sensory processing or motor control. After the first demonstration of Physicist Luigi Galvani in the late 1780's, that electric currents can induce muscle contractions in dead frogs, saw the advent of using electric currents to probe the nervous system. This long held idea about the cortex, began to change when Fritiz and Hitzig in 1870 (82), demonstrated that controlled epidural direct electrical stimulation of the mammalian cerebral cortex of the dog elicited movements of muscle groups on the contralateral side. Moreover, they found that evoked movements were found when stimulating the anterior portion of the cortex rather than the posterior portion (83, 84). This observation was one of the early indications that suggested that there was a dedicated region in the cortex involved in movement control with a dedicated motor strip. Meanwhile, neurophysiologist Charles Sherrington and his students, in 1901 did some epidural cortical stimulation experiments in different species of apes and showed the first evidence of existence of a somatotopic organization within motor cortex in apes in this seminal paper (85, 86). In parallel, neuroanatomist Brodmann's work on cerebral localization of function (87, 88) in 1909 based on cytoarchitectural studies laid the foundations of organizational principles of cerebral cortex, and their potential functional implications. Building on the work done by Charles Sherrington in 1936-37, Neurologists Foerster (89) and Wilder Penfield (84) investigated the organization of motor cortex in humans and found that there was a somatotopic organization within both sensory (S1) and motor cortices (M1) in humans. Penfield further found that these cortical areas dedicated to representing different areas of the body were uneven, with hands, feet and tongue having large areas, while trunk representation we relatively small. This visualization of cortical areas for humans was proposed by Wilder Penfield and known as the cortical homunculus (84), that we know of today.

These data obtained from non-invasive epidural cortical stimulation experiments all suggested that the motor cortex was spatially organized in a manner such that there was point-to-point (one to one) mapping of control of different body parts by different pieces of M1 cortex (90). However, this understanding changed with the advent of new techniques to deliver current without causing current spread.

The advent of metal microelectrodes and advances in extracellular recording and microstimulation in the 1940-1960's allowed neurophysiologists to invasively insert electrodes deep inside brain and record local field potentials as well as single unit discharges across the depth of cortex (91–94) as well as focally stimulate pyramidal neurons in the cortex with electric current. This method of focally stimulating the cortex, pioneered by neurophysiologist Asanuma and colleagues is known as intracortical microstimulation or ICMS (95, 96). Since then, ICMS has become an important tool to investigate the organization of motor cortex. In these early studies in humans the sensory and motor cortices showed little to no overlap. However, in early marsupial mammals such as short, tailed opossum there was a complete overlap of sensory and motor representation with a somatotopic organization (97, 98). Placental mammals, on the other hand, such as rodents, and primates were proposed to exhibit a progressive segregation of motor and somatosensory functions in the cortex (99). Early mapping studies in rodents in the 1970's -1980's, by Hall and Lindholm, Lamarche Giovanni and Donoghue and colleagues (100–106) revealed a partial sensorimotor overlap of hindlimb and forelimb regions in rats marking an evolutionary step moving towards segregation of motor and sensory cortices with little to no overlap observed in primates (99, 107). Recent ICMS studies in regions of S1 and post parietal cortex also show that motor control in the cortex is indeed distributed beyond M1 in both rodents (99, 108) as well as

primates (109). This makes the rat a popular and feasible research model to be used to evaluate changes in cortical organization after neurological injury or disease and, therefore, in this work, I used the rat model.

Differences in Cortical Processing (S1 vs M1)

Along each column in the cortex, there is a structural and functional organization that was first well characterized in S1 (93) and V1 (94). The cortex is divided into supragranular, granular and infra granular layer. Receptive field is defined as a specific region of sensory space in which an appropriate stimulus can drive an electrical response in a sensory neuron (86). In S1, the receptive field size (area of skin receptors encoded by a cortical neuron) is different, with neurons in the supragranular and infragranular layer having relatively large receptive fields compared to neurons in the granular layer (110, 111). In fact, in the adult cortex, the borders of digits representation in the adult owl monkey are abrupt such that the neurons in the granular layer in S1 (area3b), have non overlapping RFs dedicated to encoding cutaneous stimuli from the corresponding digit (112). Both the digit representation of S1 in non-human primates as well as the whisker representation in the rodent S1 have been well characterized and have discrete electrophysiological borders in the granular layer. We wanted to understand whether this organization was also consistent within the trunk sensory cortex. Surprisingly, in our investigation of the intact rodent trunk somatosensory cortex, we found that, not only where the dermatomes in the spinal level overlapping (70), receptive fields of trunk neurons in S1 in the granular layer were indeed overlapping spanning multiple dermatomes suggesting that the discrete representation with rigid borders were not a feature of entire S1. Recent studies evaluating somatosensory processing in the infragranular cortex in the rodent forepaw digit have found that the neurons are tuned to respond with different

spatio-temporal stimulus patterns to facilitate processing of more complex stimuli (113). Even if these neurons had large overlapping receptive fields resulting in loss of spatial selectivity, they can provide as an alternative, sophisticated temporal code that compensates and thereby ensure, there is sufficient information encoded about stimulus location (114, 115).

Electrophysiological recordings of local field potential (LFP) and action potential/ spiking activity of neurons reflects complementary aspects of neuronal processing (116). While LFP are input signals that integrate subthreshold activity as synaptic inputs and membrane potentials from a neuronal population at the network level, spiking activity/ action potentials are the output signals from individual neurons at the cellular level (117). In this Thesis, I examine both LFP and spiking activity to understand to understand integration of somatosensory information (tactile/proprioceptive) in the infragranular layer of trunk S1 and M1 in rodents. We did anesthetized/ awake behaving experiments in the rodent to explore the role of somatosensory input from extremities in modulating trunk S1 and M1 activity, as well as integration of trunk somatosensory input in sensory cortices such as forelimb and hindlimb.

Unlike S1, M1 has a more fractured or mosaic organization (90, 99). Though there is general topographic organization in M1 like S1, there are functional overlaps between representation of multiple body parts. These overlaps lead to cortical representation of complex movement repertoires that might be behaviorally relevant. In fact, recent mapping studies suggest that the degree of somatotopic segregation in M1 parallels the biomechanical independence of different body parts (90, 118–121).

The amount of overlap is especially more pronounced during ICMS mapping experiments with longer train durations (109, 121, 122). Movements are 3 dimensional with multiple degrees of freedom at each joint involving innumerable combinations of muscle contractions and movements. This would require the motor cortex to adopt a distributed strategy for motor control rather than one -to -one mapping with specific muscle. Therefore, the maps represent movements rather than individual muscles. In order to optimize for computational cost, it is more likely that frequently used combinations of movement called muscle synergies are represented in more locations in the M1 cortex. ICMS Studies in primates have revealed the presence of these cortically encoded muscle synergies (119, 123, 124). This fractured distributed control strategy in M1 could also provide for a greater resistance to the disruptive effects of lesion as well as injury (90).

This overlap is important when interpreting reorganization after spinal cord injury, that I study here. Unfortunately, the extent of this overlap of the trunk motor representation is unknown in the rodent cortex and, therefore, in this thesis I spent considerable effort to carefully map and understand this overlap with forelimb and hindlimb musculature and examine muscle synergies that can be recruited by trunk M1 with ICMS.

Long train Intracortical Microstimulation to evaluate movement repertoires

Goal of ICMS based mapping was to examine the different complex movement repertoires of trunk representation in M1 that includes understanding cortically evoked muscle synergies (overlapping representations / coactivation of segmental muscle groups). Longer train durations can elicit movement response at lower threshold currents compared to shorter trains (25), pilot experiments in the lab with 60ms stimulus trains showed that stimulus evoked movement represented short, truncated movements /muscle twitches while 300ms pulse trains often elicited a variety of movements ranging from simple (muscle contraction across a single joint) to more complex

movements that represented the coactivation of muscles across different segmental levels of trunk / across multiple joints. Studies utilizing long duration trains in monkeys (26, 27) and rats (9, 28, 29) argue that long duration trains represent ethologically, physiologically and behaviorally relevant timescale for activating M1 resulting in providing more insight related to function While there is concern, that it that longer stimulus trains could indeed cause artificial, random non-specific activation (30) previous studies comparing responses for short and long duration did not find that to be true, for. E.g. Ramanathan et.al 2006 showed that longer train durations represented, reproducible and sequential movement (reach, grasp, retract) as opposed to random nonspecific activation of muscle groups. (31, 32) found that short duration trains produced rather truncated versions of movement compared to long train stimulations (500ms), with limited changes in the topography within M1. (33) found that the EMG amplitude /response duration were similar for ICMS stimulus trains beyond 102 ms.

Importantly, Long train ICMS provides framework to understand changes in the organization of M1 after neurotrauma (SCI) or after rehabilitation, long duration ICMS allows the greatest opportunity for temporal facilitation of activity at each synapse along with several cascade of connections between cortex and motoneurons in the spinal-lesioned rats (9). This study and previous studies (9, 24, 34) examining M1 reorganization after SCI, also found long train parameters (300ms) did not alter the basic map structure in control rats compared to classical ICMS mapping studies (35, 36)

Both stimulation (short vs long) reveal properties of different descending systems originating from same cortical site (30). Shorter trains may largely activate more direct connections between motor cortex and motor neurons in spinal cord as observed in monkeys (37) while longer trains might be required to activate muscles that are supraspinal connected indirectly via complex propriospinal

intraneuronal system in the spinal cord (30, 38). In this thesis we used long train stimulus of 300ms to examine trunk M1 organization in intact and spinalized animals.

Cortical Plasticity – A historical perspective

Somatotopic maps can be altered or shaped by experience, environment, and sensation especially during development. Enormous changes in the brain occur during the early postnatal period of development. In the Rodent model, the whisker representation in S1 develops by postnatal day 5 followed by the emergence and refinement of trunk and extremity representation by postnatal day 20 also accompanied by changes in cellular properties of cortical neurons such as refinement in receptive field size (125). These changes in cortical neuron (firing rate properties, responsiveness to somatosensory input, receptive fields) is defined as cellular plasticity for the purpose of this thesis.

A landmark study by Hubel and Weisel in 1963, in the cat visual cortex showed that monocular visual sensory deprivation during development affected the functional architecture of visual cortex, includes both receptive field properties of neurons as well as their dominance. However, the same sensory deprivation had very little impact when imposed as adults (126). Sensory deprivation as result of whisker trimming during development also affected the whisker sensory cortex in rodents (127). Since experiments conducted by Hubel and Weisel, it was thought that the sensory cortex (visual, somatosensory) was highly plastic post development and relatively more static after adulthood.

This idea had changed in 1980's with the first demonstration of cortical plasticity in the mature mammalian brain, by neurophysiologists Micheal Merzenich, Jon Kaas and colleagues in 1983. Cortical organization of S1 was evaluated in adult monkeys after median nerve transection, that removed sensory input from the ventral portion of digits. To their surprise this resulted in massive

reorganization in the sensory cortex, with areas originally encoding for ventral portion of digits now replaced with input from dorsal skin areas (128, 129). Studies prior to this, have focused on plasticity in the visual and somatosensory cortices following sensory de-afferentation in neonatal as well as adult animal models.

This idea was extended to motor cortices as well with ICMS mapping experiments by neurophysiologist John Donoghue and colleagues in 1987, on rodents that underwent either forelimb amputation or peripheral nerve transection during development (130). They found that sensory de-afferentation during development not only affects somatosensory but also the organization of motor cortex. In fact, after a peripheral nerve transection of facial nerve in rodent, rapid motor cortex reorganization occurred within 3 hours with cortical stimulation of putative whisker representation eliciting forelimb movement instead. In neonates that underwent amputation, the putative forelimb M1 representation was smaller with regions overlapping with S1, activated by cutaneous input from shoulder and trunk instead of distal forelimb. The putative whisker representation had also expanded into the forelimb M1 region. These changes persisted well through adulthood as well (131). The organization of somatotopic maps were not only modifiable by altered sensation or injury during development and through adult, but maps were also modifiable by experience. Experiments on adult monkeys (112, 132–134) trained on a frequency discrimination task that involved controlled tactile stimulation of either one or fingertips, resulted in modifications in the organization of hand region of sensory cortex that were correlated to improvements in behavioral performance. In the late 1990's pioneering experiments by neurophysiologist Randolph Nudo and colleagues in adult squirrel monkeys showed that the motor cortex representation was modified after behavioral training of a task that required skilled use of digits (135). Follow up experiments on rodents by Nudo's research group showed that the

reorganization in the motor cortex was indeed specifically associated with skilled motor learning rather than unskilled repetitive use (136, 137).

After neurological damage to the cortex (stroke) or to the nervous system (spinal cord injury/ peripheral nerve injury), the whole brain must relearn new strategies for encoding sensation and movement, hence cortical reorganization is very likely. After injury, the affected cortical representation is usually either nonresponsive or is invaded by the neighboring representation. In case, of a stroke there is reorganization of the peri-infarct region surrounding stroke, to compensate for the sensorimotor loss (138). In case of a spinal cord injury or a peripheral nerve injury, there is massive reorganization involving changes in somatosensory input and motor output in both the unaffected (8, 139–141) and affected cortical representation (75, 142–146). This large-scale reorganization involving altered somatosensory input and motor output is defined as network plasticity for the purpose of this thesis.

Cortical plasticity both at cellular and network level, can often be either be adaptive contributing to the recovery of function or maladaptive leading to the development of neuropathic pain (147, 148). Adaptive plasticity in the cortex is accompanied compensatory strategies involving new behavioral adaptations to substitute for the sensorimotor loss. These behavioral adaptations can sometimes be detrimental to the recovery of function for e.g., in the case of a unilateral stroke, overuse of the unaffected intact limb can limit the cortical plasticity as well as functional recovery of the impaired limb (149–152). In stroke models affecting dexterous control of the hand, compensatory recovery is supported by expansion of proximal musculature representation such as elbow/shoulder in the spared regions of motor cortex followed by a further loss of distal limb musculature such as digits. Physical rehabilitation on the contrary, prevented the loss of distal limb

musculature and enhances spontaneous recovery of dexterous control (153). This is summarized with a cartoon of motor cortex in the figure below adapted from (154).

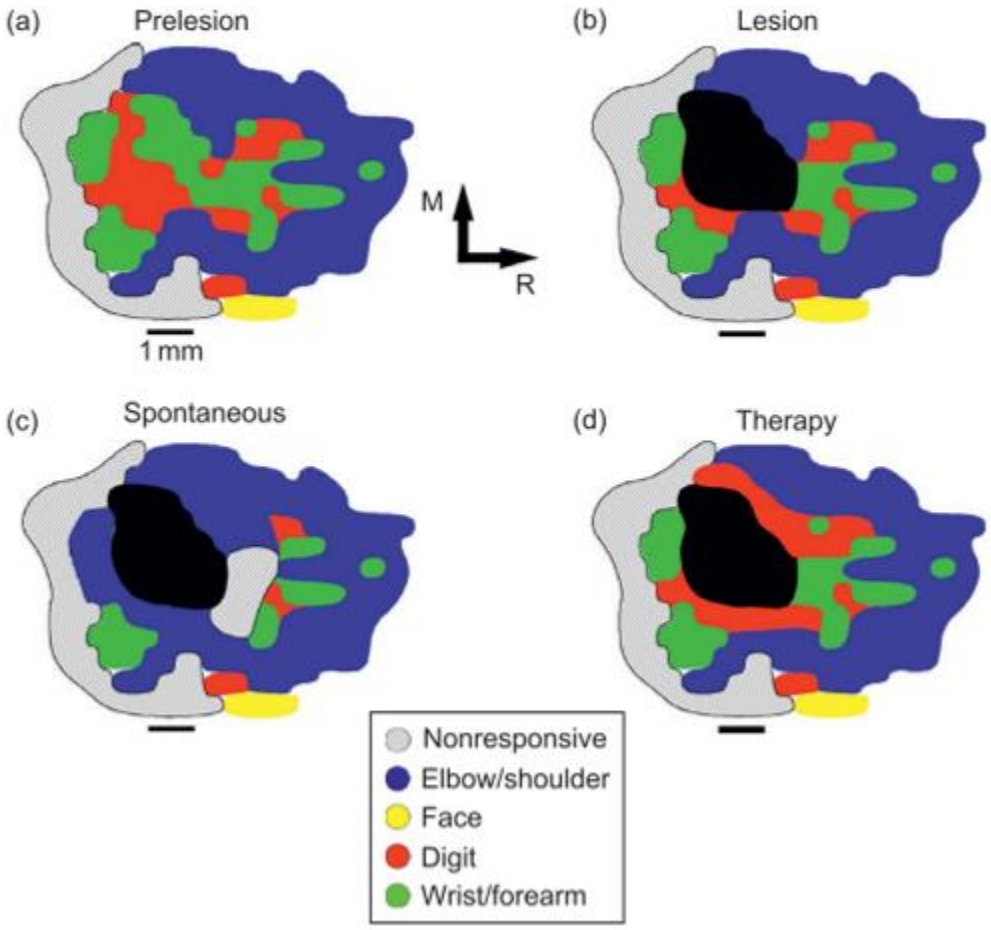

Figure 1.1 Plasticity differences in M1 associated with spontaneous recovery and rehabilitation assisted recovery of dexterous control in stroke model (adapted from Dancause, Nudo et.al 2011)

These studies from stroke models lend insight into the plasticity differences between spontaneous and rehabilitation assisted recovery after neurological damage. However, after a partial spinal cord injury, these differences are not well understood.

After an incomplete spinal cord injury, recovery of function and the associated cortical plasticity could be due to multiple reasons that could either by driven by local changes in the motor cortex organization (155–157) which includes both changes in corticospinal tract reorganization (7, 65, 67, 69, 74–76, 144) as well as altered sensorimotor integration (7, 158), sub-cortical plasticity in the brain stem (159) involving rubrospinal (160, 161), reticulospinal (162–166) or vestibulospinal tract reorganization (167, 168), plasticity in the spinal cord involving alteration in descending propriospinal interneuron network (53, 169–173) or altered spinal pre-motor neuron circuitry (43, 174–178) and motor neuron plasticity (179, 180) below the level of the injury. In fact, recent studies evaluating therapy dependent plasticity in severe injury models suggest the entire nervous system participates that includes the cortex, brain stem, spared propriospinal neurons and spinal circuits below the level of lesion (166, 181–184)

In summary, neuroplasticity in the cortex after spinal cord injury to the nervous system and the concomitant spontaneous recovery of function post injury depends on number of factors that includes age at injury (20, 54, 185–187), severity of the injury (66, 164, 188) and the type of therapeutic intervention (7, 18, 55, 57, 189) and the onset of intervention and duration (61, 190 – 193). In this thesis I examine cortical plasticity in 2 partial spinal cord injury models of varying severity to understand the underlying cortical plasticity associated with spontaneous recovery of function and therapy mediated improvement in enhancement of spontaneous recovery. Additionally, evaluating cellular and network plasticity in the cortex during the recovery process will help us understand how plasticity in the cortex changes over time and whether there the changes are correlated to behavioral improvements after the injury. This approach can help us in

lend insight in helping us understand the therapeutic window for the intervention that maximizes recovery of function as well as neuroplasticity in M1.

Role of cortex in postural control

Balance is defined as the center of pressure (COP) of the body staying within the base of support (211, 212). Postural responses are the actions taken to maintain balance, by means of pelvic roll and shifting COP within base of support. Integration of sensory information and execution of postural responses remains unclear. Postural responses have been well defined in animal models including many injury conditions, from decerebration to a range of spinal cord injuries (21, 213, 214). Sensory integration from the visual system (215, 216), vestibular system (216–218) and somatosensory feedback (213, 219) from extremities, all play a role in postural control. However, in the absence of vision (212, 216) or vestibular input (216), postural control is driven by somatosensory feedback from the extremities (220). In fact, disruption of this somatosensory feedback due to spinal cord injury impaired ability to do postural corrections (221, 222). Postural control in complete spinal cord injury models is impaired (223), despite the ability to regain stepping with step training and spinal stimulation (224, 225). The effect of therapy in improving postural control and the associated role of the cortex is unclear, especially in the partial injury model. Decerebration studies have demonstrated that cortex is not essential in the maintenance of basic postures such as standing and walking (226), and the ability to maintain balance in the tilt task (227). Despite the non-essential nature of the cortex in postural tasks, previous studies (228–231) show that many neurons in the motor cortex modulate their activity in response to postural perturbation This is in fact seen in a previous study in our lab (7) and others (20). Lesioning the reorganized cortex abolished all therapy related gains, whereas lesioning the cortex in an intact animal did not disrupt its ability to autonomously walk on a treadmill. Lesioning the reorganized

cortex in neonatally spinalized animals also increased the roll in the pelvis suggesting poor postural control. Thus, While the role of cortex is not critical during postural control prior to injury, therapy related recovery after injury is mediated by cortex (7, 54, 55).

Role of cortex in regulating locomotion.

Cortical lesions in the motor cortex affect dexterous control but does not have huge impact on locomotion especially when walking on a flat surface. In-fact after a cortical lesion in cats, they can still adapt to altered locomotor conditions such as walking with limb loaded by weights (194). Dorsal column lesion that damaged 95% of corticospinal tract resulted in only transient deficits in treadmill locomotion (195), however some deficits such as foot drag and altered interlimb co-ordination can persist during treadmill locomotion especially if the dorsolateral funiculi that contains both corticospinal as well as rubrospinal tract is damaged (161, 196, 197).

The motor cortex plays a role in skilled locomotion involving accurate paw placement in tasks that require sensorimotor co-ordination. In fact, motor cortex lesions in cats caused a lot of missed paw placements when walking on a ladder (198). It is well known that subcortical structures play a major role in the maintenance and regulation of locomotion. In fact, in a decerebrate preparation than disconnects cortex from brainstem, electrical stimulation of mid brain region in brain stem (MLR or mesencephalic locomotor region) can elicit spontaneous locomotion (199, 200), however stimulating the pyramidal tract in animals during fictive locomotion in adult cat could also alter/reset locomotor rhythm implying that the corticospinal tract can indeed modulate the activity of central pattern generators in the spinal cord (201). After SCI, in both neonatally spinalized (20) as well as adult rats (7) therapy mediated recovery of weight supported stepping in the open field is lost after lesioning the regions of the reorganized trunk motor cortex. In a recent study (166), silencing motor cortex projections to brain stem abolished therapy mediated improvement in

volitional leg movements during swimming after a severe spinal cord injury, while there was no impact in intact animals.

Recent studies have shown that repetitive motor cortex stimulation when paired with rehabilitation can improve functional recovery after SCI (202–206). Alternatively, brain-controlled neuromodulation therapies targeted at the brain stem with deep brain stimulation (DBS) (183) or targeted at spinal cord below injury level via epidural electric stimulation (EES) (31, 33, 207) have been developed. These brain controlled neuromodulation therapies, when paired with physical rehabilitation enhanced the recovery of volitional locomotor function after spinal cord injury. These studies taken together suggest that the motor cortex plays a facilitatory role rather than an obligatory role in the regulation of locomotion intact state, but however play an obligatory role in the rehabilitation assisted recovery of volitional locomotion after SCI. These reasons make M1, a compelling region to examine plasticity associated with rehabilitation assisted recovery of locomotion after spinal cord injury.

Neurons in the motor cortex have also been shown to preferentially fire at specific phases of step cycle of both the forelimbs and hindlimbs during active locomotion (194, 208–210). In fact, after spinal cord injury, the neuronal encoding of population of M1 neurons about step height during locomotion was enhanced after brain-controlled neuromodulation therapy paired with rehabilitation (33). In neonatally spinalized rats the neurons hindlimb sensorimotor cortex was more modulated to forelimb footfalls during weight supported stepping on a treadmill compared to non-weight supported steps taken (46). Forelimb somatosensory input from above the level of lesion preferentially modulated trunk M1 activity in completely spinalized rats that received a combination therapy of physical rehabilitation and pharmacotherapy (7). Hence, examining altered

sensorimotor integration in M1 and the impact of rehabilitation is essential to understand its functional relevance during in supporting weight supported stepping during treadmill locomotion. In this thesis, I examine cellular and network plasticity differences associated with spontaneous recovery and rehabilitation assisted recovery, by recording neural activity in trunk M1 in animals with moderate spinal contusion injury during treadmill locomotion.

Chapter 2: Hindlimb somatosensory information influences trunk sensory and motor cortices to support trunk stabilization

Bharadwaj Nandakumar a, b[1], Gary H. Blumenthal a,b[1], Francois Philippe Pauzin b, Karen A. Moxon a,b,c

[1]these two authors contributed equally.

a. Department of Biomedical Engineering, Science, and Health Systems, Drexel University, Philadelphia, PA.

b. Department of Biomedical Engineering, University of California Davis, Davis, CA

c. Center for Neuroscience, Davis, CA

(Cerebral Cortex 2021 (39))

Abstract

Sensorimotor integration in the trunk system is poorly understood despite its importance for functional recovery after neurological injury. To address this, a series of mapping studies were performed in the rat. First, the receptive field (RF) of cells recorded from thoracic dorsal root ganglia were identified. Second, the RF of cells recorded from trunk primary sensory cortex (S1) were used to assess the extent and internal organization of trunk S1. Finally, the trunk motor cortex (M1) was mapped using intracortical microstimulation to assess coactivation of trunk muscles with hindlimb and forelimb muscles, and integration with S1. Projections from trunk S1 to trunk M1 were not anatomically organized, with relatively weak sensorimotor integration between trunk S1

and M1 compared to extensive integration between hindlimb S1/M1 and trunk M1. Assessment of response latency and anatomical tracing suggest that trunk M1 is abundantly guided by hindlimb somatosensory information that is derived primarily from the thalamus. Finally, neural recordings from awake animals during unexpected postural perturbations support sensorimotor integration between hindlimb S1 and trunk M1, providing insight into the role of the trunk system in postural control that is useful when studying recovery after injury.

Introduction

Transmission of information between somatosensory and motor systems, or sensorimotor integration, is crucial for perception (40) and volitional control of movement (41). Understanding the substrates of sensorimotor integration is important for studies examining locomotor function. For example, sensorimotor integration has been extensively studied in the rodent whisker system (40, 42–47) giving rise to a better understanding of how rodents use their whiskers optimally to navigate and discriminate features of their environment. Furthermore, research on the forelimb (48–52) and hindlimb systems (35, 53–56) has highlighted the importance of sensorimotor integration for appropriate locomotor function. These studies found extensive integration between anatomically and topographically corresponding sensory and motor cortices, with little cross-region integration (e.g., integration between whisker sensory and hindlimb motor cortices). Yet, little is known about sensorimotor integration within the trunk cortex or between the trunk motor cortex and other sensory cortices, which can be of fundamental importance for studies examining learning and recovery after neurological injury or disease.

Classic mapping studies of the rodent primary sensory cortex (S1) and primary motor cortex (M1) have roughly outlined the location and border of trunk S1 and M1 (35, 57, 58). More recently, subregions of trunk S1 have been identified, including a ventral trunk representation (59, 60) and

a genital representation (61). Despite these findings, the internal somatotopy of trunk S1 remains ill defined, in part, due to the limited assessment of spinal dermatomes of the thoracic regions (62, 63). Similarly, trunk M1 is mentioned in most mapping studies (36, 64, 65) and some information has emerged from recent studies examining cortical reorganization after spinal cord injury (9, 11, 22, 24, 34, 66, 67). However, little is known about the internal somatotopy of trunk M1 (9, 22, 34, 66). Further study of the somatotopy of trunk S1 and M1, as well as how these cortices integrate information, is needed to understand the role of trunk cortex more fully, both in intact animals and animals that have neurological injury or disease.

Thus, the aims of the current study were to define the somatotopy of trunk S1 and trunk M1 and examine sensorimotor integration of trunk cortex. First, to examine the internal organization of trunk S1, electrophysiological mapping was performed at the spinal level to identify thoracic dermatomes and their corresponding representation in S1. Similarly, intracortical microstimulation (ICMS) was used to examine the extent and internal organization of trunk M1. Then, sensorimotor integration was assessed by examining somatosensory evoked potentials across broad regions of sensorimotor cortex and retrograde tracing was performed to understand the source of somatosensory input to trunk M1. Finally, to understand the functional role of sensorimotor integration, single neuron activity was recorded from trunk S1 and M1 in response to unexpected postural perturbations while animals stood on a tilting platform. Results from mapping studies reveal an important somatotopic organization within both the trunk S1 and M1 cortices. Furthermore, there is extensive sensorimotor integration between trunk and hindlimb systems, compared to the relatively weak integration within trunk and between trunk and forelimb cortices. Evidence from response latency and tracing studies suggest that this trunk/hindlimb sensorimotor integration is mediated predominately by thalamo-cortical projections. Importantly, this

integration of hindlimb somatosensory information with trunk M1 is activated during postural adjustments to allow the animal to stabilize the trunk and maintain balance. These insights into trunk sensorimotor organization enhance our understanding of how information is processed during postural control and thereby inform the development of effective rehabilitative strategies after spinal cord injury.

Results

Dermatomes of upper thoracic DRGs overlap more than those of lower thoracic DRGs.

To study how trunk somatosensory information is represented in the brain, it is important to understand how this somatosensory information is first represented at the spinal level. While the upper and lower thoracic dermatomes were previously mapped (62, 63, 68, 69), the mid thoracic dermatomes have not been mapped extensively in the rat, nor is the representation of these dermatomes in the cortex known. To this end, we recorded single neuron activity from DRGs at the thoracic level (T1-T13) and mapped the thoracic dermatomes (Figure 2.1A). An average of 6 +/- 3 DRGs were recorded per animal (n = 15) for a total of 86 recorded dermatomes. The thoracic dermatomes were rectangular bands with overlapping receptive fields that extended from the dorsal midline to the midline on the ventral side of the trunk. The T1-T3 dermatomes had receptive fields that extended into the forelimb, while the receptive fields of the remaining thoracic dermatomes were limited to the trunk (Figure 2.1B). The width of the thoracic dermatomes remained constant in the rostrocaudal direction along the body (One-way Repeated Measures ANOVA, F (12, 59) = 1.41, p = 0.44; Figure 2.1C), consistent with studies performed on cats (70, 71), sheep (72), and monkeys (73, 74). However, the amount of overlap between adjacent dermatomes decreased significantly from rostral to caudal (One-way Repeated Measures ANOVA, F [11, 44] = 2.52, $p < 0.05$; Figure 2.1D). This decrease in overlap was due to a shift in the average

center position of adjacent dermatomes (One-way ANOVA, F [2, 61] = 7.73, $p < 0.001$; Figure 2.1E). Tukey's post-hoc test revealed a significant increase in the average positional shift distance between adjacent dermatomes in both the mid (T5-T9; $p < 0.05$) and lower (T9-T13; $p < 0.001$) trunk regions when compared to upper trunk dermatomes (T1-T5). Therefore, rostral DRGs appeared to overlap more with neighboring dermatomes than caudal DRGs.

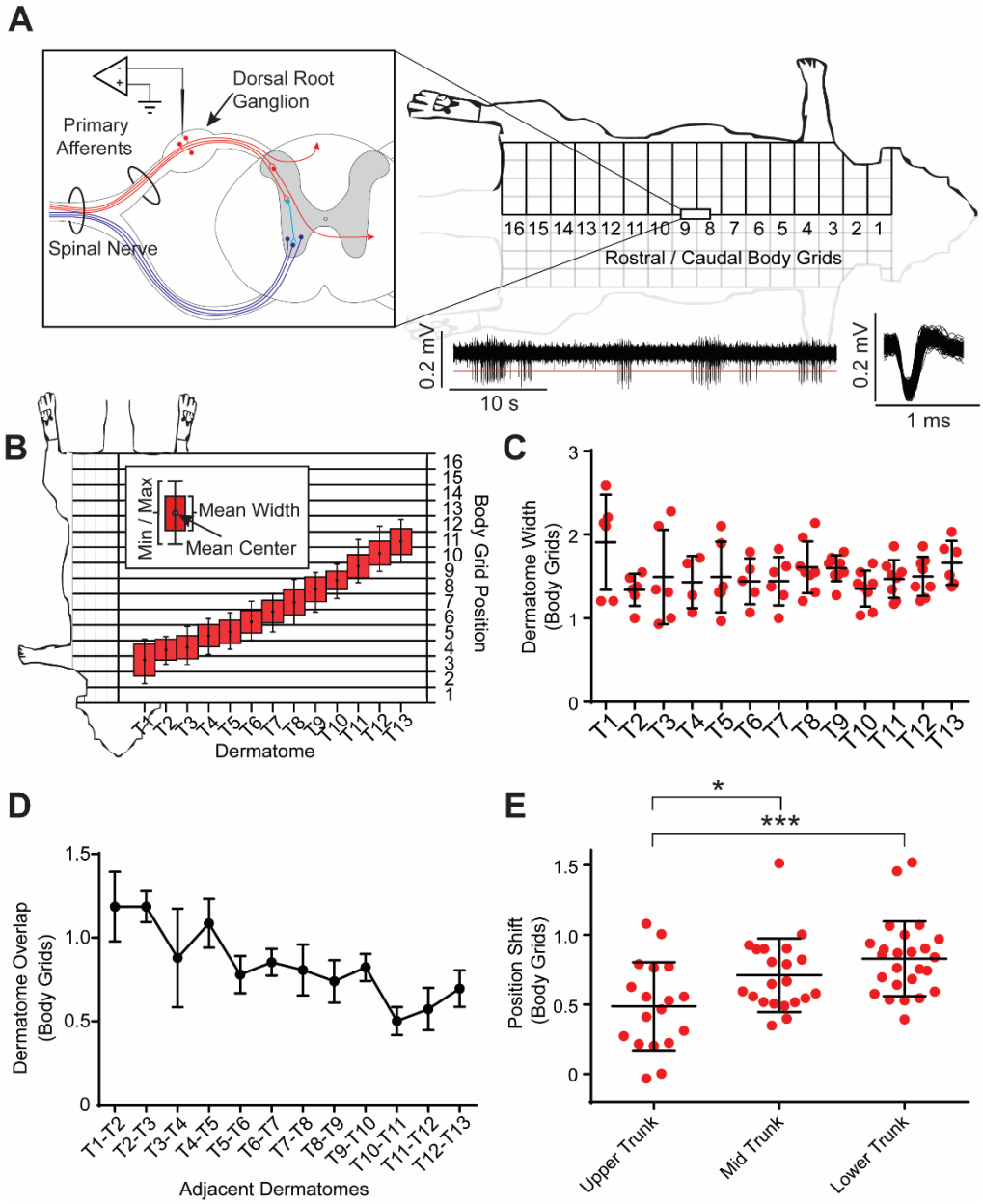

Figure 2. 1 Trunk spinal dermatomes. A) Dermatome map methodological diagram. A tungsten microelectrode was inserted into an average of 6 +/- 3 thoracic level dorsal root ganglions (DRGs) per animal (N = 15), to record from primary afferent cell bodies and identify their receptive fields (N = 86). An

example of a continuous neural trace is shown in the bottom right. B) Average dermatome width in body grid units (each grid unit is approximately 1 cm^2) and center position plotted along the rostrocaudal axis of the body. The error bar represents the most rostral and the most caudal body grid positions of each dermatome across all animals. C) Average dermatome width is similar throughout the rostrocaudal axis. D) Average overlap between adjacent dermatomes showed a shift in the rostrocaudal axis. E) Average distance in between neighboring dermatomes within the upper (T1-T5), mid (T5-T9), and lower (T9-T13) thoracic dermatomes showed a shift in the rostro caudal axis, with a significant difference for the average distance in between neighboring dermatomes between upper trunk and mid trunk and between upper trunk and lower trunk.

Sensory information from mid and lower trunk most likely to overlap within S1

A somatotopic map of TrS1 and surrounding somatosensory cortices was constructed using single unit cortical mapping data as well as information from the dermatomes. In each cortical location, the proportion of cells responding to each body part was calculated (Figure 2.2A). An average of 9 +/- 3 cortical locations were sampled per animal (N = 40 animals), with an average of 8 +/- 3 single neurons sampled per location. In total, more than 2900 neurons were recorded. TrS1 was determined to be located along the caudal edge of FLS1 and HLS1, consistent with previous studies in rats (57, 59, 60). The representation of the neck was most lateral, with the tail representation most medial (Figure 2.2B). Dorsal TrS1 was located more caudal to ventral TrS1. The ventral TrS1, consistent with previous studies (57, 59, 60), was nestled between the FLS1 (lateral) and the HLS1 (medial), and rostral to midthoracic (T6-T9) trunk representations, overlapping with the genital cortex described in previous studies (61). The full rostral extent of ventral trunk was not mapped. Nonetheless, these results show that the trunk representation is larger than previously reported (34, 35, 64).

Within the trunk representation, the thoracic dermatomes were represented from T1, laterally, to T13, medially, consistent with a study in humans (75). As might be expected, there was extensive overlap of the cortical representation of neighboring thoracic dermatomes (Figure 2.2C). The

rostrocaudal dimension of the dorsal trunk body was represented along the mediolateral axis of the cortex, with rostral trunk body represented laterally in the TrS1 (Figure 2.2C1). The mediolateral dimension of the dorsal trunk body was represented along the rostrocaudal axis of the cortex, with the most lateral part of dorsal trunk body represented rostrally in the cortex, just caudal to the ventral trunk representation (Figure 2.2C2). Unlike other sensory systems, such as whisker and limbs that tend to have RF size differences across layers (49), the RF size of neurons in TrS1 were similar across layers (N = 482) (One-way ANOVA, F [2, 479] = 1.45, p = 0.23; Figure 2.2D1). However, the RF size of trunk neurons did differ across the different regions of the TrS1 (N = 437) (One-way ANOVA, F [2, 434] = 19.71, $p < 0.0001$; Figure 2D2) with upper trunk neurons having smaller RF size compared to both mid and lower trunk neurons (5.7 +/- 3.7, 8.0 +/- 3.8, 9.0 +/- 5.0 body grids or cm^2, respectively; Tukey's post-hoc test, $p < 0.0001$; Figure 2.2D2-D3). This RF size analysis suggests that somatosensory information ascending from the thalamus is spread across large parts of TrS1 early, immediately upon arrival in layer IV, with more overlap between mid and lower trunk sensory information than that of upper trunk. This is consistent with RF sizes observed in forepaw somatosensory cortex that varied from relatively small in the digits to larger in the limb (76).

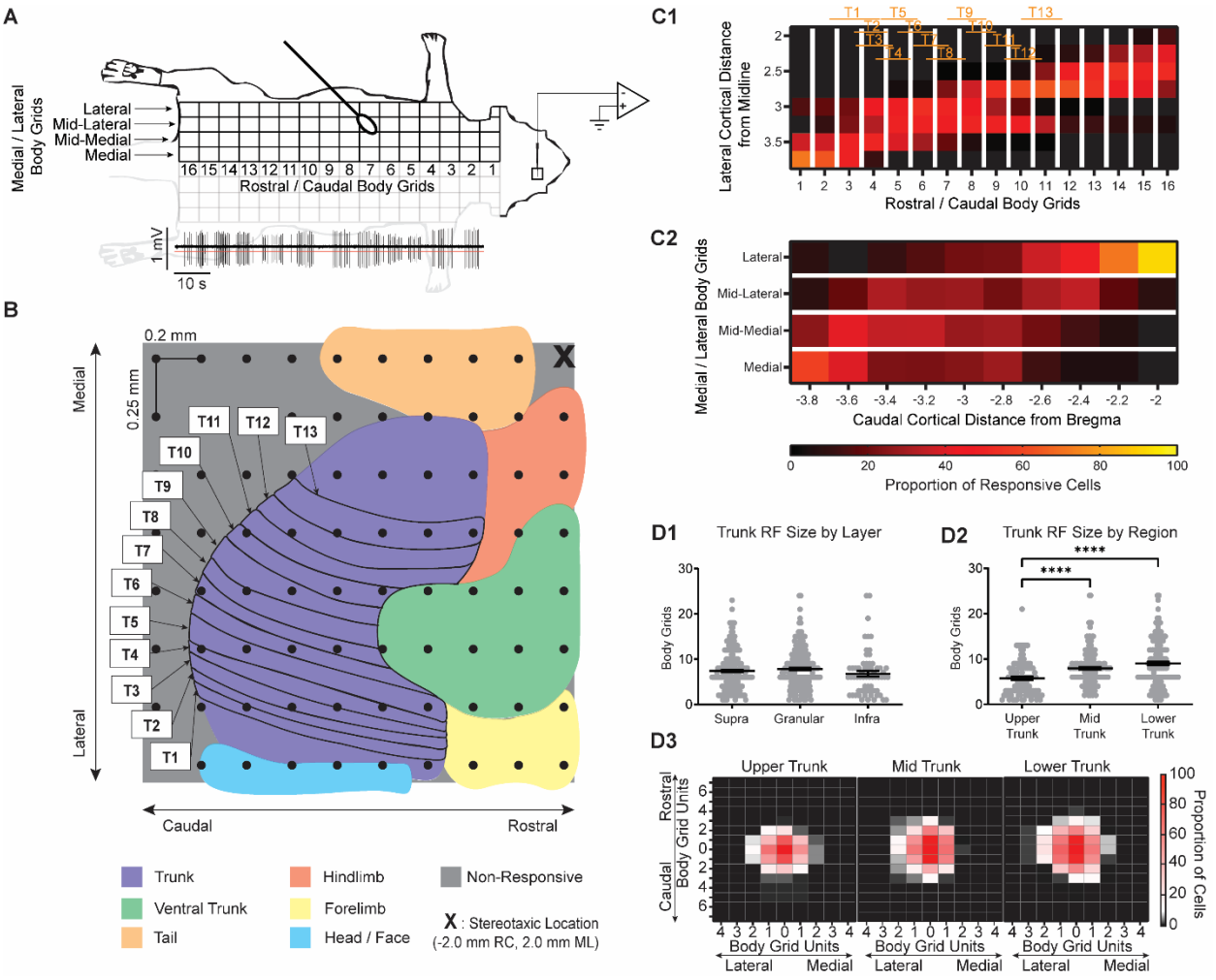

Figure 2.2 Relationship of trunk S1 organization in relationship to spinal dermatomes. A) Sensory map methodological diagram. A tungsten microelectrode was inserted into several locations within and around trunk S1. Single units were isolated, and their receptive fields were determined. B) Cortical representation of the thoracic dermatomes. The map shows the average cortical representations across cortical layers. Based on a pilot study (N = 3), 80 predefined cortical locations were chosen (black dots). They extended from -2.0 mm to -3.8 mm rostrocaudal (RC) from bregma with a resolution of 0.2 mm, and from -2.0 mm to -3.75 mm mediolateral (ML) with a resolution of 0.25 mm between locations, in order to optimally map the dorsal trunk area. 2920 neurons were recorded across all animals (N = 40) to construct the map. C1) Proportion of cells identified in the mediolateral cortical axis across all animals, associated with body grid rows, to light tactile stimulation of which the cortical cells responded. A higher proportion of rostral trunk RFs were found at lateral cortical coordinates, while a higher proportion of caudal trunk RFs were found at medial cortical coordinates. The rostrocaudal extent of the thoracic dermatomes relative to the body grid rows are also displayed. C2) Proportion of cells identified in the rostrocaudal axis across all animals, associated with body grid columns, to light tactile stimulation of which the cortical cells responded. A higher proportion of lateral trunk RFs were found at rostral cortical coordinates, while a higher proportion of medial trunk RFs were found at caudal cortical coordinates. The color scale bar at the bottom is for both C1 and C2. D1) Trunk receptive field size (body grids units) (N = 482) of neurons in the supragranular, granular and infragranular layers are similar. D2) Receptive

field size (N = 437) is significantly different for the upper, mid, and lower trunk S1 regions. D3) Receptive field centers are normalized to position (0, 0) and the proportion of cells responsive to the surrounding body grids are calculated and showed significant differences in size across trunk S1 regions (refer to D2).

Greater overlap of trunk S1 with hindlimb than forelimb S1

To understand the overlap between trunk, forelimb, and hindlimb somatosensory information, multichannel recordings were performed in TrS1, FLS1, and HLS1 in response to peripheral electrical stimulation of the mid trunk, forelimb, and hindlimb. To ensure fair comparison between the responses to the different stimulus locations on the body, the amplitudes of the SEP recorded from the granular layer at each cortical region in response to graded peripheral electric stimulation of each respective region (FL, HL, and MT) were compared (Figure 2.3A, Supplementary Figure 2.3). As expected, there was a significant increase in the SEP amplitude associated with increases in stimulus current regardless of stimulus location (Two-way Repeated Measures ANOVA, F [3, 70] = 15.47, $p < 0.0001$; Figure 2.3A). However, across stimulus location, the SEP amplitudes were similar (Two-way Repeated Measures ANOVA, F [2, 70] = 1.62, $p = 0.21$; Figure 2.3A), suggesting that the stimulus at each location activated the homologous cortical region similarly and that comparisons could be made between responses recorded from different brain regions to stimulation of the same location on the body.

To understand the overlap of trunk somatosensory information across S1, the amplitude of the SEP response to mid trunk stimulation recorded from FLS1 was compared to the SEP response recorded from HLS1. The SEP amplitudes recorded from FLS1 and HLS1 in response to low intensity trunk stimulation (0.5 mA) were similar (Independent Samples t-test, t [6] = 0.29, $p = 0.77$), suggesting trunk somatosensory information overlaps with both FLS1 and HLS1. However, when the stimulation amplitude was increased to produce twitching of the underlying muscle and further activate proprioceptive receptors (5.0 mA), the response in HLS1 was significantly greater than

that recorded from FLS1 (Independent Samples *t*-test, t [8] = 2.30, p = 0.05; Figure 3B, Supplemental Figure 2.3C-D), suggesting differences in the overlap of trunk somatosensory information in HLS1 compared to FLS1.

Next, within TrS1, the relationship between inputs to layer IV cells (SEP amplitude) and outputs of TrS1 neurons (single neuron firing rate or proportion of responding neurons) in response to low and high intensity mid trunk stimuli were examined to assess the effectiveness of the information transfer from input to output (Figure 2.3C). As noted above, SEP amplitude to high intensity mid trunk stimulation was significantly greater than the response to low intensity stimulation (Independent Samples *t*-test, t [14] = 4.76, $p < 0.001$). This increase in input results in a greater magnitude of the response (spikes per stimulus) to high intensity stimuli (Independent Samples *t*-test, t [65] = 2.59, $p < 0.05$; Figure 2.3C) without a change in the proportion of responsive neurons (χ^2 [1, N = 55] = 0.46, p = 0.50), suggesting the same cells are responding to low intensity stimuli as those that respond to high intensity.

Next, the contribution of high intensity forelimb and hindlimb stimulation to the response in TrS1 was examined. The SEP amplitude in TrS1 to forelimb stimulation was similar to that of hindlimb stimulation (Independent Samples *t*-test, t [8] = 0.36, p = 0.73). However, the proportion of neurons in TrS1 that responded to hindlimb stimulation was greater than the proportion responding to forelimb stimulation (χ^2 [1, N = 84] = 11.16, $p < 0.001$; Figure 2.3D), suggesting that the transfer of incoming somatosensory information to output is more effective for hindlimb than forelimb stimulation. In fact, too few cells responded to forelimb stimulation to allow any further analysis.

To understand if the increased proportion of responsive TrS1 cells to hindlimb stimulation was potentially influenced by the proximity of these body or somatotopic regions, recordings were performed in upper TrS1 during stimulation to forelimb and hindlimb (5.0 mA; n = 3). No

differences were found in SEP amplitude (Independent Samples *t*-test, t [4] = 0.09, p = 0.92) or the proportion of responsive cells (χ^2 [1, N = 107] = 2.95, p = 0.09) between stimuli conditions, suggesting that proximity is likely not contributing to increased responsiveness (Supplemental Figure 2.3E).

As expected, the response of TrS1 neurons to hindlimb stimulation was smaller than the response to MT stimulation (Independent Samples *t*-test, t [43] = 2.71, $p < 0.01$; Figure 2.3D-E). These results, taken together, suggest reciprocal flow of information between TrS1 and both FLS1 and HLS1, with greater influence of trunk somatosensory information in HLS1 compared to FLS1 and greater influence of hindlimb somatosensory information in TrS1 compared to forelimb information. In the last section of this paper, we explore how this organization is used to encode the cortical response to unexpected tilts in the lateral plane.

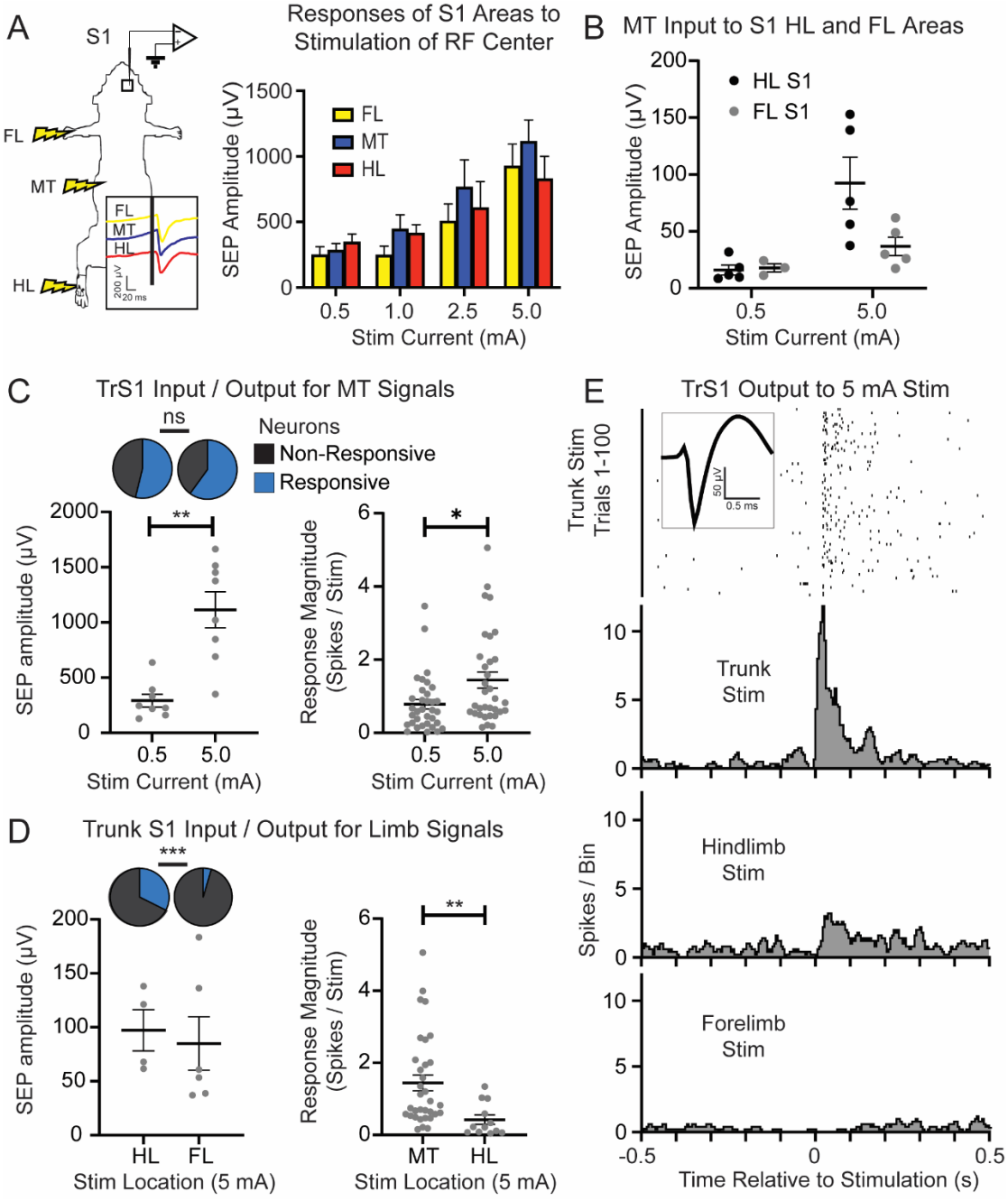

Figure 2. 3 Somatosensory integration within trunk S1. A) Electric stimulation methodological diagram. Multichannel recordings were performed in the trunk, forelimb, and hindlimb S1 in response to peripheral electrical stimulation to the mid trunk (MT), forelimb (FL), and hindlimb (HL). The SEP from each cortical region recorded from the granular layer to graded peripheral electric stimulation (0.5 mA, 1.0 mA, 2.5 mA, 5.0 mA) of each respective region (FL [N = 5, 6, 7, 8], HL [N = 7, 6, 6, 7], MT [N = 9, 7, 6, 8]) was compared (also see Supplemental Figure 2). B) SEP amplitude in the forelimb S1 and hindlimb S1 in response to the low intensity (0.5 mA; FLS1 [N = 3], HLS1 [N = 5]) and the high (5.0 mA; FLS1 [N = 5], HLS1 [N = 5]) MT stimulation. C) The relationship between sensory inputs (SEP amplitude in the granular layer, left) (0.5mA

N = 8; 5.0mA N = 8) and outputs (single neuron activity in all layers, right) (0.5mA N = 34; 5.0mA N = 33) in trunk S1 in response to low and high intensity MT stimuli. The inset on the top left represents the proportion of responsive cells for each stimulus. D) Bottom left: SEP amplitudes recorded from trunk S1 in response to high intensity HL (N = 4) and FL (N = 6) stimulation. Top left: Proportion of trunk S1 neurons responding to hindlimb or forelimb stimulation. Right: Trunk S1 response to MT (N = 33) and HL (N = 12) stimulation calculated within 100 ms from stimulus onset. E) Example PSTHs for trunk, HL, and FL stimulation (5.0 mA) in trunk S1, illustrating that trunk S1 activity is modulated more by hindlimb than forelimb.

Coactivation of trunk musculature with hindlimb is more likely than coactivation with forelimb musculature.

To gain a better understanding of the trunk cortex, it was essential to examine the extent and organization within TrM1. The extent of TrM1 was mapped using ICMS and movement representations were examined by analyzing movement and EMG responses from trunk and limb musculature (Figure 2.4A). Each of the 88 cortical locations were sampled an average of 7 +/- 2 times, across 21 animals. Each animal contributed to the data with an average of 27 +/- 2 cortical locations per animal. The average threshold current was 51.3 +/- 23.4 mA. The areas of the cortex that most likely activated the trunk musculature were within 1.5 mm ML and 0.25 mm to -2.25 mm RC, relative to bregma (Figure 2.4B). This placed the rat TrM1 medial to FLM1 and HLM1 and just caudal to whisker M1.

A much larger area than previously reported activated trunk by generally coactivating with other parts of the body, suggesting that this coactivation with forelimb and hindlimb motor cortex is functionally relevant. For each animal, the area that exclusively activated trunk musculature (ET) was quite small, and the location of ET was not consistent across animals. This suggests that there are likely to be few conditions under which trunk musculature is activated independently of the musculature of other parts of the body. In fact, it is possible to identify distinct coactivation zones between trunk and other parts of the body. The overall extent of the trunk coactivating with other

parts of the body (Figure 2.4C) spanned -2.25 mm to 0.75 mm RC and 1 mm to 2.5 mm ML relative to bregma, which is much larger than previously reported (22, 34, 64–66, 77). The area that exclusively activated trunk musculature (ET) within any given animal was restricted to within 1.5 mm lateral to midline (Figure 2.4D).

Despite this small area devoted to ET, coactivation of trunk with hindlimb musculature (HLT) was quite large (Figure 2.4E) and, not surprisingly, caudal to locations overlapping with forelimb (FLT; Figure 2.4F). In addition, consistent with an earlier study (78), in approximately half of the animals (45%), FL, HL, and trunk (synergistic trunk or FHT) coactivated in locations between the HLT and FLT representation (Figure 2.4G). In order to quantify and compare the different movement representations found within the trunk coactivation zone, responsiveness scores (12, 34) that represented the proportion of responses for each representation were compared. The responsiveness scores were different across coactivation zones ($N = 54$) (One-way ANOVA, F [7, 424] = 11.10, $p < 0.001$; Figure 2.4H). Importantly, the responsiveness score of HLT was significantly greater than FLT (Tukey's post-hoc test, $p < 0.01$), indicating that trunk coactivates more with hindlimbs across a larger region of cortex compared to forelimbs. Moreover, the responsiveness score of FLHL and FHT were very similar, suggesting that when forelimb and hindlimb coactivate, about half the time they coactivate with trunk. These results demonstrate that a large region of M1 is devoted to coactivating trunk musculature with musculature from different body parts, mainly hindlimb and less so with forelimb.

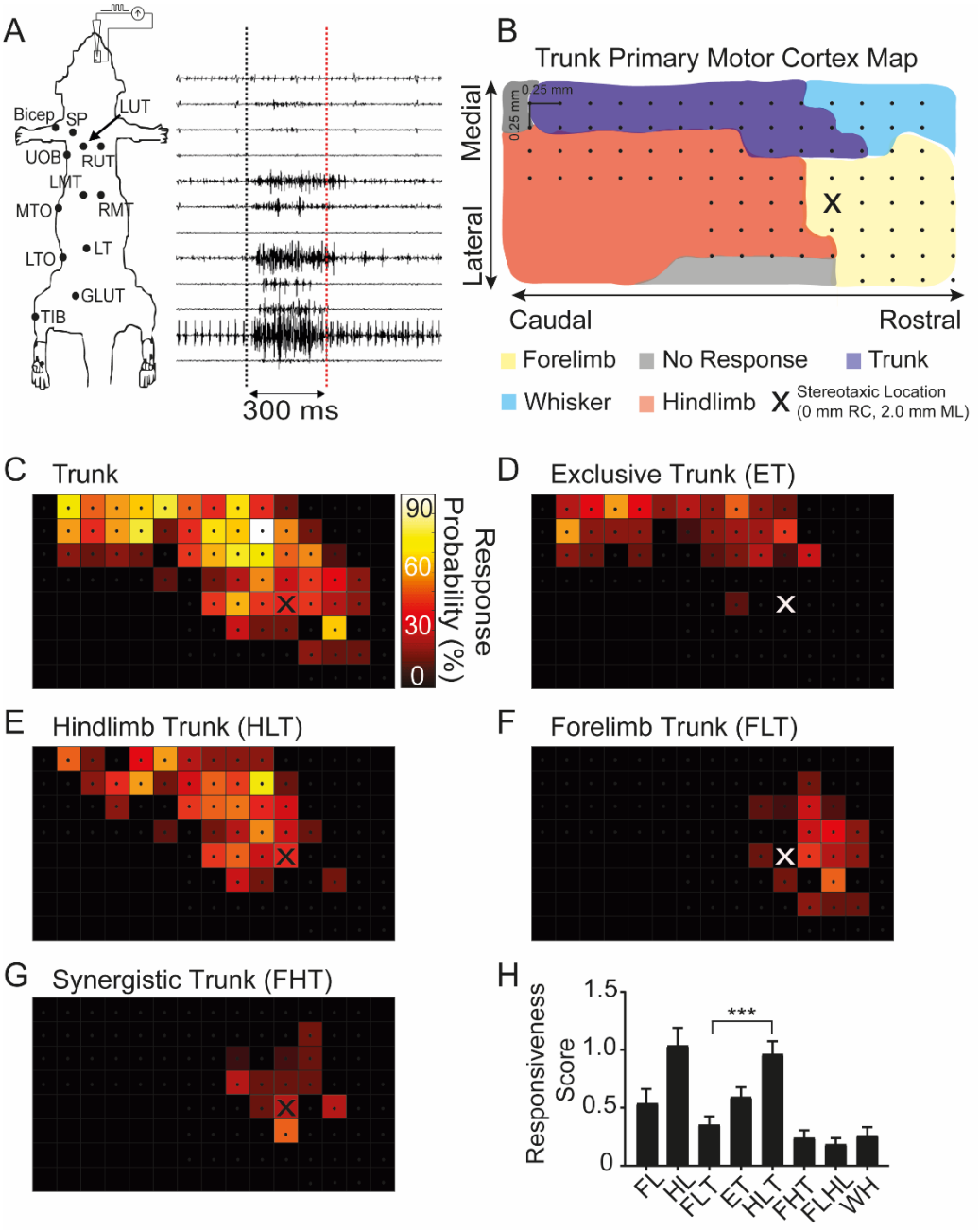

Figure 2. 4 Coactivation of trunk musculature with forelimb and hindlimb. A) ICMS methodological diagram. Motor maps were obtained by intracortical current microsimulation (ICMS) in the infragranular layer of motor cortex. Evoked muscle activity was recorded through EMG electrodes implanted along the trunk, forelimb, and hindlimb musculature (Top to bottom: forelimb bicep [bicep], spinous trapezius [SP], left upper thoracic longissimus [LUT], right upper thoracic longissimus [RUT], upper external oblique [UOB], left mid thoracic longissimus [LMT], right mid thoracic longissimus [RMT], mid thoracic external oblique [MTO], lower thoracic longissimus [LT], lower thoracic external oblique [LTO], gluteus maximus [Glut], tibialis anterior [Tib]). Observed movement and evoked muscle activity at threshold current were used to determine movement representation. B) Topography of TrM1 is based on the most predominant response across animals. The dots refer to penetration locations sampled across animals. The X location

refers to 0 mm RC, 2 mm ML, relative to bregma. C-G) Proportion of penetrations from which the following muscles were activated: (C) trunk, (D) trunk exclusively, (E) trunk and hindlimb, (F) trunk and forelimb, and (G) trunk and both forelimbs and hindlimbs. H) Average responsiveness score within trunk M1 (N = 54) was calculated for the different movement representations identified during mapping with ICMS (see Materials and Methods for explanation). FL (activation of forelimb only), HL (activation of hindlimb only), FLT (coactivation of only forelimb and trunk), ET (exclusively trunk or activation of only trunk), HLT (coactivation of only hindlimb and trunk), FHT (coactivation of forelimb, hindlimb and trunk), FLHL (coactivation of only forelimb and hindlimb), WH (activation of whisker pad).

Movement type	Visual observation	EMG response
Forelimb (FL)	Isolated movement of forelimb (wrist or multi-joint)	Exclusive EMG response- FL muscle (FL bicep)
Hindlimb (HL)	Isolated movement of hindlimb (digits or multi-joint)	Exclusive EMG response- HL muscles (gluteus, tibialis)
Forelimb Trunk (FLT)	Proximal shoulder movement	Coactivation of FL muscle and Trunk /shoulder muscles
Exclusively Trunk (ET)	Isolated movement of thoracic girdle	Exclusive EMG response- Trunk muscles
Hindlimb Trunk (HLT)	Movement of hindlimb knee /ankle along with thoracic girdle	EMG response -Trunk muscles
Synergistic Trunk (FHT)	Forepaw and HL ankle dorsiflexion movements with trunk adduction	EMG response- Trunk muscles
Forelimb-Hindlimb (FLHL)	Exclusive forepaw and HL ankle dorsiflexion movements	Coactivation of forelimb and hindlimb muscles
Whisker (WH)	Whisker movements	Absence of any EMG response

Table 2. 1 Movement type classification. Explanation of how movement types were determined for each intracortical microstimulation trial.

Trunk motor cortex is somatotopically organized.

To understand trunk musculature recruitment associated with the different coactivation zones, EMG responses were examined in more detail. As expected, stimulation of forelimb trunk cortex

(FLT) preferentially activated spinous trapezius (SP) and contralateral upper thoracic longissimus (LUT). FLT coactivation zone is thus responsible for upper thoracic trunk muscles activation (Figure 2.5A-C). Similarly, stimulation of hindlimb trunk cortex (HLT) activated the obliques along the mid and lower thoracic level and therefore HLT coactivation zone is preferentially responsible for mid and lower trunk muscles activation (Figure 2.5A-C). Interestingly, stimulation of ET cortex also activated the oblique but at all thoracic levels, suggesting that ET is important to coordinate movements of the entire trunk. Finally, stimulation of the synergistic trunk cortex (FHT) activated mostly trunk musculature at the mid thoracic level (Figure 2.5C). Therefore, the different trunk coactivation zones differentially activate segmental trunk muscles (upper, mid, and lower thoracic levels) providing topography to TrM1 motor control.

To gain more insight, we constructed two maps of trunk coactivation zone: the first to identify the proportion of penetrations across animals that activated upper trunk muscles (Figure 2.5D) and the second to identify the proportion that activated lower trunk muscles (Figure 2.5E). The mediocaudal region of trunk coactivation zone preferentially controlled lower thoracic trunk musculature while the rostrolateral region controlled upper thoracic trunk musculature. The lower trunk musculature was more influenced by the rostrolateral area of trunk coactivation zone and upper trunk musculature by the mediocaudal area of trunk coactivation zone. To demonstrate this topography along the rostrocaudal axis, the proportion of penetrations activating upper or lower thoracic trunk from mediolateral locations were averaged (Figure 2.5F). Moving rostral, there was an increase in the probability of activating upper trunk (Linear Regression, $r2 = 0.61$, $F [1, 11] = 17.82$, $p < 0.01$), whereas moving caudal, there was an increase in the probability of activating lower trunk (Linear Regression, $r2 = 0.83$, $F [1, 11] = 54.70$, $p < 0.01$). This demonstrates a clear somatotopy within the trunk coactivation zone that define subregions of TrM1: UTM1 and LTM1.

Considering that segmental trunk muscles were differentially activated within this trunk coactivation zone, the amount and extent of activation within the coactivation zone was examined using the responsiveness score. The responsiveness scores were similar across the mid, upper, and lower thoracic segmental levels (N = 54, each level) (One-way ANOVA, $F [2, 159] = 0.49$, $p = 0.54$; Figure 2.5G), suggesting that the probability of cortex to activate the different segmental levels exclusively is similar. However, despite this similarity, there were differences in the likelihood of segmental coactivation (One-way ANOVA, $F [3, 212] = 9.06$, $p < 0.001$; Figure 2.5H) with the mid and lower thoracic muscles more likely to coactivate than other segmental muscle groups (Tukey's post-hoc test, $p < 0.001$). In summary, most of TrM1 is devoted to activation with other regions of the body and cortical representation of mid and lower thoracic trunk muscles are associated with hindlimb muscle representation while upper thoracic trunk muscles are associated with forelimb muscle representation. These results were confirmed by synergy analysis using the amplitude of evoked EMG responses obtained from the different trunk musculature (Supplementary Figure 1).

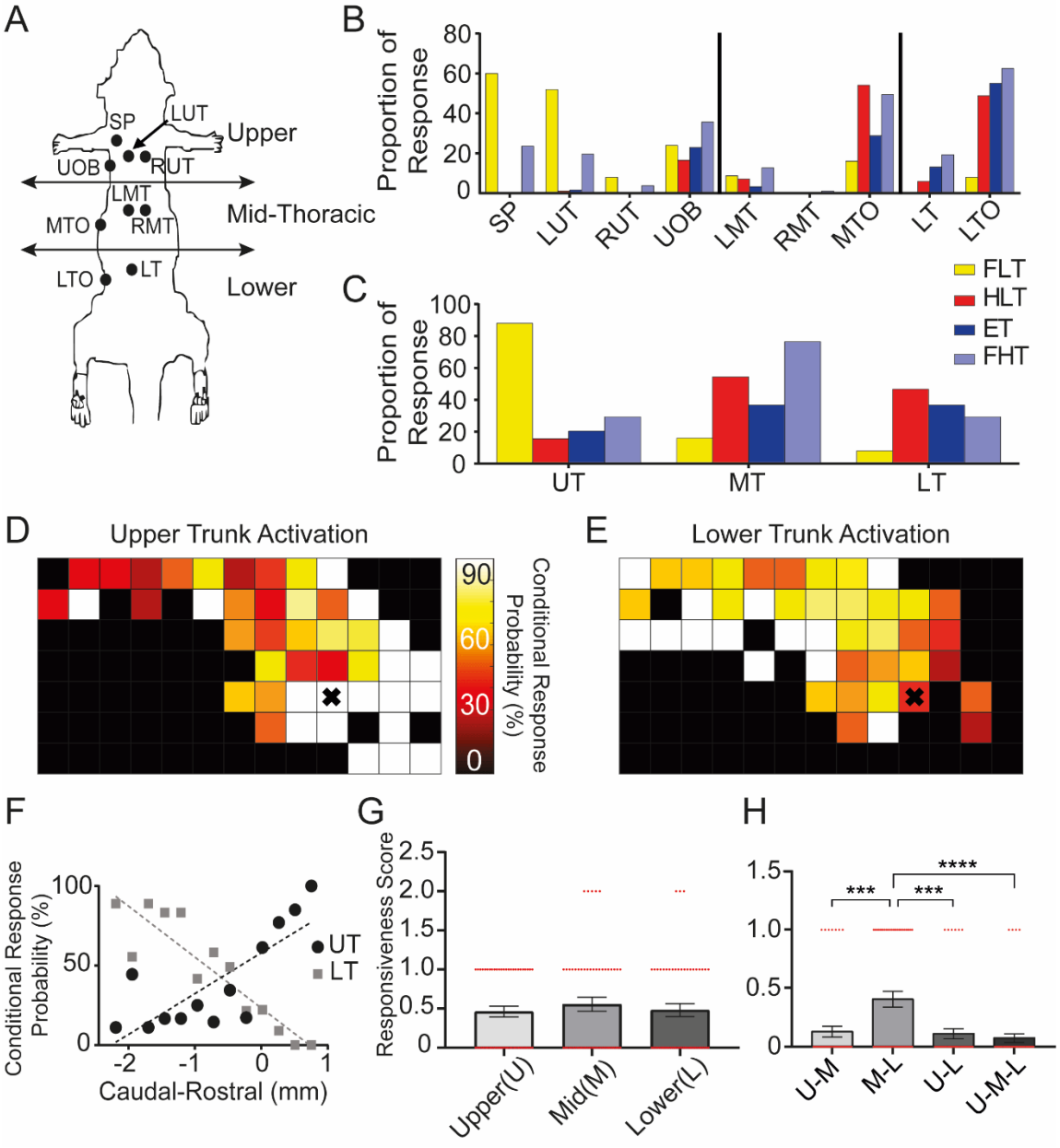

Figure 2. 5 Recruitment of trunk musculature in the different coactivation zones. A) Methodological diagram showing EMG electrode locations of trunk muscles categorized into three groups along the rostrocaudal axis of the body: upper thoracic, mid thoracic, and lower thoracic trunk muscles. B) Proportion of muscle responses in the different coactivation zones by muscle. C) Same graph as B, but muscles are grouped within the three segmental zones seen in A. Upper thoracic muscles were activated when FLT coactivation zone was stimulated and lower thoracic muscles were activated when HLT coactivation zone was stimulated. D-E) For locations within TrM1, the conditional probability of activating upper trunk musculature (D) is compared to activating lower trunk musculature (E). The X location refers to 0 mm RC, 2 mm ML, relative to bregma. F) Graph showing the conditional probability of eliciting trunk muscle responses in TrM1 based on visual observation & EMG responses of either upper or lower trunk

musculature averaged across the rostrocaudal axis G) Average responsiveness score within TrM1 (see Materials and Methods; N = 54) for the different segmental zones: upper, mid, and lower thoracic. H) Differences in the likelihood of segmental coactivation were also plotted within TrM1 for each of the segmental coactivations.

Trunk musculature type	EMG response
Dorsal Trunk	Activation of spinous trapezius or longissimus muscles at upper, mid, or lower thoracic level
Ventral Trunk	Activation of external oblique muscles at upper, mid, or lower thoracic level
Upper Thoracic Trunk (U)	Activation of spinous trapezius (SP), left upper thoracic longissimus (LUT), right upper thoracic longissimus (RUT), or upper external oblique (UOB)
Mid Thoracic Trunk (M)	Activation of left mid thoracic longissimus (LMT), right mid thoracic longissimus (RMT), or mid thoracic external oblique (MTO)
Lower thoracic trunk (L)	Activation of lower thoracic oblique (LTO) or lower thoracic longissimus (LT)

Table 2. 2 Trunk musculature classification. Muscles that were activated in response to intracortical microstimulation were classified as one of five muscle types.

Somatosensory input to trunk motor cortex is dominated by hindlimb information.

Given our understanding of somatosensory overlap within S1 and coactivation of trunk muscles with other regions of the body, we examined the integration of TrM1 with somatosensory input from the limbs by recording neural response in TrM1 supragranular and infragranular layers in response to electric stimulation of forelimbs, hindlimbs, mid trunk or upper trunk (Figure 2.6A). There was little to no response in TrM1 to low intensity stimulation (0.5 mA) applied to any of the four body locations. However, this was not the case for high intensity stimulation (5.0 mA).

Surprisingly, the SEP amplitude recorded from TrM1 in response to high intensity somatosensory stimulation of the hindlimbs was greater than the SEP amplitude to stimulation of either mid or upper trunk (Figure 2.6B-C). The response to forelimb stimulation was similar to that of trunk stimulation, solidifying that TrM1 preferentially receives somatosensory information from hindlimbs.

Due to the internal motor somatotopy along the rostrocaudal axis of TrM1 (refer to Figure 2.5F), cortical locations where SEPs were recorded were segregated into rostral (0 to –0.75 mm RC) and caudal regions (-1 to -2 mm RC). In the supragranular layer (Caudal, N = 103; Rostral N = 96), there was no effect of recording location (Two-way ANOVA, F [1, 191] = 2.34, p = 0.13), but there was an effect of stimulus location (Two-way ANOVA, F [3, 191] = 22.25, $p < 0.0001$; Figure 2.6D) such that the SEP amplitude recorded from both rostral and caudal TrM1 in response to hindlimb stimulation was greater than the response to stimulation of all the other locations (Tukey's post-hoc test, $p < 0.0001$). This result demonstrates an important role for hindlimb somatosensory integration within TrM1, but without any somatotopic organization. Surprisingly, there was no difference in the SEP amplitude in response to upper trunk stimulation compared to mid trunk stimulation (Tukey's post-hoc test, p = 0.99), suggesting no somatotopy of trunk somatosensory input within TrM1.

In the infragranular layer (Caudal N = 95; Rostral N = 85), there was again an overall effect of stimulus location (Two-way ANOVA, F [3,172] = 14.48, $p < 0.0001$; Figure 2.6E), where the SEP amplitude to hindlimb stimulation was again greater in both the caudal and rostral region of TrM1 suggesting that hindlimb somatosensory input to TrM1 was evenly distributed, across supra- and infragranular layers, between LTM1 and UTM1 as suggested by Figure 2.6C. Moreover, like the supragranular layer, there were no differences between SEP amplitude in response to mid trunk

stimulation compared to upper trunk stimulation (Tukey's post-hoc test, p = 0.95), suggesting similar organization for both supra and infragranular layers. Finally, to assess the effectiveness of high intensity (5.0 mA) hindlimb stimulation to reach the sensory or motor cortices, the SEP amplitude was compared across TrM1 (N = 8), TrS1 (N = 5), HLS1 (N = 7), and FLS1 (N = 5). There was an overall effect of cortical location (One-way ANOVA, F [3, 21] = 10.14, $p < 0.001$; Figure 2.6F), and as expected, the SEP response in HLS1 was greater than the response in any other region (Tukey's post-hoc test, HLS1 vs TrS1, $p < 0.001$; HLS1 vs TrM1, $p < 0.01$; HLS1 vs FLS1, $p < 0.001$). These results further support the extensive and preferential integration of hindlimb somatosensory input into TrM1.

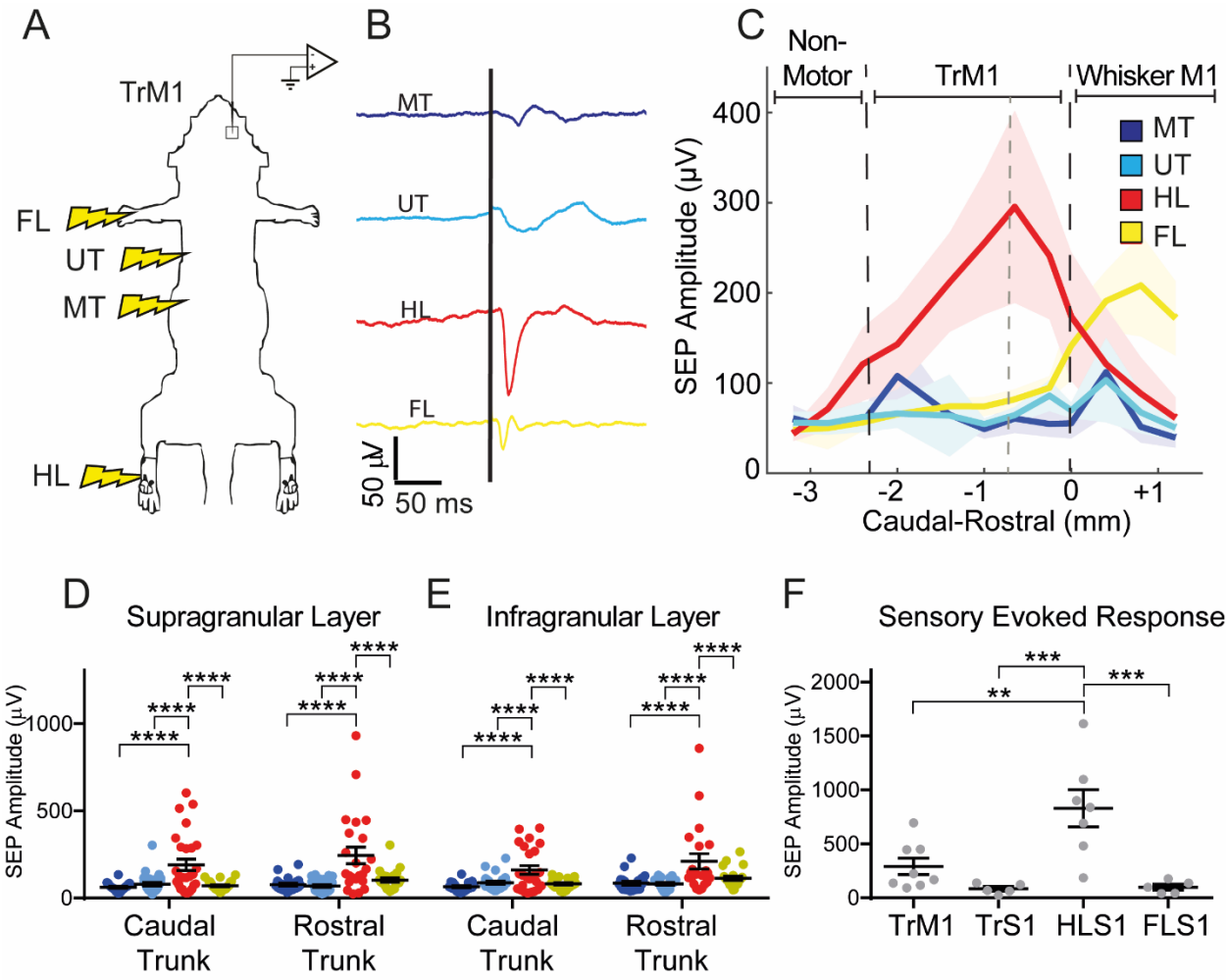

Figure 2. 6 Response to high intensity hindlimb stimulation predominates in trunk M1. A) Methodological diagram of the 5.0 mA electrical stimulation paradigm. Stimulations occurred in the dorsal hairy skin of forelimb (FL), hindlimb (HL), T4-T5 dermatome (UT), and T9-T10 dermatome (MT). B) Example of somatosensory evoked responses in TrM1 from the different stimulation locations on the body. C) SEP amplitude in the supragranular layer in response to stimulation across the rostrocaudal axis of TrM1 at 1.25 mm ML. Dotted line within TrM1 represents the distinction between caudal and rostral trunk. D-E) SEP amplitude in the supragranular (Caudal N = 103; Rostral N = 96) (D) and infragranular (Caudal N = 95; Rostral N = 85) (E) layers in the caudal region (-1 mm to -2 mm RC, relative to bregma) and in the rostral region (-0.75 mm to 0 mm RC, relative to bregma) of the TrM1. Rostral regions activate upper thoracic musculature, while caudal regions activate lower thoracic trunk musculature. F) Somatosensory evoked response in the supragranular layer of TrM1 (N = 8), TrS1 (N = 5), HLS1 (N = 7), and FLS1 (N = 5) from hindlimb stimulation.

Sensorimotor integration is cortico-cortical for trunk stimuli, thalamo-cortical for hindlimb stimuli.

Since sensorimotor integration in the cortex can be mediated by projections from the S1 cortex and the thalamus(79–81), retrograde tracing was used to better understand the relative contribution of cortico-cortical versus thalamo-cortical connections to TrM1 (Figure 2.7A). Tracer injected into the location most likely to contain the exclusively trunk region revealed that TrM1 received cortico-cortical input from ipsilateral TrS1, HLS1, and FLS1. As expected, given the variability across animals in the location of exclusively trunk cortex, the relative contribution from these sensory cortices was variable across animals (Figure 2.7B). Rats 1 and 2 had more cells projecting to TrM1 from HLS1 than from TrS1, while rat 3 showed projections exclusively from dorsal TrS1, and rats 4 and 5 showed projections predominately from dorsal TrS1. TrM1 also received input from secondary sensory cortex, dysgranular zone, whisker, and face S1 (data not shown), thereby making TrM1 a crossroad for somatosensory information.

In all animals, the projections from S1 to TrM1 were predominantly mediated by S1 cells in the supragranular and infragranular layers (Figure 7C). This laminar specificity is consistent with studies in the whisker sensorimotor system (45, 80). Tracing also revealed strong thalamo-cortical projections from the ventral posterolateral nucleus (VPL) of the thalamus to TrM1 in all animals

(Figure 7D, 7E) that likely carries proprioceptive information (82), however, tactile information from the thalamus cannot be ruled out.

To determine if the source of projections to TrM1 differed between body parts that were stimulated, SEP latency was analyzed. The mean latency of the SEP recorded from TrM1 (26.84 +/- 2.65 ms) was significantly longer than that from TrS1 (20.30 +/- 0.83 ms) when mid trunk was stimulated (Independent Samples t-test, $t [12] = 2.66$, $p < 0.05$; Figure 2.7F). This led us to conclude that the sensorimotor integration of trunk somatosensory information in TrM1 is primarily mediated by cortico-cortical projections. In contrast, the mean latency of the SEP recorded from TrM1 (23.44 +/- 1.81 ms) was similar to the that from HLS1 (21.15 +/- 1.66 ms) when hindlimb was stimulated (Independent Samples t-test, $t [12] = 0.90$, $p = 0.39$; Figure 2.7F and see Supplemental Figure 3). This led us to conclude that the integration of hindlimb somatosensory input in TrM1 is primarily mediated by thalamo-cortical projections, carrying somatosensory information, including proprioceptive. To identify how this somatosensory information might be used, next we recorded single neurons from TrS1 and TrM1 while animals were subjected to tilts in the lateral plane.

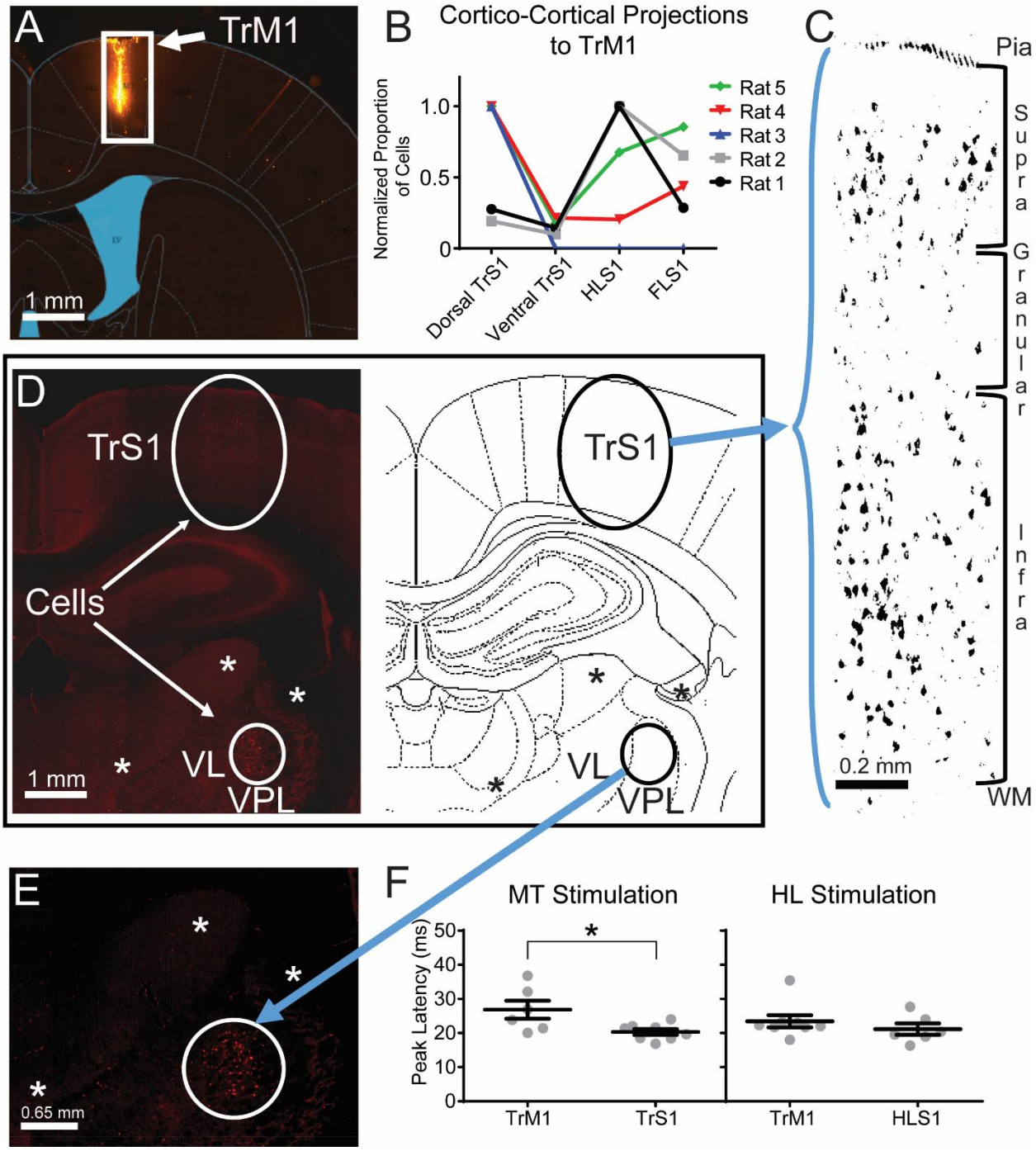

Figure 2. 7 Cortico-cortical and thalamo-cortical projections to trunk M1. A) Coronal brain slice with a superimposed rat brain atlas image (Paxinos and Watson 2007). The injection site (-0.5 mm RC, 1.25 mm ML, 1.65 mm DV, relative to bregma) was limited to TrM1. Scale bar: 1 mm. B) Proportion of cells, normalized to the maximum number of cells across all cortical regions sampled within an animal, in the different primary sensory cortices (dorsal trunk S1, ventral trunk S1, hindlimb S1 and forelimb S1; for coordinates see Materials and Methods). Most TrM1 projecting cells are located in TrS1 and HLS1. (Rat

number: raw number of cells in dorsal TrS1, ventral TrS1, HLS1, and FLS1; Rat 1: 229, 120, 830, 237; Rat 2: 62, 32, 323, 211; Rat 3: 257, 0, 0, 0; Rat 4: 1886, 404, 384, 826; Rat 5: 1344, 236, 908, 1149.) C) Black and white image of the labelled cortical cells in a coronal view of TrS1. Most of the neurons are located in the supra and infragranular layers. Scale bar: 0.2 mm. D) Image of the labelled cortical and thalamic cells in a coronal view with the corresponding modified rat brain atlas. Thalamic neurons are located in the VPL of the thalamus as the thalamic nuclei borders can be seen in both the left image and in the right atlas. The "*" indicates corresponding structures to help the viewer localizing the different thalamic nuclei. Scale bar: 1 mm. E) Zoomed in image of D to visualize the labeled cells in the VPL of the thalamus. The contrast has been increased in order to specifically focus on the presence of the labeled cells. The "*" indicates the same locations as in D to aid the viewer in locating the cells. Scale bar: 0.65 mm F) Left: peak latency of the high intensity mid trunk stimulation in TrM1 (N = 6) and TrS1 (N = 8). Right: peak latency of the high intensity hindlimb stimulation in TrM1 (N = 8) and HLS1 (N = 6).

Postural control is predominately supported by hindlimb somatosensory and lower trunk motor cortices.

To investigate the importance of sensorimotor integration between trunk and hindlimb in postural control, animals were subjected to unexpected tilts in the lateral plane during a tilt task (83), while single units were recorded from the following S1 and M1 cortices: FLS1 (n = 68), HLS1 (n = 39), TrS1 (n = 237), HLM1 (n = 124), and TrM1 (n = 325; Figure 2.8A-B). Three measures from the neuronal data were compared: responsiveness (i.e., proportion of neurons responding), magnitude of the single neuron response, and mutual information carried by the response regarding the severity of the tilt (Figure 2.8C-H). First, the proportion of responsive cells was compared between S1 regions (FLS1: 57%, TrS1: 32%, HLS1: 82%). TrS1 was less responsive than HLS1 ($\chi 2$ [1, N = 276] = 35.84, $p < 0.0001$) or FLS1 ($\chi 2$ [1, N = 305] = 14.92, $p < 0.001$), and HLS1 cells were more likely to respond than FLS1 ($\chi 2$ [1, N = 107] = 6.77, $p < 0.01$; Figure 2.8C). Moreover, the magnitude of the TrS1 response (1.87+/- 0.19 spikes per second) was smaller than that of HLS1 (3.32 +/- 0.36 spikes per second) or FLS1 cells (2.94 +/- 0.32 spikes per second) during the tilt task (One-way ANOVA, F [2, 145] = 8.63, $p < 0.001$, Tukey's post-hoc test: HLS1 vs TrS1 [$p < 0.001$], FLS1 vs TrS1 [$p < 0.05$]; Figure 2.8D). Lastly, mutual information was compared between S1 regions. The median mutual information carried by TrS1 (0.04, [0.03] bits) was significantly

less than the median mutual information carried by FLS1 (0.05 [0.06] bits) or HLS1 (0.06 [0.07] bits) during the tilt task (Kruskal-Wallis test, H [2] = 21.73, $p < 0.0001$, Dunn's post-hoc test: HLS1 vs TrS1 [$p < 0.001$], FLS1 vs TrS1 [$p < 0.01$]; Figure 2.8E). Thus, TrS1 conveyed less mutual information and was less discriminative of the type of tilt than FLS1 or HLS1. Importantly, after dividing TrS1 into LT, MT, and UT (see Materials and Methods), there were no differences between these trunk subregions in responsiveness (LTS1: 50%, MTS1: 38%, UTS1: 28%; $\chi 2$ [2, N = 237] = 5.64, $p = 0.06$). The magnitude of response significantly differed between these TrS1 subregions (LTS1: 2.25 [1.93], MTS1: 0.88 [1.23], UTS1: 1.59 [1.59]; Kruskal-Wallis test, H [3] = 6.67, $p < 0.05$); however, Dunn's post-hoc test did not reveal any significant pairwise comparisons. Additionally, there were no differences in mutual information between subregions (LTS1: 0.04 +/- 0.004, MTS1: 0.06 +/- 0.01, UTS1: 0.06 +/- 0.01; One-way ANOVA, F [2, 234] = 0.43, $p = 0.65$; Figure 2.8C-E), suggesting that the entire TrS1 is equally engaged in this task.

On the other hand, TrM1 neurons were equally likely to respond to the task compared to HLM1 neurons (HLM1: 63%, TrM1: 72%; Fisher's exact test, N = 449, $p = 0.07$; Figure 2.8F), though neither the magnitude of the response (HLM1: 3.42 +/- 0.30 spikes per second, TrM1: 4.05 +/- 0.23 spikes per second; Independent Samples t-test, t [311] = 1.46, $p = 0.14$; Figure 2.8G), nor their mutual information (HLM1: 0.07 [0.08] bits, TrM1: 0.06 [0.08]; Mann-Whitney test, U = 19112, $p = 0.40$; Figure 2.8H) differed from HLM1. Interestingly, when examining the responses from different subregions within TrM1, LTM1 was more involved than UTM1. In fact, even though neurons in LTM1 had a similar proportion of cells responding to the tilts compared to UTM1 (LTM1: 76%, UTM1: 69%; $\chi 2$ [1, N = 325] = 2.32, $p = 0.12$; Figure 2.8F), the magnitude of the response of LTM1 neurons was greater than that of UTM1 neurons (LTM1: 4.57 +/- 0.35, UTM1: 3.46 +/- 0.27; Independent Samples t-test, t [233] = 2.49, $p < 0.05$; Figure 2.8G). This

resulted in more information about the severity of the tilt being encoded by LTM1 compared to UTM1 (LTM1:0.07 [0.09] bits, UTM1: 0.06 [0.06] bits; Mann-Whitney test, $U = 11063$, $p < 0.05$; Figure 2.8H). These data suggest that LTM1 may be specialized for postural control.

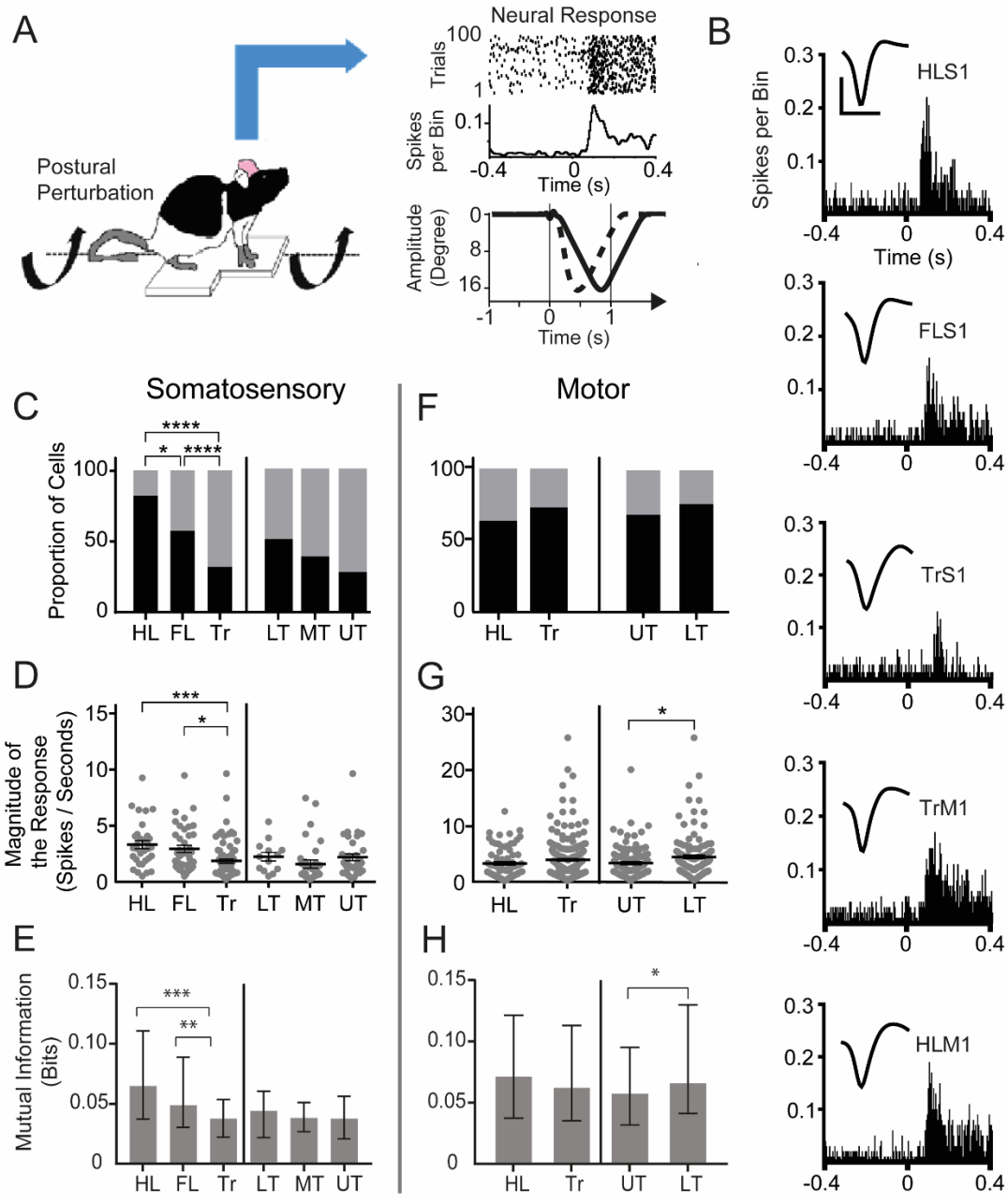

Figure 2.8 Hindlimb S1 and lower trunk M1 combine to carry the most information about postural control. A) Methodological diagram of the postural control task. The animal experienced unexpected tilts in the lateral plane while single neurons in different sensory and motor cortices were recorded (upper right panel). The bottom right panel shows the tilt profile for the fast (dotted line) and the slow (unbroken line)

tilt events, applicable for both directions (left and right). B) Example PSTHs showing a neuron response to the unexpected tilt for each recorded cortical area in the sensory and motor cortices. The waveform scale on top: y-axis: 0.05 mV, x-axis: 0.6 ms. C) Responsiveness of different sensory cortices. Data presented as cortical area: (number of responsive cells, number of non-responsive cells, % of responsive cells). HLS1: (32, 7, 82%), FLS1: (39, 29, 57%), TrS1: (80, 157, 34%), LT: (13, 13, 50%), MT: (31, 51, 38%), UT: (36, 93, 28%). D) Magnitude of the response (for responsive cells only) in different sensory cortices. E) Mutual information in different sensory cortices (represented as median +/- interquartile range for all cells [responsive and non-responsive]). F) Responsiveness of different motor cortices. Data presented as: cortical area (number of responsive cells, number of non-responsive cells, % of responsive cells). HLM1 (78, 46, 63%), TrM1 (235, 90, 72%), LTM1 (111, 51, 76%), UTM1 (124, 39, 69%). G) Magnitude of the response (for responsive cells only) in different motor cortices. H) Mutual information in different motor cortices (represented as median+/- inter quartile range for all cells [responsive and non-responsive]).

Discussion

Together, these data present an extensive view describing how cortical organization is relevant to function by demonstrating the preferential interplay between trunk and hindlimb (Figure 9). Summarizing, TrS1 and TrM1 are larger than previously reported and there is relevant somatotopy within both. In addition, TrS1 receives input from other body regions, especially the hindlimbs, and TrM1 largely coactivates trunk muscles with muscles from other body regions, especially the hindlimbs. Regarding sensorimotor integration, somatosensory information from the hindlimbs is more likely to be integrated within TrM1 than that from forelimbs or even trunk. The functional role of this integration of hindlimb somatosensory information within TrM1 for postural control was demonstrated by the relative difference in the mutual information carried by hindlimb and trunk sensory and motor cortices to tilts in the lateral plane recorded from awake animals. On the sensory side, HLS1 and FLS1 are more involved than TrS1 during postural perturbations. While on the motor side, HLM1 and TrM1 are equally involved, with LTM1 more involved than UTM1. This has important implications for recovery of function after neurological injury or disease (11, 83, 84) and is discussed below.

Methodological considerations

Choices made in our experimental design impacted data analysis. First, for sensory maps, we chose to record from as many single units as possible, identifying the extent of each cell's receptive field as our recording electrode was passed through the entire depth of S1. Therefore, it was not possible to sample the entire TrS1 within a single animal due to time constraints. Similarly, for TrM1, we chose to sample from as many muscles as possible, adding to the length of the surgery and limiting our ability to sample the entire TrM1 within every animal. Moreover, here we show that, unlike the whisker, forelimb, and hindlimb sensory systems that tend to have differences in RF size across layers (49), the RF size of neurons in TrS1 was similar across layers, within the same RF center. However, the role of urethane anesthesia in this assessment cannot be ruled out (85) Furthermore, within S1, the responses to both low and high intensity stimuli are likely to be a combination of tactile and proprioceptive information, with the low intensity stimulation predominately eliciting tactile information and the high intensity stimulation adding additional proprioceptive information. In comparison to S1, low intensity stimuli did not elicit responses within M1; however, high intensity stimuli induced muscle twitches. Thus, in M1, a greater proportion of responses to high intensity stimuli were likely proprioceptive than tactile. The tracing study suggests that somatosensory information, a mix of tactile and proprioceptive information, reaches TrM1 from S1 and thalamus. The latency studies suggest that the predominate response in TrM1 to mid trunk stimulation arrives from the somatosensory cortex. Alternatively, the predominate response in TrM1 that is elicited by hindlimb stimulation likely arrives from the VPL of the thalamus. The VPL origin of this response, which predominately carries proprioceptive information, further supports that the response in TrM1 to high intensity stimulation of the hindlimbs carries more proprioceptive information than the low intensity stimulation, although more work would need to be done to confirm this.

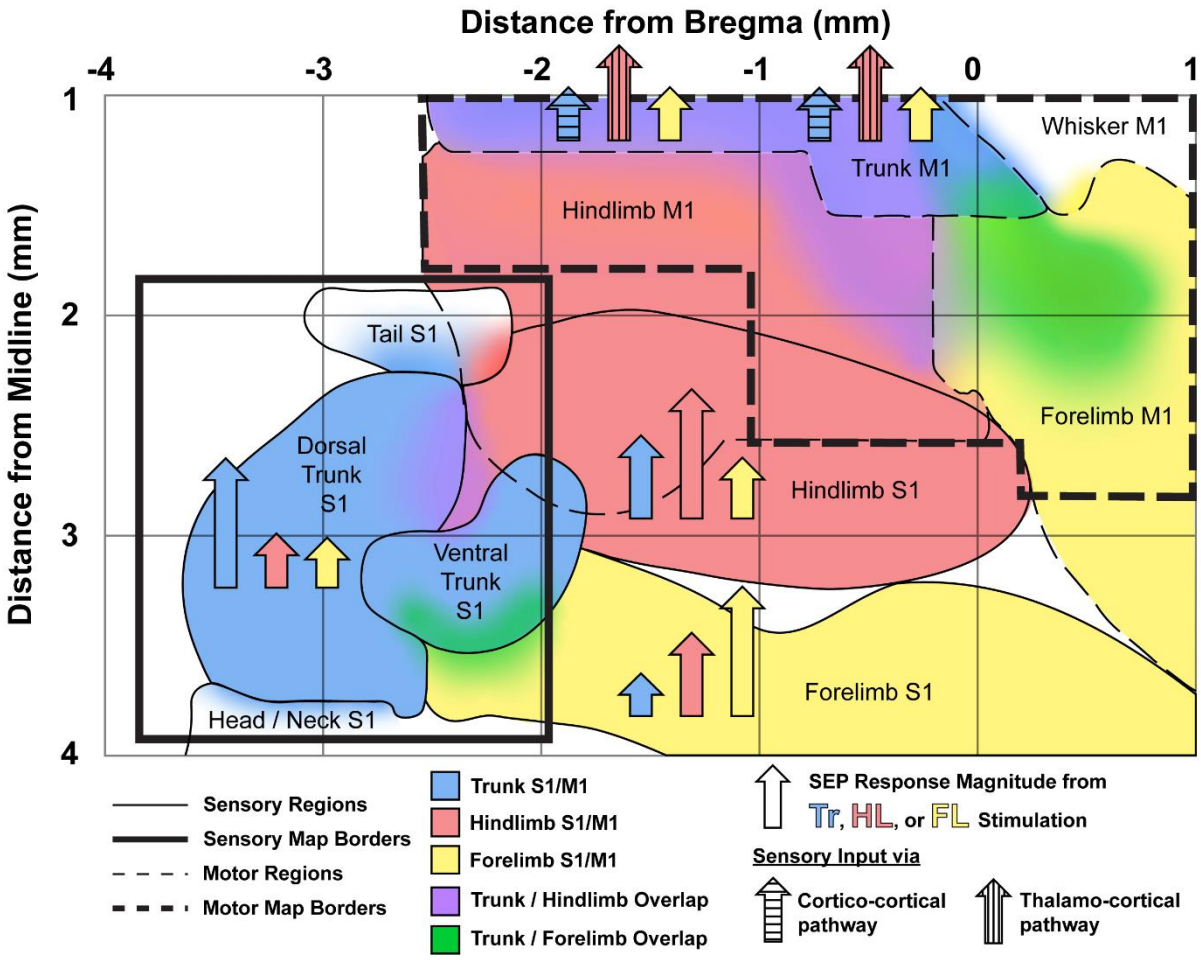

Figure 2.9 Summary of somatosensory overlap, motor coactivations and sensorimotor integration. Solid border lines indicate sensory regions while dashed border lines indicate motor regions. Bolded lines indicate the areas of S1 and M1 that were mapped in the current study. All other regions outside of these areas were adapted from (86) and (57, 87). Corresponding S1/M1 regions (e.g., trunk S1 / trunk M1) are represented with the same colors, while overlapping S1 regions or coactivating M1 regions are represented by the combined colors of the neighboring regions. Arrow height represents the relative magnitude of SEP responses within each cortical region from 5.0 mA stimulation of the trunk (blue), hindlimb (red), and forelimb (yellow). Horizontal (cortico-cortical) and vertical (thalamo-cortical) stripe patterns within each stimulation type's arrow indicates the predominate pathway for that type of sensory information to reach TrM1.

Oppositional gradient in overlap across thoracic dermatomes from DRG to trunk S1

Overlap of somatosensory information from the trunk varies along the entire neural axis. At the spinal level, overlap between thoracic dermatomes is graded such that caudal DRGs (T10-T13) have less overlap than rostral DRGs (T1-T5). At the same time, representation of these

dermatomes in S1 have the opposite gradient regarding overlap. The RF size of TrS1 neurons increased along the mediolateral axis of cortex, such that the lower thoracic TrS1 neurons had a greater RF size compared to the upper thoracic TrS1 neurons. This change in RF size across TrS1 has also been shown in the ventral trunk representation (86). Taken together, for a given stimulation to lower trunk dermatomes, the limited overlap results in fewer DRGs conveying somatosensory information to the cortex where S1 neurons with larger receptive fields amplify the signal. In contrast, for upper trunk dermatomes, the greater overlap across DRGs amplifies information to the cortex where neurons have smaller receptive fields. Therefore, the lack of overlap at the spinal level is compensated for by the greater overlap at the cortical layer and vice versa. The functional implication of this is that dorsal rhizotomy of a caudal DRG would result in a more complete deafferentation than a dorsal rhizotomy of a rostral DRG. It may be that due to the dexterous use of the forelimbs, it is considered more important to preserve upper trunk than lower trunk somatosensory information.

Trunk sensorimotor integration supports a range of functions.

The present data suggest that trunk muscles serve as a biomechanical link between the forelimbs and hindlimbs even in the absences of a neonatal spinal cord transection (20). Moreover, this linkage combines somatosensory information across the limbs and trunk, especially the hindlimbs. In the intact adult, our data show extensive overlap of trunk somatosensory signals within FLS1 and HLS1, especially in response to high intensity stimuli, thereby suggesting that HLS1 is modulated by the location and movement of trunk in space, which could be used to guide the lower limbs during locomotion (41). At the same time, somatosensory information from hindlimb and forelimb overlap within TrS1, which confirms the importance of integrating information from the limbs with trunk somatosensory processing. Within M1, trunk muscles are more likely to

coactivate with hindlimb than trunk muscles or forelimb muscles alone. Furthermore, approximately half of the animals had coactivation of forelimb and hindlimb muscles without concomitant activation of trunk muscles (data not shown). The area was located within the synergistic trunk region. This coactivation of forelimb and hindlimb was also found in other species across phylogenic scales, such as the mouse (88), tree squirrel (89), tree shrew (31), prosimian Galagos (90), and macaque monkey (91). These synchronous forelimb-hindlimb coactivations (32) are thought to be involved in a range of movement types associated with locomotion (e.g. galloping) (92). The work presented here extends this understanding by highlighting the greater integration between trunk and hindlimb than trunk and forelimb.

Classical studies showed that sensory information in M1 was mainly homotopic. For example, neurons in whisker M1, FLM1, and HLM1 received somatosensory input from the same body part that induced movement when activated with ICMS (93, 94). However, our data suggest that the TrM1 is unique in that it receives somatosensory information from trunk, hindlimbs and forelimbs, and therefore the integration of sensorimotor information within TrM1 is not strictly homotopic. Indeed, while low amplitude somatosensory stimulation of trunk, hindlimb or forelimb did not impact TrM1, high amplitude stimulation of HL produced a greater response in TrM1 than somatosensory stimulation of either trunk or forelimb. As many studies have demonstrated that somatosensory feedback to the motor cortex is critical during locomotion and recovery of function after spinal cord injury (11, 41, 84, 95–97), understanding how the post-injury sensorimotor integration differs from the integration shown here will be important for interpreting these injury studies.

Combined, this extensive sensory overlap, muscle coactivations, and heterotopic sensory integration between the trunk and the limbs supports communication between trunk sensory and

motor cortices within the broader sensorimotor cortex to achieve optimal behavior. For example, it has been previously shown that the lower thoracic trunk muscles play an important role in sexual posturing and lordosis as observed in the female rat (98). Our results show that the caudal portion of TrM1 that controls these lower thoracic muscles overlaps with the genital motor cortex (61). The extensive integration of hindlimb somatosensory information within TrM1 could be useful for sexual posturing.

Role of trunk sensorimotor cortex in postural control

The integration of HL somatosensory input across the extent of TrM1combined with the broad hindlimb-trunk coactivation zones in M1 support the role of thoracic trunk muscles synergistically acting with the hindlimbs to aid in postural control during locomotion (83, 99, 100). This coactivation likely happens through the cortico-reticulo-spinal pathway, not directly via the corticospinal pathway. In the awake animal, the vestibular system, which was not studied here, produces a fast reaction to control posture and recover balance (101). Notably, it sends direct motor inputs to the spinal cord to correct the balance. This vestibular information also ascends through the thalamus to the motor cortex to produce a coordinated neuronal response across the body musculature during the tilt (102, 103) . Interestingly, the motor cortex participates in some, but not all, aspects of postural control (102, 104), producing different responses depending on the task despite similar muscle output (105). Given the critical role of M1 for functional improvement after SCI (11), improving our understanding of how information about postural adjustments is integrated in M1 will aid in understanding how M1 contributes to recovery of function (see next section).

For example, in S1, previous studies showed that tactile and proprioceptive somatosensory feedback from the limbs are involved in postural control (106, 107). This is consistent with our data here showing that for both HLS1 and FLS1, more cells respond, and the magnitude of their response was greater compared to that of TrS1, such that FLS1 and HLS1 convey more information about the tilt than TrS1. But, within TrS1, the different areas of trunk (LT, MT, and UT) are equally responsive, conveying similar amounts of information about tilt. We can deduce that the response in TrS1 is predominately mediated by trunk proprioceptive information because the trunk is not in contact with the platform. Furthermore, because this study showed that a significant proportion of neurons in TrS1 responded to HL somatosensory information during the tilt task, the somatosensory information reaching TrS1 comes from the position of both the trunk and hindlimb in space, allowing significant integration of this proprioceptive information, along with tactile and vestibular, to allow the animal to maintain its balance.

In the motor cortex, a similar proportion of HLM1 and TrM1 cells were likely to respond with a similar magnitude of response, conveying a similar amount of information about the tilt, suggesting that these two regions are equally active in controlling muscles when the animal is maintaining its balance in response to the tilt. Interestingly, within TrM1, the region that controls lower thoracic muscles (LTM1) was more engaged in the task compared to the regions that control upper thoracic musculature (UTM1). Given that more of the weight of the animal is over the hindlimbs, these data suggest that extensive coactivation across hindlimb and lower thoracic muscles is used for postural control.

Hindlimb somatosensory feedback to the trunk motor cortex: Pathophysiological implications

Pathologies resulting in postural deficits in humans are associated with changes in cortical organization (108), motor planning (109), and recruitment of trunk musculature (110) The integration of hindlimb proprioceptive information in TrM1 cortex identified here provides an opportunity for a new understanding of how therapy after mid thoracic spinal cord injury improves function. For a complete spinal transection, we previously showed that therapy produced sprouting of descending corticospinal axons from HLM1 cortex into thoracic spinal cord that could be used to control trunk musculature. This produced a larger representation of the TrM1 cortex whose extent was correlated to recovery of function and overlapped with expansion of the FLS1, creating a new circuit of forelimb somatosensory and trunk motor integration (34). If this reorganized cortex was lesioned, functional gains were lost (11). Our new understanding of the extensive sensorimotor integration in intact animals presented here makes it clearer that the sensorimotor integration in animals that receive therapy after SCI is not a novel sensorimotor integration, but a necessary restoration of a system that operates on strong sensorimotor organization.

While the role of limb proprioception after more severe injuries is less understood, our group previously showed that after complete spinal transection, when somatosensory input from the hindlimb is not possible, epidural stimulation induces somatosensory feedback from the trunk into the deafferented hindlimb sensorimotor cortex that carries information about the animal's behavior (84). This study now makes clear that this somatosensory feedback is likely to be trunk proprioceptive information that provides input to hindlimb S1 and M1 cortices in intact animals. Therefore, therapy to improve function could take advantage of this pre-existing sensorimotor integration to restore function.

This role of sensorimotor integration extends to models of partial spinal lesion. Proprioceptive information has been suggested to be critical for recovery of function after mid thoracic spinal cord injury (111, 112). For example, epidural stimulation of spinal circuitry below the level of the lesion restored volitional locomotion in rats (18, 84, 113–115), non-human primates (116), and humans (114, 117, 118). Stimulation is conducted at lateral sites, over or near the DRGs and it has been suggested that this epidural stimulation activates proprioceptive afferents (114, 119).

Therefore, the work outlined in this paper supports the idea that facilitation of sensorimotor integration across broad regions of the cortex is key to improving treatment outcomes after neurological damage or disease (120) and we now understand that this sensorimotor integration is the operational model of the trunk cortex in intact animals. Moving forward, our understanding of the sensorimotor integration in the intact system could be used to tailor rehabilitative strategies to optimize sensorimotor integration or recovery of function.

Materials and Methods

Subjects

One hundred and six adult, female Sprague Dawley rats (225-250 g; Envigo) were maintained on a 12/12-hour light/dark cycle with ad libitum food and water. Fifteen animals were used to map the representation of each thoracic dermatome at the spinal level, 40 animals were used to map the internal representation of trunk S1, 21 animals were used to examine the movement representation of trunk M1, 14 animals were used to examine the integration of somatosensory information within

and between sensory and motor cortices, five animals were used for anatomical tracing, and 11 animals were used to study sensorimotor integration relevant for postural control.

For all anesthetized experiments, animals were secured on a stereotaxic frame (Neurostar, Sindelfingen, Germany) and body temperature was maintained at 37°C using a temperature-controlled heating pad (FHC Inc., Bowdoin, ME). In addition, heart rate, SpO2, and anesthetic state (whisking/toe pinch reflex/corneal reflex) were constantly monitored. All experimental procedures were approved by UC Davis or Drexel University IACUCs and followed NIH guidelines.

Body grid system to map receptive fields.

To identify receptive fields (RFs) consistently across animals, a standardized grid was outlined on each animal's dorsal trunk (121). The dorsal trunk was shaved and a grid of 128 equally spaced squares was drawn indelibly. The grid spanned from the skull's base, parallel to the intertragic notch of the ear, to the tail's base (16 grids in the rostrocaudal orientation), and from the dorsal trunk's midline to its lateral aspect at the base of the limbs on each side of the animal (8 grids in the mediolateral orientation; Figure 2.1A). Each grid square was approximately 1 cm^2 and was consistent across animals due to the similarity of both size and weight. In addition, a photograph of the animal with the drawn grid was taken to assist in defining RFs during S1 mapping experiments (Supplementary Figure 2.1).

Mapping thoracic dermatomes

Animals were anesthetized with urethane (1.5 g/kg, IP) and maintained at Stage III-3 anesthesia (122). An incision was made along the midline of the trunk and axial musculature was separated from the vertebral column to expose the thoracic vertebrae. The spinous processes, lamina, and

transverse processes of the selected thoracic vertebrae were carefully removed to access the dorsal root ganglion (DRG) on one side of the body. The animal's spinal column was secured in place by attaching locking forceps to the transverse process rostral to the T1 vertebrae and caudal to the T13 vertebrae. A single high-impedance (4-10 MΩ) tungsten microelectrode (FHC Inc., Bowdoin, ME) was attached to the stereotaxic manipulator and a ground wire was placed in contact with the body cavity. The electrode was positioned over a single DRG and lowered slowly until a single cell was identified. The neuronal signal (digitized at 40 kHz) was amplified (20000x), band pass filtered (150 - 8000 Hz; Plexon Inc., Dallas, TX) and monitored with an oscilloscope and through audio speakers. The cell's receptive field was then identified using light tactile stimulation (49, 57). First, the dorsal cutaneous surface of the animal was tapped with a cotton brush, both within and outside the body grid to gain insight of the neuron's RF. If the RF was located within the trunk body grid, it was then mapped with a 0.25 body grid square resolution by applying light tactile stimulation to the cutaneous surface using a wooden probe (4 mm diameter). If the RF was found outside the grid, it was not included in the mapping of thoracic dermatomes. When mapping of that neuron's RF was complete, the electrode was lowered at least 50 μm dorsoventral (DV) before another cell was identified to ensure that the same cell was not mapped twice. This process was repeated until the electrode punctured through the entire DRG. Each DRG was sampled at least three times, so as to cover the DRG's rostrocaudal extent (Wessels et al. 1994). A trunk dermatome was defined as the union of all trunk grid locations on the skin that were found to be responsive to at least one cell in the respective DRG. The width of a dermatome was defined as the number of trunk grid locations within its rostrocaudal extent. Center position of a dermatome was defined as the center of this rostrocaudal extent. Dermatomal overlap was defined between two adjacent

dermatomes as the distance between the rostral extent of the more caudal dermatome and the caudal extent of the more rostral dermatome.

Mapping trunk sensory cortex

Animals were anesthetized with urethane (1.5 g/kg, IP) and maintained at Stage III-3 anesthesia (122). A craniotomy was performed on the right hemisphere to expose hindlimb S1 (HLS1), trunk S1 (TrS1), and parts of forelimb S1 (FLS1). Based on a pilot study (n = 3), 80 predefined cortical locations relative to Bregma were chosen. They extended from -2.0 mm to -3.8 mm rostrocaudal (RC) with a resolution of 0.2 mm, and from 2.0 mm to 3.75 mm mediolateral (ML) with a resolution of 0.25 mm between locations. At each location, the electrode was slowly lowered into the brain, up to a depth of -2.0 mm DV, while light tactile stimulation was applied to the cutaneous surface of the trunk. If a neuron was responsive, the neuron's receptive field was categorized into either trunk, ventral trunk, head/face, forelimb, hindlimb, tail, or a combination of body parts. If the RF included the trunk, the RF was further analyzed relative to the body grid with a 1.0 body grid square resolution and calculated separately for the supragranular, granular, and infragranular layers. A somatotopic map of the trunk and surrounding somatosensory cortices was constructed. At each cortical location, the proportion of cells that responded to each body part was investigated. A body part was assigned to a cortical location if at least 25% of the neurons in that location were responsive to that body part. If there were multiple body parts that meet the criterion, the body part with the highest proportion of responsive neurons was assigned (Figure 2.2B).

To locate the cortical representation of the thoracic dermatomes within TrS1, all cells that had RF centers within trunk were used. For a given cortical location, the rostrocaudal positions of the RF centers on the body grid from all cells of that location were averaged. The dermatome with the

closest center position to the average cortical RF position defined the corresponding dermatome of that cortical location. Cortical locations that represented the same dermatome were grouped to generate the representation of thoracic dermatomes in the cortex. All RFs belonging to the same dermatome representation were used to calculate the amount of overlap between the neighboring dermatome representations. To analyze the size and extent of trunk RFs, only neurons that were completely contained within the borders of the trunk grid were used. Average RF size was calculated by averaging the number of responsive body grid squares for all cells.

Local field potential recording in response to peripheral electrical stimulation

Electrical stimulation was chosen to compare the S1 and M1 responses to stimulation across the hindlimb, forelimb, and trunk. First, bipolar electrodes placed in the hairy skin of the hindlimb, forelimb, and trunk, were used to activate afferents between the two poles of the electrode. Second, to ensure fair comparisons across stimulus locations, the response of HLS1, FLS1 and TrS1 to stimulation of their RF centers was titrated to produce similar magnitudes of response across the three sensory cortices. This would be difficult to accomplish with other stimulation modalities. Although mixing of tactile and proprioceptive afferent activation cannot be ruled out, a low intensity stimulus (0.5 mA) was used to predominantly activate tactile receptors between the two poles of the electrode, while a high intensity stimulus (5.0 mA) was used to elicit muscle twitches and slight movements that further activate proprioceptive afferents and nociceptive afferents (123, 124). This higher amplitude stimulus was necessary to identify sensory responses in trunk M1. Specifically, bipolar stimulating electrodes were inserted subcutaneously into the dorsal hairy skin at four locations: hindlimb (HL), forelimb (FL), T4-T5 dermatome of the upper trunk (UT), and T9 dermatome of the mid trunk (MT; approximately the midpoint of the trunk between the FL and HL), contralateral to the recording location (Figure 2.3A, Supplementary Figure 2). For the trunk

locations, the bipolar electrodes were placed approximately 5 mm apart from each other and approximately 20 mm from the midline of the animal (approximately halfway between the midline and the grid line border of the ventral trunk). Electrical stimulation, consisting of 100 pulses (1 ms duration) was delivered every 2 s at varying stimulation intensities (see Results).

To record local field potentials, animals were anesthetized with urethane (1.5 g/kg, IP). A craniotomy was performed on the right hemisphere to expose the sensory and motor cortices. A 32-channel, four shank recording electrode array (A4x8-5mm-200-400-177; NeuroNexus, Ann Arbor, MI) was positioned over the fixed locations either spanning M1 (-3.2 to 1.2 mm RC, 1.25 mm ML), TrS1 (-3.4 mm to -2.2 mm RC, 3 mm ML), HLS1 (-1 mm to -2.2 mm RC, 2.5 mm ML), or FLS1 (0.5 mm to -0.7 mm RC, 3.5 mm ML). The array was lowered perpendicularly into the cortex to a depth of 1.8 mm where it was fixed in place.

The extracellular local field potential (LFP) was acquired simultaneously from all 32 channels (Intan Technologies, Los Angeles, CA), digitized at 20 kHz, amplified (192x) and band pass filtered (0.1 Hz – 7.5 kHz). To ensure fair comparisons between the stimulation responses of different locations on the body, the responses of each region to stimulation of their RF centers were compared (RF center identified using light tactile stimulation, see above). A high pass filter of 5 Hz was used to mitigate slow wave activity that developed under urethane anesthesia (85, 125) in the cortical LFP. A window of 1 s centered on the stimulation time was extracted from the high pass filtered LFP data (5 Hz, Butterworth order 2, zero-lag) of each recording site. The data in that window was then averaged across stimulation trials to obtain the somatosensory evoked potential (SEP). A representative channel from the supragranular (400 µm DV), granular (800 µm DV), and infragranular (1200 µm DV) cortex was selected for further analysis (Supplemental Figure 3). For each layer, the SEP was considered responsive if the amplitude exceeded the mean

background activity by three standard deviations. SEP amplitude was evaluated as the absolute value of the first negative peak of the SEP, normalized to the background activity. Peak latency of the SEPs was calculated as the time of the SEP peak amplitude post stimulus. Only responsive SEPs with a latency less than or equal to 50 ms were considered for further analysis to capture the short latency response. In addition, the LFP from each electrode was filtered (300-8000 Hz) and single neurons were discriminated using PCA and visual inspection using Offline Sorter (Plexon Inc., Dallas, TX).

Single neuron spike times were used to construct peri-stimulus time histograms (PSTH) to determine the magnitude of the response of a neuron to the peripheral electric stimulation using previously published methods(11, 76, 126–128). The PSTH consisted of spike counts within 5 ms bins averaged across 100 trials within a window of 100 ms from the time of stimulus (Figure 3E). A neuron was considered responsive if at least two consecutive bins in the PSTH exceeded three standard deviations above the background window. Response magnitude and the proportion of responsive neurons were quantified from neurons recorded across all layers in S1.

Mapping trunk motor cortex

The representation of trunk primary motor cortex (TrM1) was examined by analyzing evoked movement and EMG activity in response to stimulation of infragranular neurons in M1 using previously published methods (34). Animals were anesthetized with ketamine (63 mg/kg, IP), xylazine (6 mg/kg, IP) and acepromazine (0.05 mg/kg, IP) and administered dexamethasone (5 mg/kg, IM) to control blood pressure and brain swelling. Supplemental doses of ketamine (20 mg/kg, IP) were administered, when necessary, to maintain the animal at light Stage III-2 anesthesia throughout the entire mapping procedure (122, 129). Animals were placed in a

stereotaxic frame in a prone position such that the limbs could hang freely. Eight bipolar intramuscular electromyogram (EMG) electrodes (stainless steel, 7 strands, AM-Systems Inc., Sequim, WA) were implanted on dorsal (longissimus) and ventral (external oblique) trunk muscles at the upper thoracic (T4-T5), mid thoracic (T9-T10) and lower thoracic (T12-T13) levels. One EMG electrode was implanted in each of the contralateral shoulder/trunk (spinous trapezius), contralateral forelimb (forelimb bicep), contralateral hindlimb hip (gluteus maximus) and hindlimb ankle (tibialis anterior; Figure 4A). Based on previous studies on rats (24, 34, 130), a craniotomy exposed the medial post bregma area and the caudal forelimb area (1 mm to –3.5 mm RC, 1 mm to 3 mm ML). Similar to the somatosensory mapping procedure, 88 predefined cortical locations were chosen spanning the craniotomy. The medial portion (<1 mm) could not be mapped reliably due to methodological constraints related to the high density of blood vessels in this region that limits access to the cortex. Previously Donoghue and Wise 1982, (36) reported that responses could not be evoked from these medial regions. This region, often referred to as medial agranular cortex or M2, is cytoarchitecturally different from M1.

A low impedance glass insulated tungsten electrode (100-500 kΩ; FHC Inc., Bowdoin, ME) attached to a stereotaxic manipulator was inserted into one of the 88 predefined cortical locations. In order to assess microstimulation waveform quality, the voltage drop across a 10 kΩ resistor interposed in series between animal ground and the isolated current pulse stimulator (Model 2100, A-M systems, Sequim, WA) was monitored with an oscilloscope. At each M1 location, the electrode was lowered to the infragranular layer (1.5 mm DV) and a long train ICMS was applied (25, 131), consisting of 0.2 ms cathodal leading bipolar current pulses (10 to 100 µA) delivered at 333 Hz for 300 ms. This long train was used to evoke muscle synergies (overlapping representations/coactivation of segmental muscle groups) that represent complex movement

repertoires. Pilot experiments with 60 ms stimulus trains showed that stimulus-evoked movement represented short, truncated movements and muscle twitches. while 300 ms pulse trains often elicited a variety of movements ranging from simple (muscle contraction across a single joint) to more complex movements that represented the coactivation of muscles across different segmental levels of trunk / across multiple joints consistent with other studies (9, 26–29, 31, 32). The stimulation current was gradually increased in steps of 10 μA until a reliable movement or EMG response was found.

EMG signals and current stimulus times were sent to a data acquisition system (Intan Technologies, Los Angeles, CA). EMG was sampled at 5 kHz, zero-lag band pass filtered (40-400 Hz) and rectified. An EMG envelope was obtained by further filtering the data (zero-lag Butterworth low pass filter, 20 Hz, 5th order). The EMG envelope was normalized to its peak value to account for changes in EMG response due to electrode placement, impedance mismatch, signal to noise ratio, and muscle size (132). Motor evoked potentials (MEPs) were then obtained by averaging the processed EMG over a time window of 1 s centered on the current stimulus timestamps. If the amplitude of a MEP exceeded the background EMG activity by five standard deviations, it was considered a responsive EMG. The minimum current required for eliciting a movement/EMG response was defined as the threshold current for that cortical location. Once a reliable threshold current was found, the current was increased to 100 μA (suprathreshold), and the movement and EMG responses were recorded. A minimum of five separate stimulations were performed in every cortical location. If no movement or EMG response was evoked with the 100 μA current, the cortical location was determined non- responsive. If there were more than three consecutive non-responsive locations, the closest responsive location was rechecked to identify the limits of motor cortex. A combination of visual observation of movements and reponsive EMG

locations were used to classify cortical locations into movement types (Table 2.1). Recruitment of trunk musculature via stimulation of the TrM1 was examined based on EMG response. Trunk musculature responses were classified into different categories based on the location of responsive trunk EMG along the thoracic level at both threshold and suprathreshold currents (Table 2.2, Figure 2.5A). At threshold, the proportion of responsive EMG was compared across thoracic levels.

The muscle responses (muscle identification and movement type) associated with the stimulation of each cortical location were used to calculate a responsiveness score (12, 34). For each movement type (or trunk musculature type), the proportion of responses in each location was determined and transformed to a score as follows: ranges of 0, 1-33%, 34-66%, and 67-100% received a score of 0, 1, 2, or 3, respectively. For example, if only one animal responded to cortical stimulation at a cortical location out of five animals that were stimulated at that spot, the occurrence rate would be 0.2 or a score of 1. A score of 0 meant that no movement and no EMG response were recorded and a score of 3 meant that the muscle movement (or EMG response) was elicited for 67 -100% of the cortical stimulation. The average responsiveness score for a specific movement type and/or EMG response was calculated by averaging the score across cortical locations. To control for the fact that not every cortical location was sampled equally, a responsiveness score was only included in the analysis if there were at least five penetrations in a given location.

Retrograde tracing

To gain insight into the regions of the brain that project sensory input to TrM1, a tracing study was performed. Results from the ICMS mapping showed that only a small location in the brain exclusively activated trunk musculature and most of TrM1 included coactivation with other body

parts. However, the location of this exclusively trunk area was variable across animals. Although a ICMS study prior to tracer injection could have located this exclusively trunk region in each animal, this would have severely damaged the tissue and made the tracing unreliable. Therefore, the tracer was injected into the most likely location that exclusively activated trunk musculature. Animals were anesthetized with ketamine (63 mg/kg, IP), xylazine (6 mg/kg, IP), and acepromazine (0.05 mg/kg, IP). A craniotomy was made over TrM1 (-0.5 mm RC, 1.25 mm ML, 1.65 mm DV) and 300 nL of 10% fluorescent microbeads (Lumafluor Inc., Naples, FL.; Figure 2.4D, Figure 2.7A) were injected with a Hamilton syringe (tip diameter: 0.1 mm). Three days after the injection, animals were perfused with saline followed by 4% PFA and brains were removed. 50 µm coronal sections were mounted under Permount (Fischer Chemical, Geel, Belgium) on microscope slides. Brain slices were then imaged using a wide field microscope (5x/.012 numerical aperture; ZEISS, Oberkochen, Germany) and cell counting was performed using ImageJ (National Institutes of Health, Bethesda, MD). Images were transformed to an 8-bit grey scale image and thresholding was done to minimize artifacts caused by autofluorescence. Automated cell counting (minimum size: 100 pixels) was conducted in the region of interest (ROI). The different ROIs, corresponding to the different somatosensory cortices were identified based on electrophysiological sensory mapping data (Figure 2.2B). For locations outside of TrS1, ROIs for HLS1 and FLS1 were identified based on (133). Only ipsilateral projections were identified. The location of thalamic nuclei was identified by superimposing our images on to the rat brain atlas.

Postural control task (tilt task)

The tilt task was used to understand sensorimotor integration in the cortex relevant for postural control. Microwire arrays (32 channel each [8*4], 250 µm resolution, Microprobes, Gaithersburg, MD) were implanted bilaterally in the infragranular layer of the cortex, spanning TrS1, HLS1, and

FLS1 on the left hemisphere and TrM1 and on the right hemisphere. For chronic microwire implantation refer to previously published methods (76, 83, 134). Single neuron activity was recorded from the different cortices in response to sudden unexpected postural perturbation in the lateral plane. Four different tilt types were tested, two to the left and two to the right. For each direction, there was a slow speed (max speed: 26.2°/s; duration to final amplitude: 0.9 s) and a fast speed (max speed: 76.5°/s; duration to final amplitude: 0.5 s). The final angle for all tilt types had the same final amplitude of 16.5° (Figure 2.8A). The task was adapted from (83) and engaged the cortex bilaterally. Based on the mapping results, the recording electrodes in M1 were grouped based on the region of the body they most likely activated. Electrodes spanning caudal TrM1 (-1 mm to –2 mm RC, 1.25 mm to 1.5 mm ML; Figure 2.5F) preferentially activated lower thoracic trunk musculature and were defined as lower thoracic trunk primary motor cortex (LTM1). Electrodes rostral to LTM1 (0 mm to -0.75 mm RC, 1.25 mm to 2.0 mm ML) were more likely to control upper thoracic muscles and were labelled upper trunk primary motor cortex (UTM1). Regions lateral to LTM1 (-1 mm to –2 mm RC, 1.75 mm to 2 mm ML) preferentially controlled hindlimb musculature and were defined as hindlimb primary motor cortex (HLM1). Similarly, for each of the electrodes spanning the somatosensory cortex (left hemisphere), the corresponding RF center (i.e., stimulus location that produced the largest SEP amplitude) was identified in response to peripheral electric stimulation (0.5 mA, tactile) of the different body parts (forelimb, hindlimb, upper, mid, and lower trunk). The electrode was then labelled as recording from FLS1, HLS1, UTS1, MTS1 or LTS1 based on the RF center.

Responsiveness in the different cortices was calculated as the proportion of responsive neurons to at least one tilt type. A neuron was considered responsive to a tilt if the neuronal activity in the response window (400 ms from start of tilt) was significantly different from the background and

there were at least five consecutive bins (bin size 5 ms) in the response window that exceed the background activity by two standard deviations. The magnitude of response (spikes per second) was defined as the change in the average neuronal firing rate from the background (average firing rate in response window – average background firing rate). Shannon's mutual information was used to quantify the information about the tilt type provided by the neuronal response of each single neuron within the region (135). If a neuronal response and a tilt type are completely independent from each other, mutual information is 0 bits, and if they are perfectly correlated, the mutual information is defined by the entropy of the stimulus (tilt type) and is 2.0 bits (i.e., $\log_2(4)$, n = 4 tilt types) of information.

Statistical Analysis

Statistical analyses were conducted using GraphPad Prism 9.0.1. Continuous variables with a normal distribution are reported as mean + standard error; variables with a non-normal distribution are reported as median (interquartile range). Differences between two independent groups were assessed using an Independent Samples t-test for normally distributed data, or a Mann-Whitney U test for non-normal data. Differences between three or more independent groups were assessed using analysis of variance (ANOVA) with a Tukey post-hoc test for normally distributed data, or a Kruskal-Wallis test with a Dunn's post-hoc test for non-normal data. Frequencies were compared using Pearson χ 2 or Fisher's exact test. A value of $p < 0.05$ was considered significant and significant group effects were subjected to Tukey's honest significant difference post-hoc test. $p < 0.05$ is denoted by *, $p < 0.01$ by **, $p < 0.001$ by ***, and $p < 0.0001$ by ****.

Acknowledgements

This work was supported by grant R01NS096971 from the National Institutes of Health and grant 1933751 from the National Science Foundation.

Chapter 3: Exercise therapy guides cortical reorganization after spinal contusion injury to enhance control of lower thoracic muscles below the lesion supporting interlimb coordination

Abstract

Postural control is critical for locomotion, including gait changes, obstacle avoidance and navigating rough terrain. A major problem after spinal cord injury is regaining the control of balance to prevent falls and further injury. While the circuits for locomotor patterns reside in the spinal cord, balance control consists of multiple, complex networks that interact at the spinal, brainstem and cortical levels, to maintain posture. After complete SCI, cortical reorganization establishes novel control of trunk musculature that is required for weight-supported stepping. In this study we examined the role of cortical reorganization in the more clinically relevant models of midthoracic contusion injury in the rat and demonstrate that cortical reorganization supports weight-supported stepping and exercise therapy further improves outcome by improving interlimb coordination through control of lower thoracic muscles. This information can be used to improve physical therapy after SCI by considering changes along the entire neural axis.

Introduction

Maintaining postural stability is critical to recovery of unassisted locomotion after spinal cord injury (SCI). Efficient control of posture is equally important for standing and walking (136–138) as it is for providing support of voluntary limb movements (139). The spinal cord contains intrinsic

circuitry needed to respond to external postural perturbations. Spinal circuits are sufficient to generate postural limb responses based on somatosensory inputs from load and position afferents (140) (141, 142). (143). (144) (145) (146, 147). However, supraspinal signals, including the reticulospinal (RS(148–156)), vestibulospinal (VS(157)), rubrospinal (RbS(158)) and corticospinal (CS(105, 142, 159) tracts provide both tonic and phasic excitatory drive. Thus, two closed-loop mechanisms are involved, with sensory inputs contributing to both circuits (160)

Damage to descending and ascending spinal pathways, caused by a spinal cord injury (SCI), results in an impairment of postural control (161). Postural deficits depend on the location and extent of SCI. The behavioral effect of a complete lesion of the spinal cord in the thoracic region has been well studied (162–165). Notably, some control (e.g. brief standing episodes) may remain (166) depending on the animal model and can be improved with training (167–170). While the spinal cord may contain intrinsic circuitry that can generate postural movements, humans and animals with spinal cord injuries fail to maintain lateral stability even after the recovery of spinal postural reflexes (155, 156, 168, 169, 171). Of note, the monosynaptic spinal cord reflexes recover within days of injury in rats whereas polysynaptic reflexes only appear after weeks of recovery (172, 173), suggesting that these circuits rely on supraspinal signals to generate stabilizing corrective responses after injury (174, 175). (147). In fact, our recent work showed that after a complete midthoracic spinal lesions, cortical reorganization of the trunk representation in primary motor cortex (TRM1) was necessary for functional improvement, with descending corticospinal fibers making contact above the level of the lesion to control muscles that span the lesion, stabilizing the trunk and allowing animals that received physical therapy to take weight-supported steps in the open field (11)

However, much less is known about the more clinically relevant contusion injury. Spontaneous recovery of motor control after SCI is limited in both human patients as well as in animal models (176–178). Physical rehabilitation either alone (16, 179–181) or in combination with electrochemical/ pharmacological strategy (2, 117, 182, 183) can potentiate functional recovery further, by means of increased activation of spared neuronal networks that bypass lesion site (13, 184, 185). But most studies utilized specific lesions with the hemi section injury model most widely used to examine therapy mediated functional improvements after incomplete SCI (2–4, 186). While the injury is less variable, the approach is not in line with pathophysiology encountered in SCI patients (5). On the contrary contusion injuries in the rat model are variable, but constitute a clinically relevant model of incomplete SCI (6, 7). Partial lesion studies demonstrate that ventral pathways are critical for postural control with dorsal pathways less important (155, 156, 165). Animal models of contusion injury generally apply loads at the dorsal surface, destroying the dorsal pathways and leaving some ventral pathways intact. Cortical plasticity associated with differential sparing of ventral tracts, their relationship to sponataneous recovery and rehabilitation assisted plasticity is not known. To address this, we studied the effect of moderate treadmill exercise therapy on two models of mid-thoracic contusions – moderate and severe – on cortical reorganization in the rat model. Results show that after contusion SCI, cortical reorganization establishes novel control of trunk musculature. In this study we examined the role of cortical reorganization in the more clinically relevant models of midthoracic contusion injury in the rat and demonstrate that cortical reorganization supports weight-supported stepping and exercise therapy further improves outcome by improving interlimb coordination through control of lower thoracic muscles. This information can be used to improve physical therapy after SCI by considering changes along the entire neural axis.

Results

Moderate exercise improves behavioral recovery.

In the moderately contused animal, moderate treadmill exercise therapy (30-minute per day, 5 days/week for 5 weeks) after moderate midthoracic SCI (mSCI) improves recovery of weight supported stepping in the open field (Figure 1). Animals that received therapy were more likely to consistently take weight-supported steps (BBB>10) and to have good interlimb coordination (BBB>13) [therapy: $F(1,30) = 15$, $p=0.0005$] although there was spontaneous recovery of function regardless of therapy [time: $F(3.5,100) = 203$, $p<.0001$; time*therapy: $F(5,145) = 5.3$, $p = .0002$]. Note that 73% (11/15) of SCI-EX animals had consistent weight support and co-ordination (BBB >13) while 18% (3/17) of the SCI-NX animals improved co-ordination. In fact, exercise therapy accelerates improvement in recovery [week 1: $p=0.230$; week 2 $p=0.008$; week 3, $p= 0.001$; week 4, $p=0.005$; week 5 $p =.048$]. Therefore, as expected, exercise therapy after SCI enhanced the spontaneous recovery of weight supported stepping and interlimb coordination in the open field, in line with previous work (180, 187–189). This was unlikely to be due to difference ins spared white [therapy: $F(1,12)=0.70$, $p=0.420$; distance from epicenter: $F(4,35)=41$, $p<0.000$; interaction: $F(28,243)=0.70$, $p=0.870$] or grey matter in the cord [therapy: $F(1,12)=0.54$, $p=0.48$; distance from epicenter: $F(3.4,30)= 46$, $p<0.000$; interaction: $F(28,244)=0.74$, $p=0.830$]. The spared matter analysis suggests that the improvement in BBB score due to therapy was not related to the spared matter in the spinal cord and therapy did not affect the amount of sparing of the white matter tracts in the spinal cord.

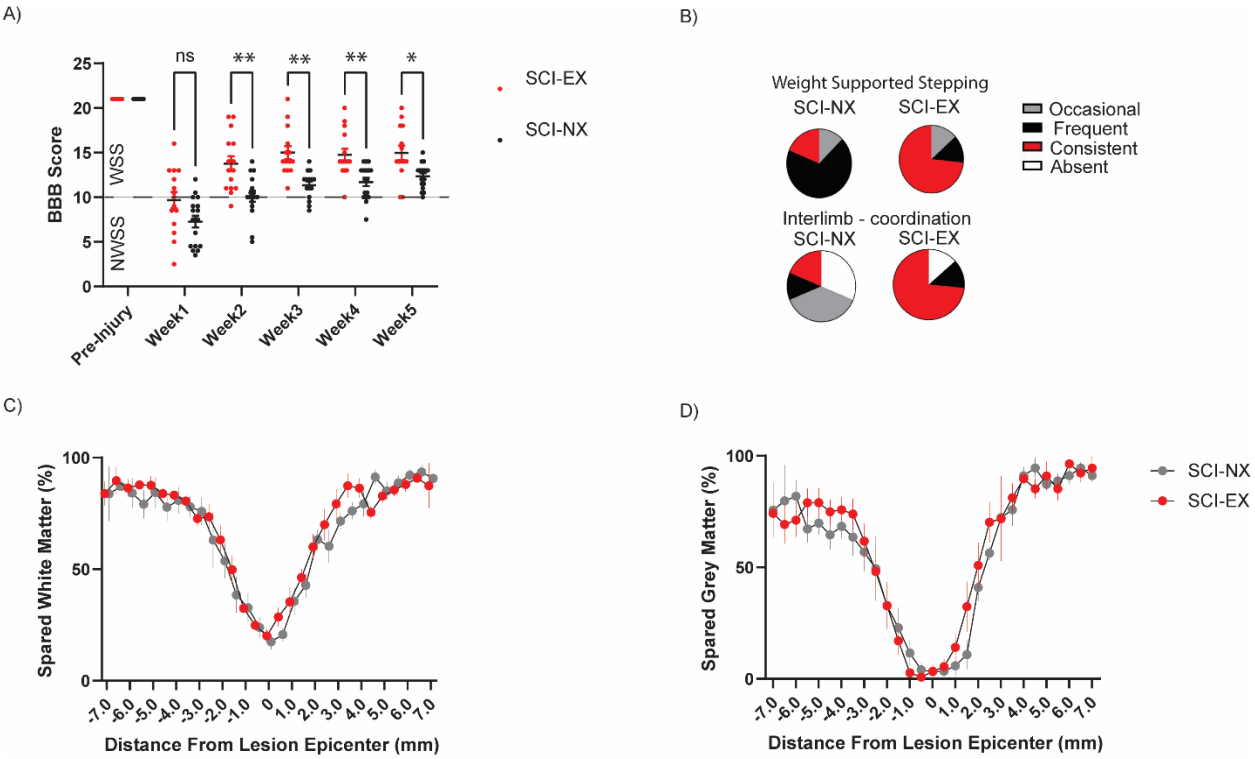

Figure 3. 1 Exercise therapy after SCI improves behavior recovery in open field without differences in in lesions. Left Panel: Effect of moderate SCI and treadmill therapy on behavior. A. Comparison of the change in BBB score with time between groups. B. Comparing BBB scores achieved between groups by week 5. C Comparison between groups of spared white and D. Grey matter.

Within Trunk M1, there is an internal somatotopy relevant for locomotor function.

For comparison to the injured animal, we first studied the internal somatotopy within trunk M1 in an intact rat (Figure 2). As we previously reported, regions that are highly likely to control trunk musculature are located medially (Figure 2B), overlapping with regions that control forelimb musculature (rostral and lateral) (Figure 2C) and extensively overlapping with regions controlling hindlimb musculature (Figure 2D)(190). Regions that are more likely to control lower thoracic trunk muscles are located medial and caudally (purple box, -0.5mm to-2.5mm RC, 1-1.5mm ML) with extensive preferential overlap with those that control hind limb musculature. This region is defined as the putative lower thoracic Trunk M1 (LTM1) (Figure 2E). Alternatively, regions that

are more likely to control upper trunk musculature are located rostral to LTM1, with the regions rostral to bregma (blue box, 0 to 0.5mm rostral, 1-2.5mm lateral) having overlap with regions that control forelimb. This region is defined as the putative upper trunk M1 (UTM1) (Figure 2F). Both the UTM1 and LTM1 are equally likely to recruit mid thoracic trunk musculature. Therefore, putative TRM1 is organized in a functional manner relevant for posture control during locomotion, providing a framework to compare the impact of exercise therapy on cortical reorganization after injury.

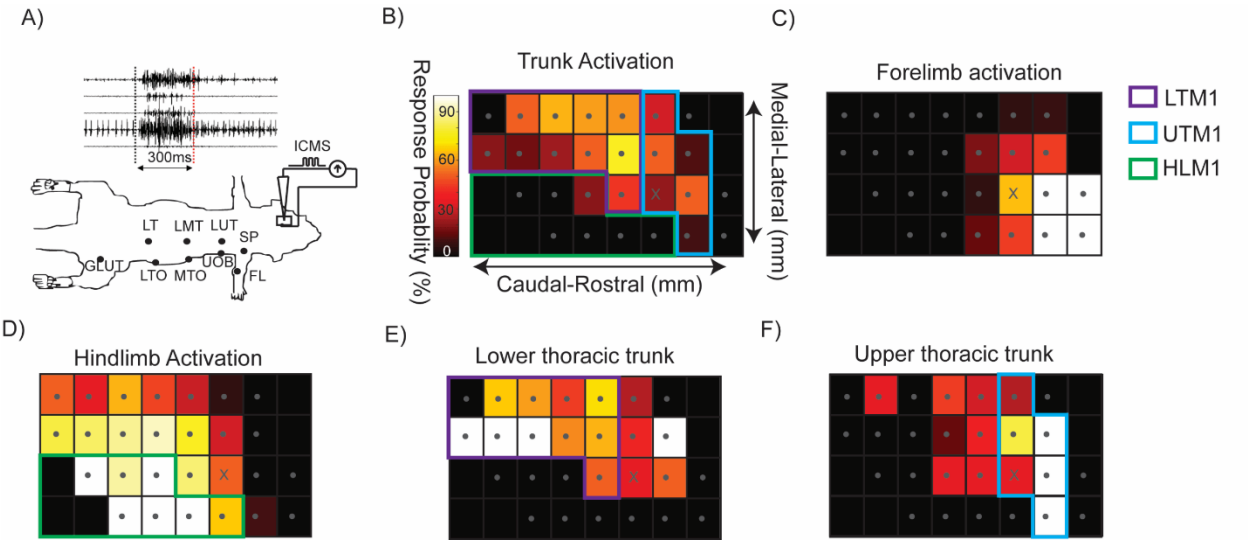

Figure 3.2 Somatotopic organization of Trunk M1 in Intact rat. A) ICMS methodology, Movement maps constructed by ICMS stimulation of infragranular layer of M1with resolution (500µm). Muscle activity recorded through EMG electrodes implanted along forelimb, trunk and hindlimb musculature (Right to Left: FL bicep (FL), spinous trapezius (SP), LUT (Upper thoracic Longissimus), UOB (Upper thoracic External Oblique), LMT (Mid thoracic Longissimus), MTO (Mid thoracic External Oblique), LT (Lower thoracic Longissimus), LTO (Lower Thoracic External Oblique), Glut (Gluteus Maximus)). Observed movement and evoked muscle activity at threshold current defines the movement representation B) Likelihood of activating trunk musculature plotted across intact animals (9.5 +/- 0.67 samples/location), grey dots indicate locations with sufficient sampling with atleast 6 electrode penetrations /location. X represents location: 0 Caudal to bregma, 2 mm Lateral to midline. C-D) Likelihood of activating any hindlimb musculature (C) and forelimb musculature (D) plotted across animals, Regions defined by green box (HLM1) are more likely to exclusively recruit hindlimb. Forelimb is likely recruited rostral and lateral to bregma, with relatively less overlap with Trunk M1 compared to the extensive overlap of Hindlimb with trunk M1. E-f) Conditional probability of recruit any lower (E) thoracic trunk muscle / Upper thoracic trunk muscle (F) plotted across animals, Regions Caudal and medial to bregma (purple Box) are more likely to

preferentially control lower thoracic (defined as putative LTM1), while regions rostral (blue box) are more likely to preferentially control upper thoracic trunk muscles (UTM1).

Spinal cord injury shifts TrM1 Caudal & lateral towards HLM1.

Motor maps were constructed 5 weeks post mSCI to assess the impact of moderate treadmill exercise on reorganization of TRM1 (Figure 3). As expected, despite the fact that animals recover weight supported stepping, injury abolishes ICMS activation of HL muscles in line with previous studies on incomplete spinal cord injury (191–194). Interestingly, TRM1 expands into putative HLM1, regardless of therapy group, suggesting TRM1 shifts lateral and caudally. But generally, the somatotopy, with lower trunk more caudal and upper trunk more rostral is maintained. These observations can be seen across the population (Figure 3B). First, regardless of therapy, the Center of gravity of trunk representation is shifted caudal [$F(2, 30)= 3.794$, $p= 0.024$; SCI-NX vs Intact, $p = 0.060$; SCI-EX vs Intact, $p = 0.020$; SCI-EX vs SCI-NX, $p = 0.931$] and lateral [$F(2, 30)=23.26$, $p<0.001$; SCI-EX vs. INTACT $p<0.0001$; SCI-NX vs INTACT $p<0.0001$; SCI-EX vs SCI-NX, $p = 0.398$] after SCI irrespective of whether they had therapy (Figure C) This is due in part to a significant increase in the likelihood to activate trunk musculature after injury specifically within HLM1 [Figure 3D, $\chi^2(2, N = 334) = 20.480$, $p< 0.001$; INTACT (3/62), SCI-NX (39/157), SCI-EX (41/115); SCI-EX vs INTACT $p<0.0001$; SCI-NX vs INTACT $p<0.001$] but there is no difference between therapy groups (SCI-EX vs SCI-NX $p=0.18$), even if we examine the different muscles groups (lower, mid and upper) separately (DATA NOT SHOWN) [Lower Trunk Muscles: SCI-NX (12/39), SCI-EX (14/41): SCI-EX vs. SCI-NX $p=0.813$; Upper Trunk Muscles: SCI-NX (20/39), SCI-EX (18/41): SCI-EX vs. SCI-NX $p= 0.502$; Mid Trunk Muscles: SCI-EX (31/41), SCI-NX (25/39): SCI-EX vs SCI-NX $p=0.33$].

Notably, the internal somatotopy of trunk M1 is preserved after SCI regardless of therapy (Figure 3E; Lower thoracic trunk: INTACT: $r^2 = 0.64$, $p<0.053$; SCI-NX: $r^2= 0.86$, $p<0.005$; SCI-EX: $r^2 =0.96$, $p< 0.001$). But there is a shift of the curves down for both injury groups relative to intact that reflects the expected de-efferentation of lower trunk spinal cord, below the level of the lesion, from the cortex (Upper thoracic trunk: INTACT: $r^2 = 0.69$, $p<0.05$, SCI-NX: $r^2= 0.89$, $p<0.005$, SCI-EX: $r^2 =0.99$, $p<0.001$). Here, there is a shift of the curves up for both injury groups relative to INTACT, suggesting an increase in activation of upper trunk muscles across the rostro-caudal extent of M1 after SCI in response to de-efferentation of spinal circuits recruiting lower thoracic trunk muscles below the injury level.

Yet, the total area devoted to trunk in M1 is greater for SCI-EX compared to SCI-NX (SCI-EX: 2.9 mm^2 vs SCI-NX: 1.8mm^2, $p<0.05$, Figure 3F). This difference in area devoted to trunk between SCI-EX and SCI-NX is not due to difference within putative HLM1 as shown in Figure 3D. Therefore, next, we investigated whether this difference was due to differences within putative LTM1 and/or UTM1. The overall difference in area between groups combined with the lack of difference in the activation of trunk muscles between SCI-EX and SCI-NX within HLM1, suggested to us that regions within TRM1 might account for the difference in area.

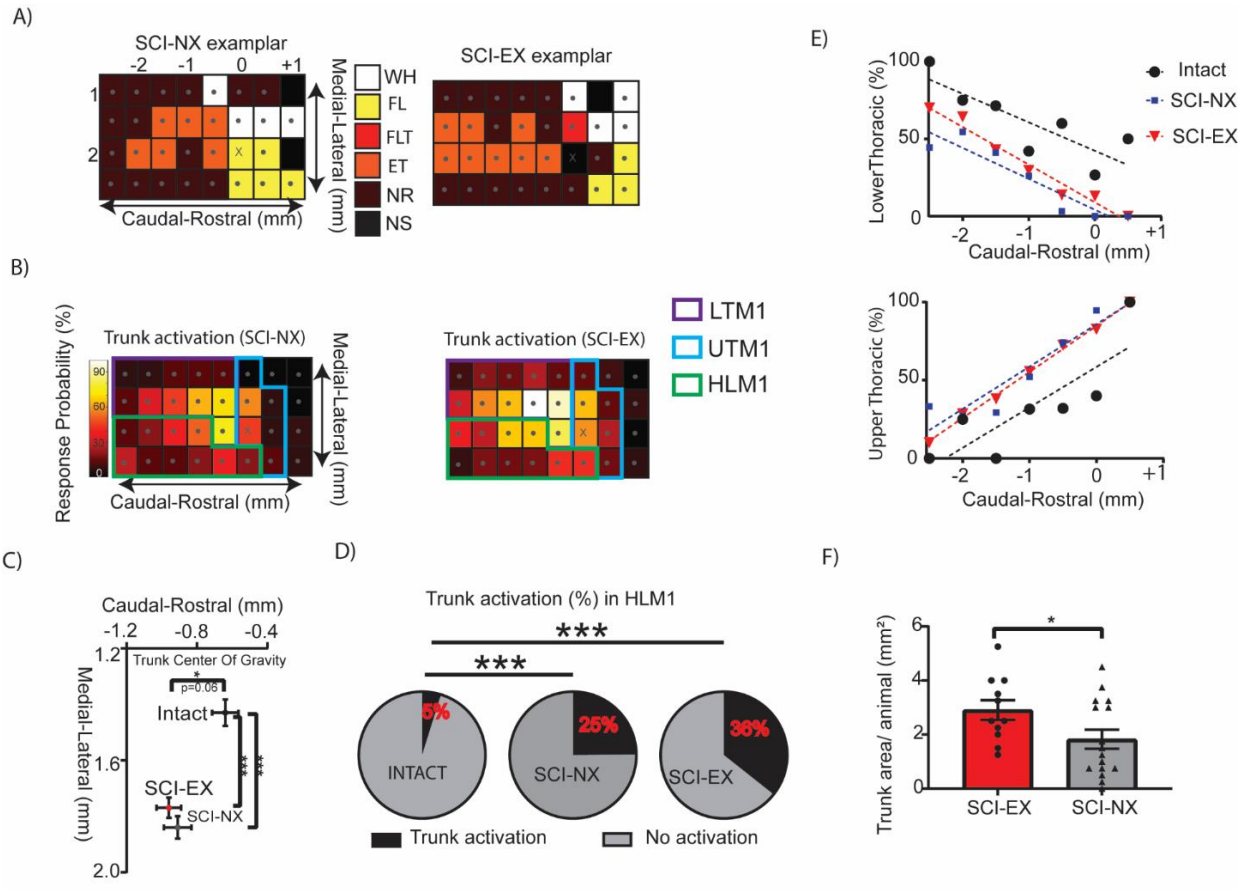

Figure 3.3 Spinal cord injury shifts trunk M1 Caudal & lateral towards HLM1. A) Exemplar Movement map of animals constructed 5 weeks post injury in (SCI-NX, BPS247) non-therapy and animals (SCI-EX BPS147) that received exercise therapy. Hindlimb activation abolished after SCI, all the movement types depict exclusive activation (WH- whisker, FL- forelimb, FLT- forelimb trunk coactivation, ET- Exclusive trunk, NR- nonresponsive location), The grey dots indicate sampled locations. Despite ability to recover weight supported stepping, cortical control of hindlimb with ICMS is absent. There is also a loss in the likelihood to recruit trunk in the most medial portion of M1 after SCI B) Probability distribution of trunk movement maps plotted between SCI-NX (n=16 animals, 15.53 +/- 0.14 samples /location) and SCI-EX (n=14 animals, 12.06 +/- 0.24 samples/location) animals. There is an increase in the likelihood to recruit trunk muscles in the de-efferent HLM1 (green box) after SCI compared to intact animals (Figure 2B), quantified as the likelihood to recruit trunk within HLM1 (Figure C), the increase in trunk recruitment in HLM1 is not therapy dependent. D) The center of gravity (COG) of Trunk representation plotted between Naïve, SCI-EX and SCI-NX animals, the trunk COG shifts caudal and lateral relative to naïve animals. * Represents $p<0.05$, *** represents $p<0.001$, all measurements expressed as mean +/- 1 SEM. E) Conditional probability of recruiting lower thoracic trunk musculature and upper thoracic trunk musculature plotted. Rostral regions have higher probability to recruit upper thoracic while caudal regions have higher probability to recruit lower thoracic trunk muscles. This internal somatotopy of trunk M1 is conserved after SCI and unaltered by therapy. Slopes were compared with simple linear regression analysis F) The area of Trunk/ animal plotted; SCI-EX animals (n=11) have bigger area of trunk compared to SCI-NX animals (n=16). Animals with adequate sampling throughout M1 alone considered (at-least 75% penetrations across M1).

Reorganization of upper trunk M1 is independent of therapy.

Within putative UTM1, there is loss of lower thoracic muscle activation and a concomitant, increase in upper thoracic trunk muscle recruitment after SCI regardless of therapy group (Figure 4). As might be expected, there is no effect of therapy on the probability of recruiting trunk musculature from within the putative UTM1 (INTACT 21/64, SCI-NX = 20/96, SCI-EX 26/77; χ^2 (2) = 4.417, p=0.110, data not shown). However, mSCI decreased the probability of activating lower thoracic muscle with a concomitant increase in activating upper thoracic trunk muscle regardless of therapy group (Figure 4A). To quantify this, we separately compared lower thoracic trunk muscle activation [Figure 4B; INTACT (7/21), SCI-NX (0/20), SCI-EX (2/25); χ^2 (2)=10.75, p<0.005; SCI-NX vs INTACT p<0.001, SCI-EX vs Intact (p<0.001, SCI-NX vs SCI-EX p = 0.1] and upper thoracic trunk muscle activation (Figure 4C; INTACT (12/21), SCI-NX (19/20), SCI-EX (22/25); (2)=10.78, p<0.005, SCI-NX vs Intact p<= 0.01, SCI-EX vs Intact, p=0.06. This loss of lower thoracic muscle activation is mainly due to a loss of co-activations of upper and mid thoracic muscles with lower thoracic muscles seen in intact. In fact, co-activation with lower thoracic muscles converts to exclusive activation of upper thoracic trunk or coactivation with upper and mid thoracic muscles. This in interesting to demonstrate but not unexpected given the injury. Therefore, regardless of therapy, the concomitant reduction of lower thoracic muscle activation and increase in upper thoracic muscle activation likely reflects the damaged axons that no longer reach the lower thoracic spinal cord.

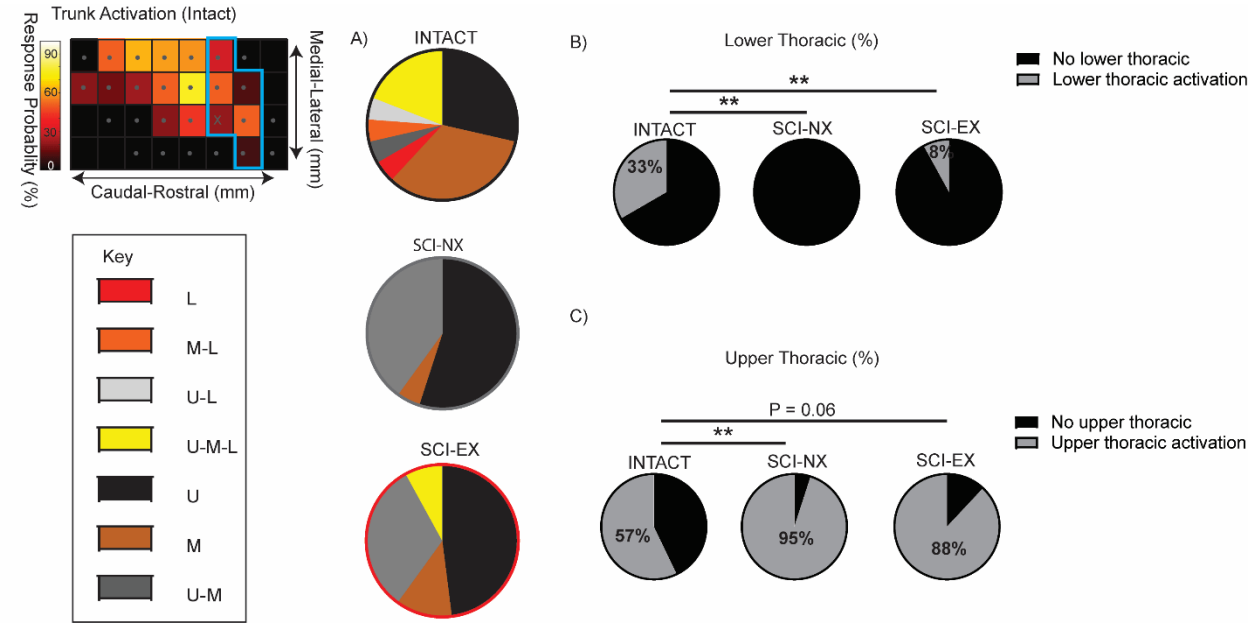

Figure 3.4 Within putative UTM1, there is a loss of lower thoracic, increase in upper thoracic trunk muscle recruitment after SCI independent of therapy. A) The likelihood of activating trunk musculature within putative UTM1 (refer to inset, reproduction of Figure 2B with UTM1 marked in blue for reference) compared between Intact (21/64 penetrations), SCI-NX (20/96 penetrations) and SCI-EX (25/77 penetrations) animals. Pie charts represent segmental co-activation along with other trunk musculature within putative UTM1 between intact (, (U /M/L represents exclusive thoracic trunk musculature activation of upper or mid or lower thoracic trunk muscles respectively, U-M represents (exclusive co-activation of Upper& mid thoracic trunk muscles), M-L (Exclusive lower and mid thoracic) , U-L (Upper and Lower), U-M-L (Upper, mid and lower) activation B) Conditional probability of recruiting any lower thoracic (B), upper thoracic (C) quantified between groups within putative UTM1, there is a loss of lower thoracic trunk while there is an increase in the likelihood to recruit upper thoracic trunk muscles after SCI, (Chi- sq test, fischer's exact test with bonferroni correction *p<0.05, **p<0.001

Exercise therapy rescues LTM1 function

For motor maps within LTM1, SCI-NX show a reduction in trunk activation compared to INTACT but not SCI-EX [Figure 5A: Intact (53/111), SCI-NX (55/172), SCI-EX (69/138), $\chi^2(2, N = 421) = 12.22$, $p<0.01$; SCI-NX vs INTACT $p< 0.05$, SCI-EX vs SCI-NX $p<0.01$, SCI-EX vs INTACT, $p=0.80$]. This is likely the reason for the reduction in area devoted to trunk activation in NEX

compared to NEX (refer Figure 3F). This increase in trunk activation is due to an increase in likelihood to recruit both upper and lower thoracic muscles with no difference in mid thoracic muscle recruitment when comparing SCI-EX to SCI-NX [Upper: SCI-NX (29/172) vs SCI-EX (38/138) $p < 0.05$, Mid: SCI NX (38/172) vs SCI-EX (38/138) $p = 0.2$, Lower: SCI-EX (25/138) VS SCI-NX (12/172), $p < 0.01$, data not shown]

Considering only those trials when trunk is activated, there is no difference in the proportion of recruited muscles between SCI-EX and SCI-NX. However, compared to INTACT, there is an increase in the likelihood to recruit upper [INTACT (29/53), SCI-NX (38/55), SCI-EX (29/69), $\chi^2(2, N=177) = 11.85$, $p<0.005$, SCI-EX vs SCI-NX $p =2.55$, SCI-NX vs INTACT $p < 0.05$, SCI-EX vs INTACT $p< 0.01$, data not shown] and a decrease in the likelihood to recruit lower thoracic muscles [Figure 5B; INTACT (32/53), SCI-NX (12/55), SCI-EX (25/69); $\chi^2(2, N= 177) = 17.23$, $p<0.001$; SCI-NX vs NTACT $p<0.001$, SCI-EX vs INTACT $p<0.05$, SCI-EX vs SCI-NX $p=0.33$] with no change in the likelihood to recruit mid thoracic muscles [INTACT (32/53), SCI-NX (38/55), SCI-EX (38/68); $\chi^2(2, N=177) = 2.269$, $p=0.32$, data not shown]. This lack of difference in the proportion of mid thoracic muscles recruited between therapy groups could be due to the fact that these muscles span the lesion and there is an equal probability of losing control to muscles below the lesion but increase in sprouting of those axons above. Note that there is still an overall decrease in activating trunk muscles in SCI-NX compared to SCI-EX.

However, there are important differences in the way lower thoracic muscles are recruited between groups (Figure 5C). When examining trials when lower thoracic muscles were activated, exercise increases probability to exclusive activate lower thoracic trunk muscles, similar to intact [INTACT (14/32), SCI-NX:(2/12), SCI-EX (14/25)] but different from SCI-NX (Figure 3D; SCI-EX vs SCI-NX $p<0.05$). For example, 7/14 SCI-EX animals could activate lower thoracic trunk muscles with

ICMS stimulation in LTM1 at threshold, of these 5/7 could recruit lower thoracic trunk exclusively. Moreover, while 6/13 SCI-NX animals were able to activate lower thoracic trunk in LTM1, only 1 of these 6 could exclusively recruit lower thoracic trunk. Therefore, NEX is more likely to coactive lower thoracic muscles with mid thoracic muscles compare to SCI-EX, suggesting exercise prevents axons that normally pass below the level of the lesion from dying back to midthoracic spinal cord (see discussion for more details).

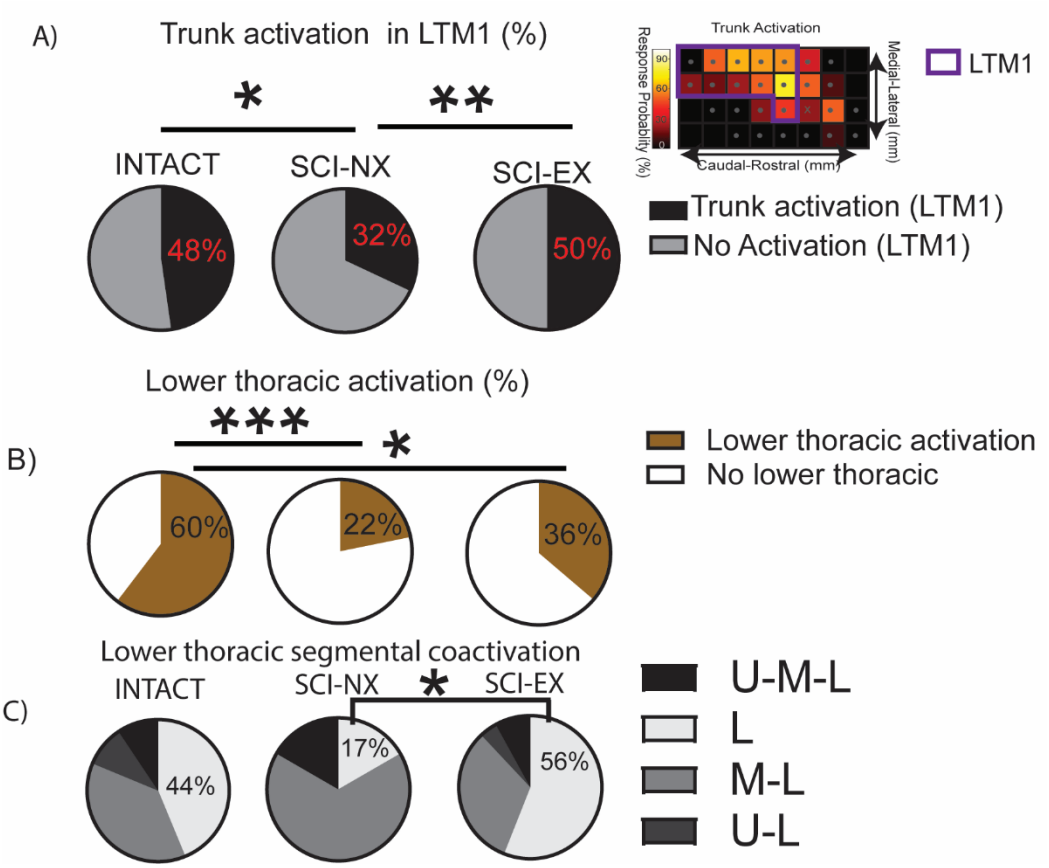

Figure 3. 5: Within LTM1, exercise therapy rescues activation of trunk muscles induced by ICMS. A) The likelihood of activating trunk musculature within putative LTM1 plotted between Intact (total 111 penetrations), SCI-NX (172 penetrations) and SCI-EX (138 penetrations). B) Conditional probability of recruiting any lower thoracic quantified between groups within putative LTM1 plotted in the same order Intact (53), SCI-NX (55), SCI-EX (69). The loss in likelihood to activate trunk in LTM1 after SCI is rescued in animals that had exercise therapy C) In LTM1, Segmental co-activation of Lower thoracic with another musculature plotted between Intact (32), SCI-NX (12), SCI-EX (25). Lower thoracic muscle can either be exclusively activated (L), coactivate with mid thoracic trunk musculature (M-L), co-activate with mid and upper thoracic trunk (U-M-L) or exclusive co-activate with upper thoracic trunk (U-L) muscles. While the

likelihood to recruit lower thoracic trunk, musculature is not significantly altered by therapy, the likelihood of co-activating with mid thoracic musculature at the level of injury differs. Therapy promotes exclusive lower thoracic trunk muscle recruitment in LTM1 while non therapy animals preferentially recruit lower thoracic trunk below injury via coactivation with mid thoracic trunk muscles at the level of injury. Comparisons between groups were done with (Chi- sq omnibus test, posthoc: Fischer's exact test with Bonferroni correction *p<0.05, **p<0.001).

Exercise attenuates loss of muscle activation below the level of the lesion.

The minimum current required to recruit trunk muscles with ICMS was significantly higher after injury regardless of therapy, suggesting that therapy had no effect of corticospinal excitability [INTACT (49 +/-2.1 μA), SCI-EX (64.4 +/ 2 μA), SCI-NX (64.3 +/- 2.2 μA) data not shown; $F(2) = 13.19$, $p < 0.0001$; SCI-NX vs Intact $p<0.001$, SCI-EX vs Intact $p<0.001$, SCI-NX vs SCI-NX $p = 0.1$. Notably, when comparisons were made within the non-de-afferent representation such as FLM1 and compare threshold currents between intact, SCI-EX and SCI-NX animals, no difference suggesting that this excitability change in the cortex is not global [$F(2, 121) = 202.778$, $p = 0.520$ INTACT (n= 15) (48+/3.4 μA), SCI-EX (n=60) (47.83 +/- 3.2 μA), SCI-NX (n=46) (52+/- 2.5 μA).

Therefore, the amplitudes of the MEPs in response to ICMS (100 μA) were compared between SCI-EX and SCI-NX separately for dorsal and ventral muscles below, at and above the level of the lesion. Below the injury, exercise attenuated the reduction in MEP amplitude known to occur after SCI for both dorsal and ventral trunk musculature [LTO (ventral) (SCI-NX=9, SCI-EX=24) $p<0.05$; LT (dorsal) SCI-NX=7, SCI-EX=14 $p<0.05$]. Surprisingly, within LTM1 when evaluating locations that recruited mid thoracic musculature, MEP amplitude in dorsal trunk muscles recorded from animals that did not receive therapy were higher than those that received therapy, indicative of aberrant sprouting at the level of lesion [LMT (dorsal) SCI-NX N=29, SCI-EX N=21, $p<0.05$;

MTO (ventral) SCI-NX N=30, SCI-EX N=23, p= 0.93]. As expected, there were no differences in the EMG amplitude above the level of the injury [LUT (dorsal) SCI-NX N=24, SCI-EX N=13, p = 0.07; UOB (Ventral) SCI-NX N=25, SCI-EX N=21, p = 0.48]. This greater MEP amplitude recorded from SCI-EX compared to that of SCI-NEX represents a maintenance of recruitment of lower thoracic trunk muscles by LTM1 because the MEP amplitude of lower thoracic muscles recorded from SCI-EX was similar to that of intact animals (2.6+/ - 0.3 a.u, refer chapter 1) (190). To test whether this was compensated for by differences between recruiting ventral or dorsal trunk muscles, the proportion of dorsal muscles recruited was compared to the proportion of ventral muscles between groups.

Results show that the difference in the proportion of dorsal or ventral trunk muscles recruited at suprathreshold current, between SCI-EX and SCI-NX supports the differences in the MEP amplitude. Below the injury level, the conditional likelihood of recruiting ventral trunk muscles with ICMS in LTM1 were significantly higher in SCI-EX compared to SCI-NX (SCI-EX: 28/55, SCI-NX: 8/47, $p<0.001$) while dorsal trunk musculature recruitment was similar (SCI-EX: 11/55, SCI-NX: 4/47, $p=0.16$)

At the injury level, the conditional likelihood of recruiting ventral trunk muscles (SCI-EX: 27/55, SCI-NX: 33/47, $p<0.01$) and dorsal trunk muscles (SCI-EX: 20/55, SCI-NX: 30/47, $p<0.01$) were significantly higher in the SCI-NX animals compared to SCI-EX animals.

Above the injury level, the conditional likelihood of recruiting ventral trunk muscles (SCI-EX: 19/55, SCI-NX: 27/47, $p<0.01$) and dorsal trunk muscles (SCI-EX: 14/55, SCI-NX: 41/47, $p<0.01$) were significantly higher in the SCI-NX animals compared to SCI-EX animals.

Therefore, therapy rescues loss of LTM1 control of lower thoracic muscles and promotes control of lower thoracic trunk muscles like intact animals suggesting that trunk control strategy is different between SCI-EX animals and SCI-NX animals. This result reveals underlying differences between rehabilitation assisted plasticity and spontaneous compensatory plasticity after spinal cord injury. In fact, ICMS in LTM1 of SCI-EX animals was more likely to recruit ventral trunk muscle with greater MEP amplitude below the level of the lesion, with reduced likelihood to recruit dorsal trunk muscles with reduced MEP amplitude. Moreover, there was reduced likelihood of co-activation with ventral trunk muscles at and above the level of injury.

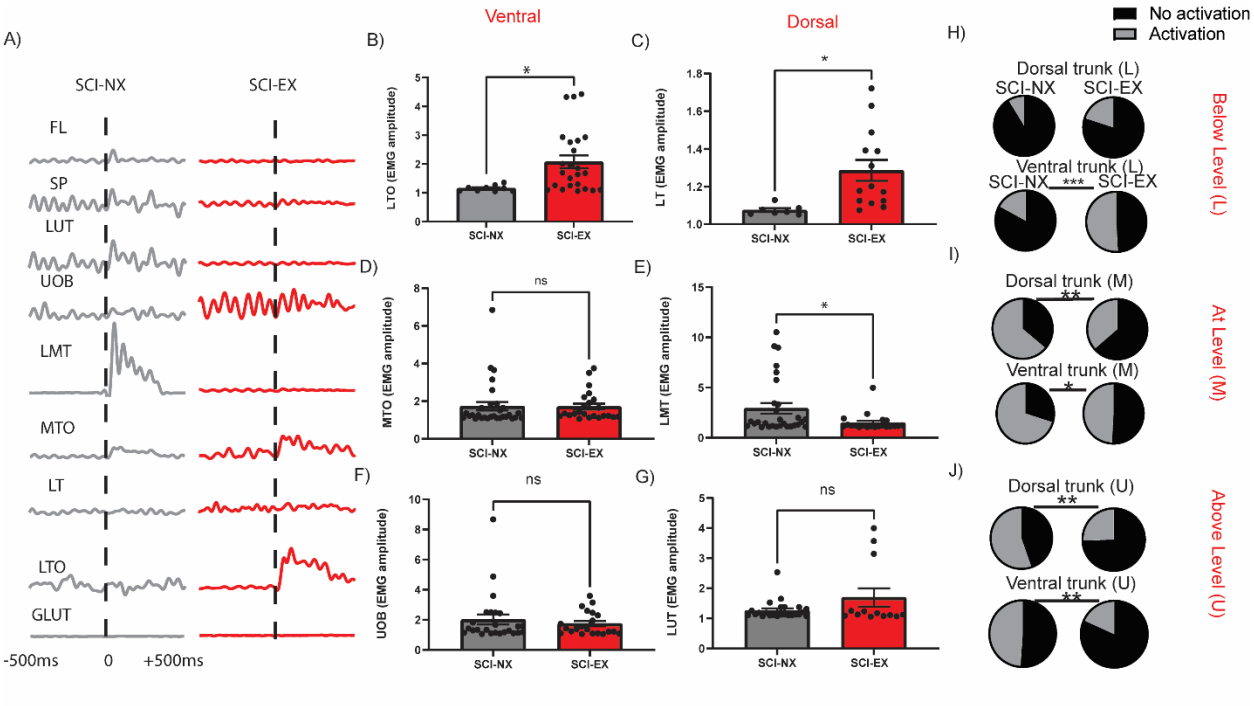

Figure 3. 6 Within LTM1, exercise attenuates loss of EMG amplitude due to mSCI. Left Panel: EMG exemplar traces from muscles recorded at, above and below the level of the lesion. FL- forelimb, SP-, LUT -, UOB -, LMT -, MTO -, LT -, LTO – GLUT – gluteus. Middle Panel: Comparison of muscles amplitude between SCI-NX and SCI-EX for muscles below (B-C), at (D-E) and above (F-G) the level of the lesion. Right Panel: Conditional likelihood of recruiting dorsal/ventral trunk musculature below (H), at (I) and above (J) level of injury with ICMS in LTM1 at suprathreshold current represented as pie charts between SCI-NX and SCI-EX animals.

Severe SCI contusion shows expansion of trunk into putative HLM1 that is dependent on the extent of recovery, not exercise therapy.

These difference between EX and NX in this moderate contused animal model where all animals regain WSS, raises interesting questions when compared to more severe injuries. Previous work from our research group has shown that a combination of active body weight supported treadmill and pharmacotherapy after complete spinal cord injury resulted in improvement in weight supported stepping in the open-field concomitant with the expansion of trunk motor cortex into the de-efferent HLM1 (11). Therefore, we wanted to understand whether this difference between our moderately contused animal data and this complete spinal transection was due to the partial lesion or severity of lesion. Therefore, we repeated this work in severely contused animals (Figure 7).

For moderate contused animals, there was a significant correlation between the likelihood to activate trunk musculature in LTM1 and functional recovery. This is expected based on the ability of LTM1 to exclusively activate lower thoracic trunk muscles [see Discussion; $F(1,27) = 6.266$, $p<0.05$, $r^2=0.2$, Figure 7A]. However, for the severely contused animals, there was no difference in the BBB score between exercise groups [therapy: $F(1,12) = 0.4316$, $P = 0.52$; week: $F(3.7, 43.02) = 185.5$, $p<0.001$; interaction: $F(10, 116) = 0.87$, $p=0.55$, Figure 7B] and, therefore, no correlation between trunk muscle activation and BBB score [$F(1,2)= 6.266$, $p = 0.02$, $r^2=0.001$, Figure 7C]. In fact, there were no differences in the likelihood of LTM1 to recruit thoracic muscles between therapy groups (Data Not shown): SEV-EX: (43/104), SEV-NX (22/54), Fischer's Exact Test 1 sided test $p = 0.54$, which our moderately contused study suggests requires the benefits of therapy to be effective. This result is not surprising because the therapy was moderate, scaled back compared to the full transect study ((11); see Methods).

However, regardless of whether the severe animal received exercise, some animals achieved weight-supported stepping, and some did not. Based on the data from previous study from Manohar et.al 2017, we hypothesized that animals that regained the ability to achieve weight supported stepping will demonstrate expansion of trunk into de-efferent HLM1, but, based on the moderate contusion above, as there was no effect of exercise, there would be no difference in the representation of trunk in LTM1. To accomplish this, animals were separated by behavioral recovery (BBB>10 compared to BBB<=10). By week 10 post injury 8/14 animals (BBB>10) regained the ability to take weight supported steps at-least occasionally. Comparing the motor map of an animal that received WSS (Figure 7E) to one that did not (Figure 7D), it is evident that the likelihood of recruiting trunk musculature was significantly higher in HLM1 in animals that gained weight supported stepping (SEV-WSS) compared to animals that did not. This is quantified by the likelihood for penetrations in putative HLM1 to activate trunk musculature [SEV-WSS (39/77) 51%, SEV-NWSS (20/60) 33%, Fischer's Exact test, 1 - tailed, p= 0.03)] (Figure 7F). However, there were no differences in likelihood to recruit trunk from LTM1 [% activation of trunk in LTM1 SEV-WSS (SEV-WSS: 37/88 42%, SEV-NWSS: 28/63 44%, p=0.44) (Figure 7G). These data, combined with our early work on complete spinal transection and the work on moderate confusion, suggest expansion of trunk into putative HLM1 is dependent on recovery of WSS independent of therapy. Reorganization within TRM1 is dependent on therapy induced improvement in function.

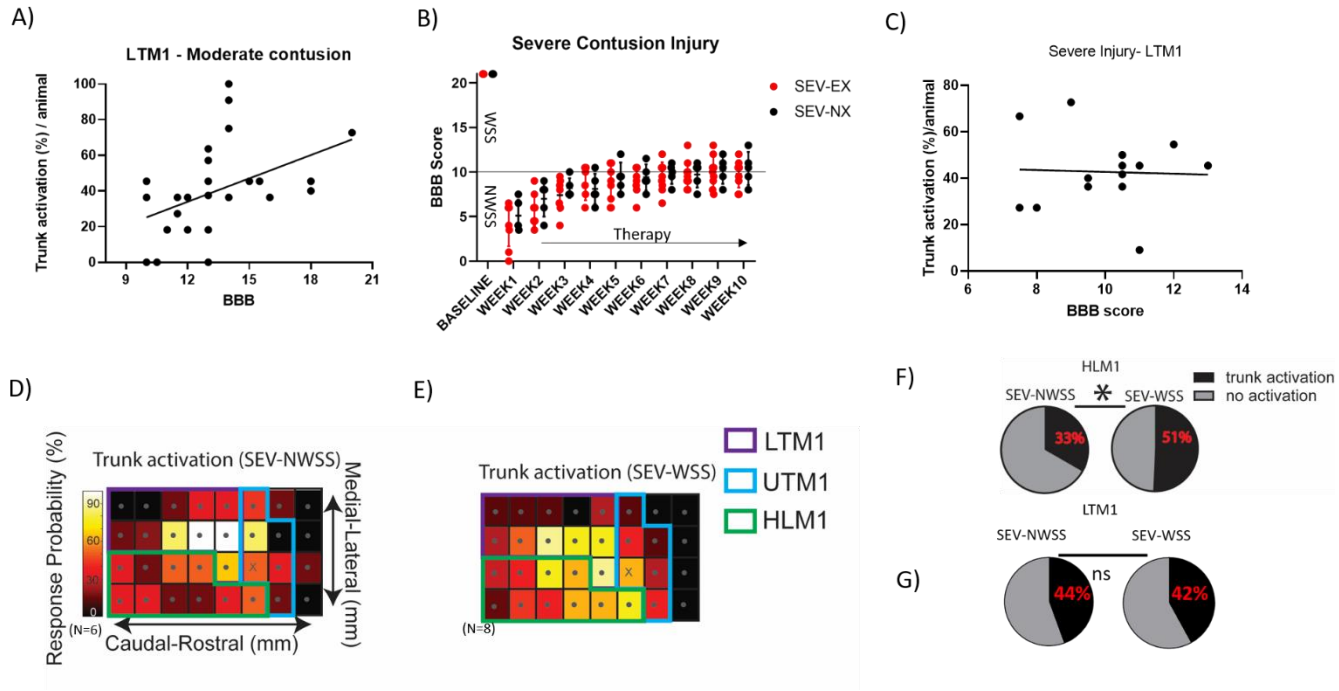

Figure 3.7**:** For severely contused animals, moderate treadmill exercise did not improve behavioral outcome but differences in WSS predicted differences in cortical reorganization. A. For moderately contused animals, the likelihoods to recruit trunk muscles was correlated to BBB score. B. For severely contused animals, exercise did not impact BBB score. C) There was no correlation between the likelihood to activate trunk and BBB score (C). D, E. Difference in the motor map were related to difference in whether animals achieved WSS. E. There were no differences in the likelihood to recruit trunk muscles from LTM1 between WSS and NWSS however, HLM1 was more likely to recruit trunk muscles with ICMS if animal achieved weight supported stepping.

Discussion

The contusion model of SCI is more clinically relevant than specific lesion studies but variance across animals is high. However, when we can combine information from specific lesion models, the rat model of SCI represents an important avenue to allow insight into the mechanisms for physical therapy and the relationship to functional recovery (e.g., achieving weight-supported stepping). While spontaneous recovery in the moderately contused rat model of SCI results in most animals achieving weight supported stepping, therapy promotes further improvement resulting in more consistent weight supported stepping and better inter-limb co-ordination. This is

achieved by engaging the putative lower thoracic trunk motor cortex to restore some control of both dorsal and ventral lower thoracic muscles. Animals that do not receive therapy have a loss of activation of lower thoracic trunk muscles and increased activation of mid-thoracic trunk muscle, suggesting that axons damaged by the injury die back further in the absences of therapy. Taken together with earlier studies on the effect of injury on descending corticospinal neurons ((195)), these results suggest that therapy promotes the sprouting of damaged axons just above the lesion enabling continued control of lower thoracic muscles while the ability to achieve weight-support in the absences of therapy is compromised and the axons die back, making contact at the mid-thoracic level. Taken together these results suggest that animals that have undergone spontaneous recovery that achieves weight-support, increase access to thoracic muscles use the trunk muscles at/above injury for propulsion, however with therapy, there are likely to also engage ventral muscles below injury. Understanding the details of cortical control of trunk muscles after therapy and those that are recruited during spontaneous recovery can help us better design and evaluate therapeutic interventions that rely on trunk control for recovery of weight supported stepping after spinal cord injury.

Methodological considerations

The goal of this study was to assess cortical reorganization associated with physical rehabilitation and assess differences between spontaneous and physical therapy mediated recovery. Data from intact animals were part of a previous study (see Chapter 1). For that study, the resolution penetrations were greater, and maps were made by combining data across animals for a complete map. Therefore, in this study, each penetration was considered an independent sample when calculating the measures assessing cortical reorganization within M1 and the statistic is interpreted

as samples from M1 (or subregions within M1, e.g., LTM1 or UTM1) rather than a population statistic.

We did not perform a lesion study and, therefore, at this time it is premature to imply any causal relationship between reorganization in the trunk motor cortex and functional recovery observed in this moderate thoracic spinal cord contusion model. However, given that the reorganization of trunk cortex into putative HLM1 was necessary in the full transect model and, here we show that that reorganization exists in animals that achieve WS, we suspect that the lesion study will show this reorganization is necessary for contusion models as well.

For our mapping study we identified a reduction in cortical excitability after SCI independent of therapy group. However, when we examined corticospinal excitability changes in non-de-afferented representation such as FLM1, comparing threshold currents between intact, SCI-EX and SCI-NX animals, no difference was found [$F(2,DOF)=202.78$, $p=0.520$; INTACT n= 15, 48+/3.4 mA; SCI-EX n=60, 47.83 +/- 3.2; SCI-NX n=46, 52+/- 2.5uA] suggesting that this excitability change in the cortex is not global (data not shown).

Finally, it is important to acknowledge the potential translational limitation of our study focusing on quadrupedal instead of bipedal stepping. Indeed, the novel cortical sensorimotor circuit developed in our rats – integrating sensory information from the ventral forepaws and motor control to the muscles of the spine – suggests that the closed-loop control of trunk musculature that is sufficient for quadrupedal functional improvement might be irrelevant for bipedal locomotion. However, it can be argued that patients attempting to recover locomotion after a spinal cord injury make significant use of the upper limbs to handle their walking aids, so that locomotion behavior switches from the normal bipedal pattern to an assisted quasi-quadrupedal pattern (196) From this quasi-quadrupedal perspective, this novel supraspinal control of trunk stability might

become critical to achieve locomotion in recovering patients with spinal cord injury, as in our animals.

Expanded cortical control of trunk musculature is critical for recovery of weight-supported stepping.

Similar to our work with complete transection, recovery of WSS requires expansion of trunk M1 into HLM1. For both the moderate and severely contused mid-thoracic model used here, it was possible for animals to achieve WSS even without physical therapy. We suggest that it is the role of the expanded trunk cortex into M1 that permits this functional recovery. Trunk muscles do extend from above to below the level of the injury, thus providing a biomechanical substrate for bypassing the lesion by activating these muscles at the mid-thoracic level. The idea is that animal that achieve WSS learned to activate the trunk musculature to reduce the load on the hindlimbs while balancing on the forelimbs, which allowed the central-pattern-generators below the level of the lesion to be activated, resulting in weight-supported hindlimb stepping. This explanation is supported by previous observations in neonatally spinalized rats (20, 197, 198) which can develop unassisted weight-supported stepping (199, 200). Importantly, the motor recovery of neonatally spinalized rats is not due to any reconnection within the spinal cord (201, 202) but is instead causally related to sensorimotor cortical reorganization (22, 67, 128, 198, 203–205). Recovery of unassisted weight-supported hindlimb stepping after complete spinal cord injury was believed to remain restricted to neonatally spinalized rats, due to the higher cortical plasticity at neonatal age compared to adulthood (22, 205) but we recently showed this was possible in the adult complete transection(11). Our results here extend this idea to the contusion model, both moderate and severe, and suggest it is independent of therapy.

Compensatory Sprouting Pathways

Current understanding of the impact of these therapeutic interventions after SCI suggests functional improvement relies on plasticity along the entire neural axis which includes changes in the spinal networks below the level of lesion as well as supraspinal networks in the brain-stem (206, 207) and the sensorimotor cortex (8, 9, 12, 18, 128, 208–210). In fact, recent studies showed that neuroplasticity in M1 is required to maintain therapy induced functional improvements after SCI (11, 17, 198, 211)

On the one hand even without rehabilitation, studies in humans (212, 213) and in animal models (214, 215) point out that cortical plasticity in M1 parallels spontaneous recovery of function after incomplete SCI. This is likely since the cortex has to relearn new strategies for motor control. The role of physical rehabilitation in altering cortical plasticity in M1 after incomplete SCI, is not clear especially when spontaneous recovery is a confounding factor. The underlying plasticity differences in M1 reorganization associated with rehabilitation assisted recovery and spontaneous use dependent recovery is not known after incomplete SCI. The central question of this study improves our understanding about rehabilitation driven learning strategies adopted by the cortex. Moreover, this suggests that rehabilitation driven behavioral improvements are not a mere enhancement of compensatory plasticity associated with spontaneous recovery but represent a novel capability. In this case, restoration of control by LTM1 of lower thoracic muscles. We suspect this is because of exercise preventing dieback of the damaged corticospinal fibers and allowing them to sprout above the level of the lesion, but follow-on studies are needed to confirm this.

Conclusions

Our results demonstrate that the ability to achieve WSS stepping in the contusion models studied here does not require therapy but is associated with expansion of the trunk motor cortex into the putative HLM1. However, to achieve further behavioral improvements that are therapy dependent are associated with restoration of LTM1 control of lower thoracic trunk muscles, most likely through connections that span the lesion site. Therefore, therapy induced improvements are more than just further enhancements of spontaneous mechanism underlying functional recovery. These results suggest that consideration of cortical plasticity in the design of therapeutic interventions is important.

Methods

Overview:

Thirty-two, female Sprague Dawley rats (225-250 g; Envigo) were maintained on a 12/12-hour light/dark cycle with ad libitum food and water. All animals received spinal cord injury. A subset of the animals (n=15) received quadrupedal treadmill training starting week 1 to week 5 post spinal cord injury. Locomotor recovery was assessed weekly followed by a terminal cortical mapping experiment at week 5-6 post SCI. All experimental procedures were approved by UC Davis or Drexel University IACUCs and followed NIH guidelines.

Spinal cord contusion

Animals were anesthetized with ketamine (63 mg/kg), xylazine (5 mg/kg) and acepromazine (0.05 mg/kg) via IP injection. Animals were considered sufficiently anesthetized with the absence of a toe pinch reflex. The skin and musculature overlying the spinal column was retracted from spinal levels T4 to T12 and a laminectomy was performed at vertebral level T10. The spinal cord was stabilized by securing locking forceps to the transverse processes of T9 and T11. SCI rats received a moderate bilateral mid thoracic contusion injury at vertebral level T10 using the Infinite Horizon

impactor device (Precision Systems and Instrumentation, LLC; Fairfax Station, VA) with 150 kdynes of force and a 1 s dwell time. The musculature was then sutured in layers and the skin was closed with wound clips. Laminectomy controls underwent the same procedure, except the spinal cord was not impacted. Animals were post-operatively hydrated with saline (7 ml), prophylactically administered an antibiotic (enrofloxacin, 5 mg/kg), and allowed to recover on a heated water pad. Animals were administered fluids and antibiotics once daily for seven days and bladders were manually expressed twice daily until they regained autonomic bladder control.

Exercise therapy

Therapy for moderately contused: Animals receive moderate intensity quadrupedal treadmill training for 5 weeks post SCI, 5 days/week for 30 min, starting at 1 week post SCI. Pre-SCI, all animals are acclimated to the motorized treadmill. Post SCI, animals assigned to either SCI-NX or SCI-EX at random, paired such that for every animal that has therapy had a sham therapy partner. The goal for each session was to encourage weight supported plantar placement and stepping throughout the entire duration. Minimum body weight support was provided as and when required by either supporting the pelvis for lateral support, holding distal end of tail for vertical support. External support was provided in a manner to allow opportunity for the animals to maintain balance and correct for postural instability during treadmill locomotion. Treadmill speed is adjusted between 8-14m/min) and personalized for each animal and adjusted throughout training session to allow the animal to also adapt interlimb co-ordination throughout the session. If the animal was not able to take plantar steps during the early phase of training, the ventral surfaces of the hind paw was gently stroked in a rhythmic manner and plantar placement of the paws onto the treadmill surface was done (216). The median speed, time spent on treadmill & the distance travelled, notes on quality of stepping were documented for each session.

Therapy for severely contusion*:* Therapy consists of body-weight-supported treadmill training and pharmacotherapy 5 days per week, beginning 2 weeks after SCI and continuing until 10 weeks post injury. Ten minutes before treadmill training, animals are injected with 5-HT agonists (8, 11, 217) consisting of 0.125 mg/kg of quipazine (1 mg/ml) and 0.125 mg/kg of 8-OH-DPAT (1 mg/ml), as this dose had a maximal effect on cortical reorganization (8, 11, 34, 217). The 2 week recovery period following SCI allowed upregulation of 5HT receptors caudal to the lesion level(200, 218). Sham therapy animals received an equivalent volume of saline injections.

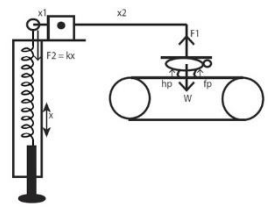

spring mass system for body weight support during quadrupedal locomotion (adapted from Manohar et.al 2017)

Then, animals receiving therapy are placed in a body weight support harness and step training is provided for 30 min 5 days/week at 8-14m/min. The harness provides fixed lateral and adjustable vertical body weight support by means of a spring. The body weight support provided is adjusted by altering the extension of the spring with a rotary knob until the animal reaches a load bearing failure point. %BWS is assessed weekly on Mondays as the load bearing-failure point(219) defined as the minimum % body weight support (%BWS) needed for the animal to step with its hindlimbs for 3 consecutive step cycles when initially placed on the treadmill. %BWS assessment is done on all animal's post SCI, regardless of group, after injection of 5-HT agonists but before treadmill training. Note that animals receiving therapy are provided 30 min of treadmill training with this %BWS for the rest of the week (5 days M-F).

Behavior Assessment (BBB)

Locomotor functional recovery was measured using the Basso, Beattie, and Bresnahan (BBB) locomotor rating scale (220). Animals were placed in an open field (76.20 x 91.44 cm) and were

observed by two trained experimenters blinded to the animals' experimental condition for 4 mins. Each hindlimb was assessed for the presence of joint movements, weight support, quality of stepping, forelimb-hindlimb coordination, paw placement, and toe clearance and these observations were converted into a BBB score for each hindlimb. Scores on this scale range from 0 to 21, where a score of 0 represents a complete paralysis of the hindlimbs, while a score of 21 represents the locomotor function of an uninjured rat. All BBB testing in severely injured animals were without any drug administration.

Motor maps and EMG recordings: (Refer Chapter 1 Methods)

Perfusion and Histology: Lesion analysis

Histological verification of the spinal cord lesion was conducted on subset of animals. At the conclusion of behavioral testing five weeks post-SCI, animals were transcardially perfused with cold saline followed by 4% paraformaldehyde (pH 7.4). During spinal cord tissue removal, the vertebral level of the lesion site was confirmed. Tissue was post-fixed in 4% paraformaldehyde for 24 hrs and placed in 30% sucrose until the tissue sank to the bottom of the specimen container, indicating that the tissue had been cryoprotected. A 14 mm section of spinal cord surrounding the lesion site was dissected and frozen in Shandon M1 embedding matrix (Thermo Fisher Scientific, Waltham, MA). 25 µm coronal sections of cord were collected using a freezing microtome and every 20th slice was mounted onto charged slides (Thermo Fisher Scientific premium frosted microscope slides) to preserve 500 µm spacing between section. Sections were air dried overnight. To stain, the slides were dehydrated in increasing concentrations of ethanol baths (75%, 95%, 100%) for 3-6 mins each, cleared using Citrisolv (DeconLabs Inc., King of Prussia, PA) for 20 mins, rehydrated in decreasing concentrations of ethanol baths (100%, 95%, 75%) for 3-6 mins each, and were then rinsed with distilled water. The slides were stained for myelin using a Cyanine

R / $FeCl_3$ solution for 10 min. Slides were rinsed and placed in differentiation solution for 1 minute using 1% aqueous NH_4OH. After additional rinsing, slides were stained for Nissl in a Cresyl Violet solution for 20 minutes, rinsed, and dehydrated once again using ethanol. Slides were coverslipped using Vectashield mounting medium (Vector Laboratories, Burlingame, CA), and digital images were taken of each section 24 hours later.

Lesion analysis was done in a subset of 7 animals from each group (SCI-EX, SCI-NX) animals. To determine if there was an association between spared matter around the lesion site, the amount of spared white and grey matter in each section was calculated using Image J Software (NIH, Bethesda, MD) (221). Tissue was considered spared if staining was uniform and it was absent of extensive cellular debris or vacuoles. All measured sections were then normalized to the section with the largest amount of total spared tissue and converted to a percentage of spared tissue. The section with the least amount of total spared tissue was considered the lesion epicenter.

Data Analysis

Behavior: BBB scores were compared between groups across time within injury model (moderate or severe) using a two-way mixed model ANOVA with two factors: therapy (SCI-EX v. SCI-NX) and week (pre, 1-5). Since therapy began after the first week, week 1 was considered a pre-therapy week. Where appropriate Sidak multiple comparisons were performed as a post-hoc test. For the severely contused model we compared the change in BWS needed to allow the animals to take weight-supported steps during therapy using using a two-way mixed model ANOVA with two factors: therapy (SCI-EX v. SCI-NX) and week (pre, 1-5). Since therapy began after the first week, week 1 was considered a pre-therapy week. Where appropriate Sidak multiple comparisons were performed as a post-hoc test.

Histology: Spared white and grey matter were compared between groups at week 5 for moderate and week 10 for severe using a two-way mixed model ANOVA with two factors: therapy (SCI-EX v. SCI-NX) and distance from epicenter (0. +/- 10mm, 0.25 mm increments).

Motor Maps*:* Previously published methods were used to assess changes in motor maps. Animals with at least 75% sampling of each region (LTM1, UTM1 and HLM1) were considered for quantification of trunk area/animal (28, 34) and trunk center-of-gravity (22, 24). Trunk area/animal was calculated as the total trunk site/animal scaled by the resolution (0.25 mm^2). Unpaired-t-test was done to compare trunk area between SCI-EX and SCI-NX animals. Center of gravity (CoG) was calculated separately for mediolateral and rostrocaudal shifts. CoG was defined as the mean rostrocaudal-extent or media-lateral extent of trunk representation across animals. Separate one-way ANOVAs were used to evaluate differences in trunk CoG for rostro-caudal and medio-lateral directions. Tukey post-hoc was applied where appropriate to assess difference between groups (INTACT, SCI-EX, SCI-NEX). Finally, the motor cortex was also divided into regions (LTM1, UTM1, HLM1) and the probability (%) of recruiting any trunk musculature was calculated. If ICMS at a particular location recruited trunk musculature, the conditional probability of recruiting segmental trunk musculature (upper/mid or lower) was calculated. It is important to note that this ICMS recruitment was not necessarily exclusive, and the segmental co-coactivations of trunk musculature were represented as pie charts. Independent Chi-square test done to test for significant differences in the likelihood to recruit trunk/segmental trunk musculature between INTACT, SCI-NX and SCI-EX animals. Fischer's exact test, Bonferroni adjusted post-hocs using chi- square test were done where appropriate. Finally, the likelihood to activate trunk musculature in LTM1 was compared between animals that received exercise therapy and those that did not.

EMG Analysis*:* Motor evoked potentials (MEPs) were obtained by averaging the processed EMG over a time window of 1 s centered on the onset of the current stimulus. If the amplitude of a MEP exceeded the background EMG activity by five standard deviations, it was considered a responsive EMG. MEPs were averaged across animals and compared between groups. MEP amplitude was defined as the ratio of the average EMG amplitude in the response window relative to the mean background activity. The EMG amplitude of muscles in response to ICMS was compared between SCI-EX and SCI-NX separately for muscles below, at and above the level of the lesion using unpaired Student's t-test.

All p's provided are adjusted for multiple comparisons and presented as * $p<0.05$, ** $p<0.01$, *** $p<0.005$ and **** $p<0.001$ in the figures.

Chapter 4: Functional relevance of therapy mediated cortical reorganization in neuronal encoding of posture and weight supported stepping on a treadmill after moderate, mid-thoracic spinal cord injury in the rat

Introduction

Postural responses are the actions taken to maintain balance, by means of pelvic roll and shifting COP within base of support. Decerebration studies have demonstrated that cortex is not essential

in the maintenance of basic postures such as standing and walking (222), and the ability to maintain balance in the tilt task (223). Despite the non-essential nature of the cortex in postural tasks, previous studies (83, 159, 224, 225) show that many neurons in the motor cortex modulate their activity in response to postural perturbation. In fact, postural responses have been well defined in animal models including many injury conditions, from decerebration to a range of spinal cord injuries (138, 163, 226). Postural control in complete spinal cord injury models is impaired (175), despite the ability to regain stepping with step training and spinal stimulation (227, 228). The effect of therapy in improving postural control and the associated role of the cortex is unclear, especially in the partial injury model.

Similarly, motor cortex (M1) plays a facilitatory role rather than an obligatory role in the regulation of locomotion in the intact state. However, M1 plays an obligatory role in the rehabilitation assisted recovery of volitional locomotion after SCI. In fact, after SCI, in both neonatally spinalized (9) as well as adult rats (11) therapy mediated recovery of weight supported stepping in the open-field is lost after lesioning the regions of the reorganized trunk motor cortex. In a recent study (211), silencing motor cortex projections to brain stem abolished therapy mediated improvement in volitional leg movements during swimming after a severe spinal cord injury, while there was no impact in intact animals.

Neurons in the motor cortex have been also been shown to preferentially fire at specific phases of step cycle of both the forelimbs and hindlimbs during active locomotion (107, 229–231). In fact, after spinal cord injury, the neuronal encoding of population of M1 neurons about step height during locomotion was enhanced after brain-controlled neuromodulation therapy paired with rehabilitation (115, 203).

Additionally, evaluating cellular and network plasticity in the cortex during the recovery process will help us understand how plasticity in the cortex changes over time and whether there the changes are correlated to behavioral improvements after the injury. This approach can help us in lend insight in helping us understand the therapeutic window for the intervention that maximizes recovery of function as well as neuroplasticity in M1.

These reasons make M1, a compelling region to examine cellular plasticity and altered neuronal encoding strategies associated with rehabilitation assisted recovery of locomotion after spinal cord injury.

In this chapter, I examine cellular and network plasticity differences associated with spontaneous recovery and rehabilitation assisted recovery changes over time, by recording neural activity in trunk M1 in animals with moderate spinal contusion injury chronically over time during postural control on a tilt platform and during weight supported stepping on a treadmill.

Result

Exercise therapy improves postural control during locomotion by reducing hindlimb base of support.

The base of support (BOS) was evaluated in animals that were able to achieve weight supported stepping throughout an entire run on the CatWalk® as the animal volitionally walked over a glass plate. Base of support was quantified 5 weeks post injury in SCI-EX (n = 6) and SCI-NX (n = 7) animals. In a subset of animals, therapy was continued for up to 9 weeks post SCI and changes in BOS relative to pre-injury baseline calculated. The base of support in the forelimb was not significantly affected post injury at week 5 (unpaired t-test, p = 0.29, Figure 1A). Surprisingly, therapy decreased rather than increased hindlimb BOS seen in SCI-NX animals (unpaired t- test, p = 0.03, figure 1B). This reduction in the HL BOS was likely to be maintained at week 9 (unpaired

t-test, p = 0.01, figure 1c). In addition, the FL base of support increased in animals that received therapy at week 9 (unpaired t-test, p = 0.01, Figure 1d)

The relative increase in HL BOS from pre-injury levels reflects the compensatory behavioral strategy adopted by SCI-NX animals by widening their base of support in hindlimbs leading to better stability during walking. Animals that received therapy (SCI-EX) were able to maintain postural control while walking on a glass plate by reducing the base of support of their hindlimbs compared to pre-injury levels reflecting a novel adaptive behavioral compensation.

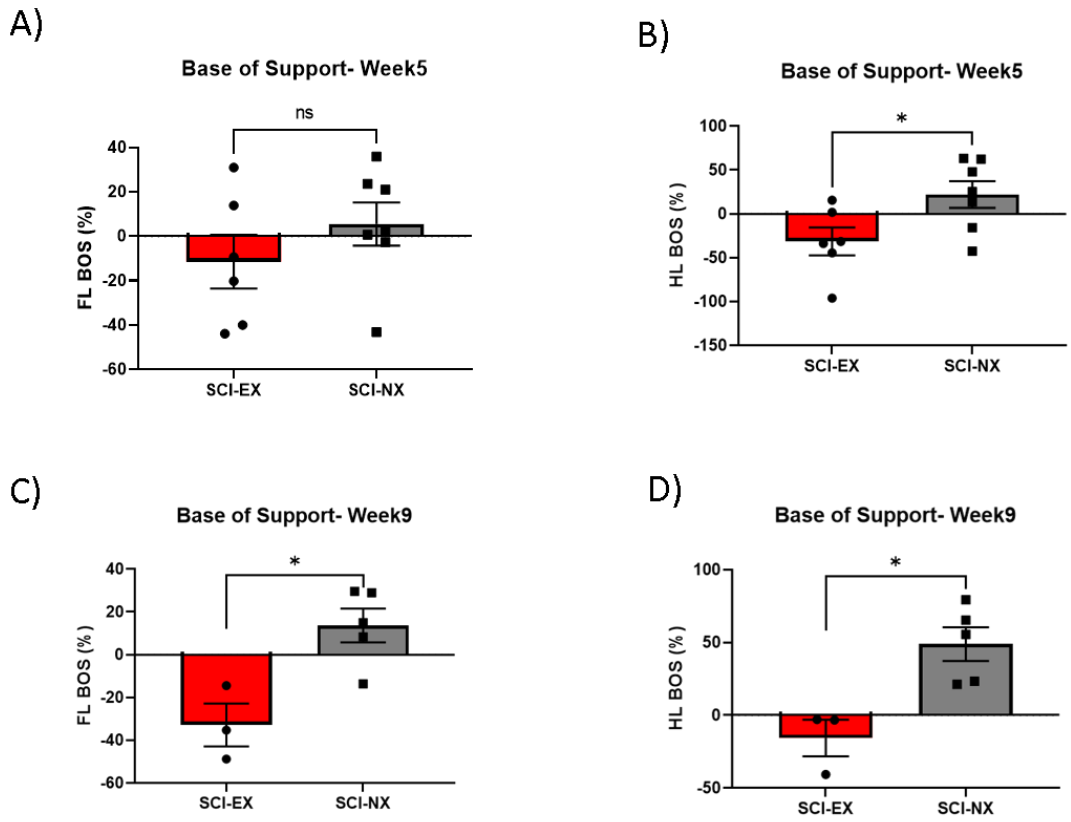

Figure 4. 1 Exercise therapy after SCI improves postural control during locomotion. Base of support evaluated in SCI-NX (n=7) and SCI-EX (n=6) at week 5 and week 9 post SCI, in animals that can take weight supported steps. Relative changes in hindlimb base of support compared to pre-injury level quantified at week 5 and week 9 respectively, therapy prevented the increase in HL BOS seen in SCI-NX animals post injury A) FL BOS at week 5 not impacted by therapy B) HL BOS reduced in animals in SCI-EX animals, while

increased in SCI-NX animals C, D) Therapy impacted both forelimb and hindlimb base of support at week 9. error bars represent mean +/- 1SEM, unpaired –t –test, * represents p <0.05.

Exercise therapy post SCI prevents loss of neuronal responsiveness to postural perturbations. PSTH's of single neuron activity in the reorganized cortex were constructed to evaluate responsiveness to slow and fast tilts. Neurons can modulate their firing rate by increasing their firing rate above background (excitatory response), decreasing its firing rate below background (inhibitory response) or have phases during the tilt where there is both an excitatory as well as inhibitory response (active inhibitory). If the neuron did not have any of the above physiological response, it was considered nonresponsive. The proportion of responsive neurons in the reorganized cortex to both slow tilt and fast tilt were evaluated irrespective of the tilt direction for SCI-EX and SCI-NX animals across weeks. There were no significant differences in the total number of neurons recorded per animal across time [2 Way ANOVA Time: $F(3, 40) = 0.37$, $p = 0.77$] or between therapy and non-therapy animals [2 Way ANOVA therapy: $F(1, 40) = 1.028$, $p = 0.31$, *Figure 2B*]. Hence, the total number of neurons sampled between groups (SCI-EX /SCI-NX), and the total number of neurons sampled per animal remained consistent across weeks from week 1 to week 9 post injury. The proportion of neurons maximally responsive to a fast tilt decreased with time in SCI-NX animals (χ^2 (3, N=501) = 13.92, $p = 0.003$). In fact, by week 9, the proportion of responsive neurons were significantly lower compared to pre-injury levels (Bon ferroni adjusted Fisher's exact test, $p_{adj} = 0.01$). Surprisingly, in SCI-EX animals the proportion

of responsive neurons to fast tilts remained consistent after SCI (χ^2 (3, N=806) = 0.146, *p = 0.985)*. Proportion of neurons responsive to fast tilts were in fact similar between SCI-EX and SCI-NX animals pre-injury (Bon-ferroni corrected Fisher's exact test, $p_{adj} > 0.1$) and at 1 week post injury (Bon-ferroni corrected Fischer's exact test, $p_{adj} = 0.72$) prior to therapy onset. Moreover, SCI-EX animals were significantly more responsive to fast tilts compared to SCI-NX animals at week 5 (SCI-EX vs SCI-NX week5, $p_{adj} < 0.001$) and week 9 post injury (SCI-EX vs SCI-NX week9 $p_{adj} < 0.0001$).

Similarly, for slow tilts the proportion of responsive neurons decreased with time in SCI-NX animals (χ^2 (3, N=501) = 9.373, *p = 0.024*). In fact, the proportion of neurons responsive to slow tilts 9 weeks post SCI were significantly lower than pre-injury levels in SCI-NX animals (Bon-ferroni corrected Post Hoc, fisher's exact test $p_{adj} = 0.016$). On the contrary, the proportion of responsive neurons in SCI-EX animals remained consistent after injury with no differences across weeks.

χ^2(3, N=806) = 13.92, *p = 0.00)*. Moreover, the proportion of responsive neurons were significantly higher in SCI-EX animals compared to SCI-NX animals 9 weeks post injury (Bon ferroni adjusted fisher's exact test, $p < 0.001$). These results suggest that exercise therapy modulates the cellular plasticity after SCI in the reorganized cortex (LTM1 and HLM1).

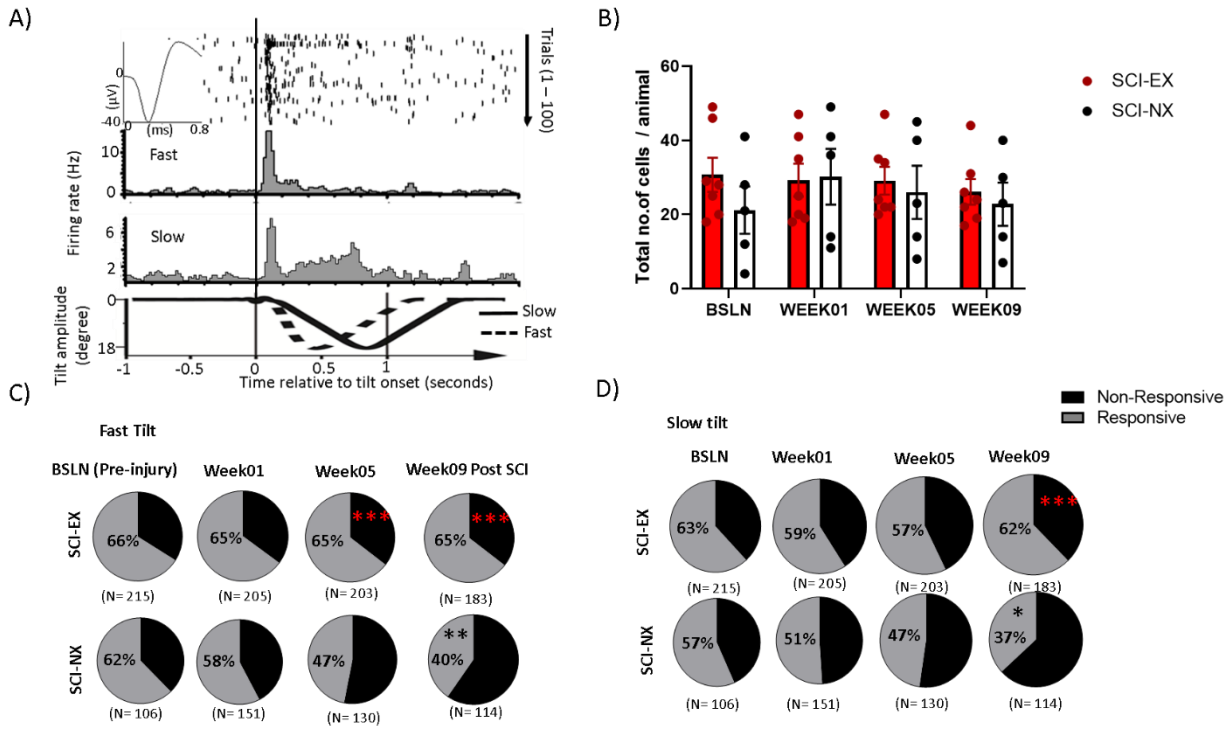

Figure 4. 2 Therapy prevents loss of neuronal responsiveness in the reorganized cortex (LTM1, HLM1) to postural perturbation A) Exemplar PSTH of a neuron in SCI-NX animal responsive to both slow and fast tilt 9 weeks post SCI B) The no. of cells recorded / animal for both animals that received the exercise therapy (SCI-EX =7) and animals that did not SCI-NX = 5) remained consistent across weeks and between groups. The error bars represent mean +/- 1 SEM C, D) Pie charts represent the proportion of neurons that modulated their firing rate (neuronal responsiveness) to fast and slow tilts respectively in SCI-EX and SCI-NX animals. N represents total no. of neurons recorded in each group. Therapy prevents the attenuation in the proportion of neurons responsive to both fast tilt by week 5 and slow tilts by week 9 post SCI in SCI-NX animals. Statistical comparisons for proportions done with chi-square test to test the differences across time separately for SCI-EX and SCI-NX animals, bon ferroni corrected Fisher's exact test done to test differences between SCI-EX and SCI-NX between groups. * - represents comparisons between SCI-EX and SCI-NX groups at a particular time point, * - represent comparisons within group (SCI-EX/SCI-NX) between different time points (* p< 0.05, *** p < 0.001)

Neural encoding associated with tilt detection impaired after SCI.

In the intact cortex both HLM1 and LTM1 were highly specialized for postural control (see chapter 1). Hence, to understand changes in neuronal encoding associated with 'slow and fast speed' tilt detection, mutual information was quantified in this reorganized region comprising of HLM1 and LTM1, at baseline (BSLN), week01, week05 and week09 post injury. The mutual information was

normalized to the pre-injury baseline (z scored) and statistical comparisons between time and impact of therapy were made with a 2-way ANOVA.

First, during fast tilts the amount of single neuron information in the re-organized cortex decreased after spinal cord injury (Time: *F (1, 2210) = 19.136, p <0.001*) with the information at week 1, 5 and 9 post injury significantly reduced compared to pre-injury baseline level (Sidak's Post Hoc BSLN vs week1, 5 and 9, p<0.0001). However, there was no impact of therapy (Therapy: F (1,2210) = 1.638, p = 0.2, Figure 2A) on the changes in mutual information in detecting fast tilts.

Similarly, there was a decrease in the mutual information in the cortex to detect slow tilts after injury (2 Way ANOVA time F (3, 2094) = 12.782, p < 0.0001) with the information at week 1, **5** and 9 post injury significantly reduced compared to pre-injury baseline level (Sidak's Post Hoc BSLN vs week1, 5 and 9, p<0.0001). Surprisingly, this decrease in mutual information post SCI was attenuated in SCI-EX animals (Therapy: F (1, 2094) = 3.964, p = 0.047, figure 3B) with no significant interaction. These results suggest that neurons in the reorganized cortex decrease their neuronal encoding to detect tilts on a single trial basis.

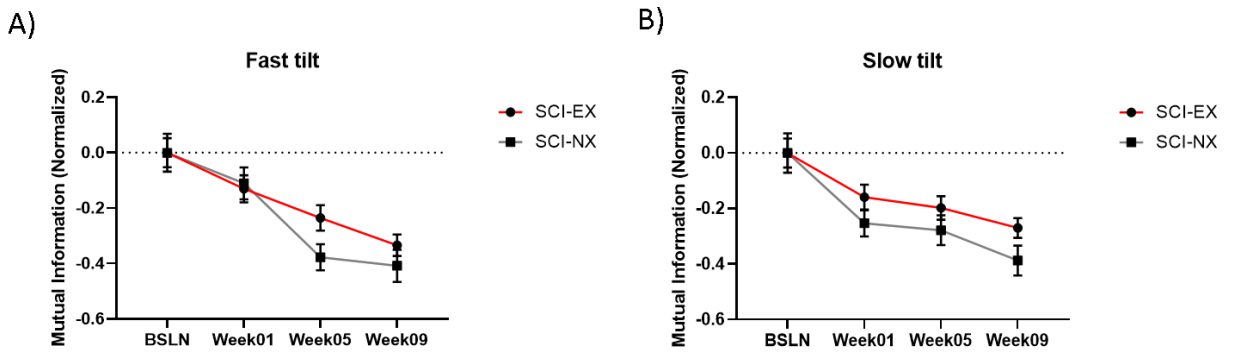

Figure 4.3: Neural encoding associated with tilt detection impaired after SCI. Single neuron mutual information about tilt type, normalized to pre-injury baseline level (Z-score) evaluated across weeks between SCI-EX (n =7) and SCI-NX (n = 5) animals. The no. of response between two groups (SCI-EX, SCI-NX) at each week are as follows (BSLN (362, 197), Week01 (306, 279), Week 05 (302, 220) and week 09 (283, 153))). Mutual information pre-injury about slow tilt (SCI-EX: 0.11+/- 0.007 bits, SCI-NX: 0.13+/- 0.01

bits) and fast tilts (SCI-EX: 0.14+/- 0.007 bits, SCI-NX: 0.13+/- 0.008 bits) were similar between both groups. A) Mutual information in cortex in encoding for fast tilt reduces regardless of therapy B) Mutual information about slow tilts also decrease with time. All the error bars represent mean +/- 1 SEM.

After SCI, firing rate of responsive cortical neurons decrease, latency onset increases in response to postural perturbation.

To gain insight on the neural encoding strategy in cortex about tilt, the firing rate properties of responsive neurons (average response firing rate and first bin latency of response from tilt onset) to a slow/ fast tilt was quantified.

Average firing rate of neurons responsive to fast tilts decreased after SCI in both SCI-EX and SCI-NX (2 Way ANOVA, Time: *(F (3, 1265) = 12.82, p <0.0001, Figure 4A)* animals regardless of therapy. SCI-NX animals reduce their firing rate to fast tilts early, by week 5 post SCI [2 WAY ANOVA, time* therapy: *F (3, 1265) = 2.742, p <0.05, Sidak's multiple comparison SCI-EX BSLN, Week05, p < 0.0001*) and remained consistent, at week 9 *(Sidak's multiple comparison SCI-EX Week05, Week09, p = 0.99)*. In animals that did not receive therapy the neurons that were responsive did not decrease the firing rate until week 9 post injury *(Sidak's multiple comparison SCI-NX (BSLN, Week09, p = 0.0012)*.

Similar reductions in response firing rate were observed in neurons responsive to slow tilts regardless of therapy (2 Way ANOVA, Time: $F(3, 1077) = 10.12$, *p <0.0001, Figure 4B)*. Responsive neurons in SCI-EX animals reduce their firing rate as early as week 5 (2 WAY ANOVA, time* therapy: F (3, 1077) = 4.232 p *<0.01), Sidak multiple comparison SCI-EX (BSLN, Week05), p < 0.001*) while the responsive neurons of non-therapy animals decrease their firing rate by week9 post SCI *(Sidak's multiple comparison SCI-NX (week5 Week09, p = 0.001))*.

Not surprisingly, the latency onset of responsive neurons to fast tilt increased in both groups regardless of therapy after SCI (2-way ANOVA time: $F(3, 1265) = 7.262$, $p < 0.0001$). There was no impact of therapy or interaction between therapy and time, however. The latency onset was significantly higher compared to pre-injury condition by 5 weeks post SCI (Sidak's multiple comparison BSLN vs week5, $p = 0.004$).

Latency onset of responsive neurons to slow tilts also increased after injury *(2-way ANOVA Time $F(3, 1077) = 10.12$, $p < 0.0001$)* by week 5 post Injury (Sidak's multiple comparison, *$p = 0.002$*), however the increase in latency was attenuated in SCI-EX animals (2-way ANOVA Therapy: $F(1, 1077) = 23.76$, $p < 0.001$))

In summary, responsive neurons in animals that received therapy modulate their firing rate as early as week 5 for both and fast tilts and have attenuated increases in latency onset to the slow tilt compared to non- exercise animals. Taken together these suggest an altered strategy of neurons to encode for fast and slow tilts by reducing their firing rate and increasing the latency onset after SCI.

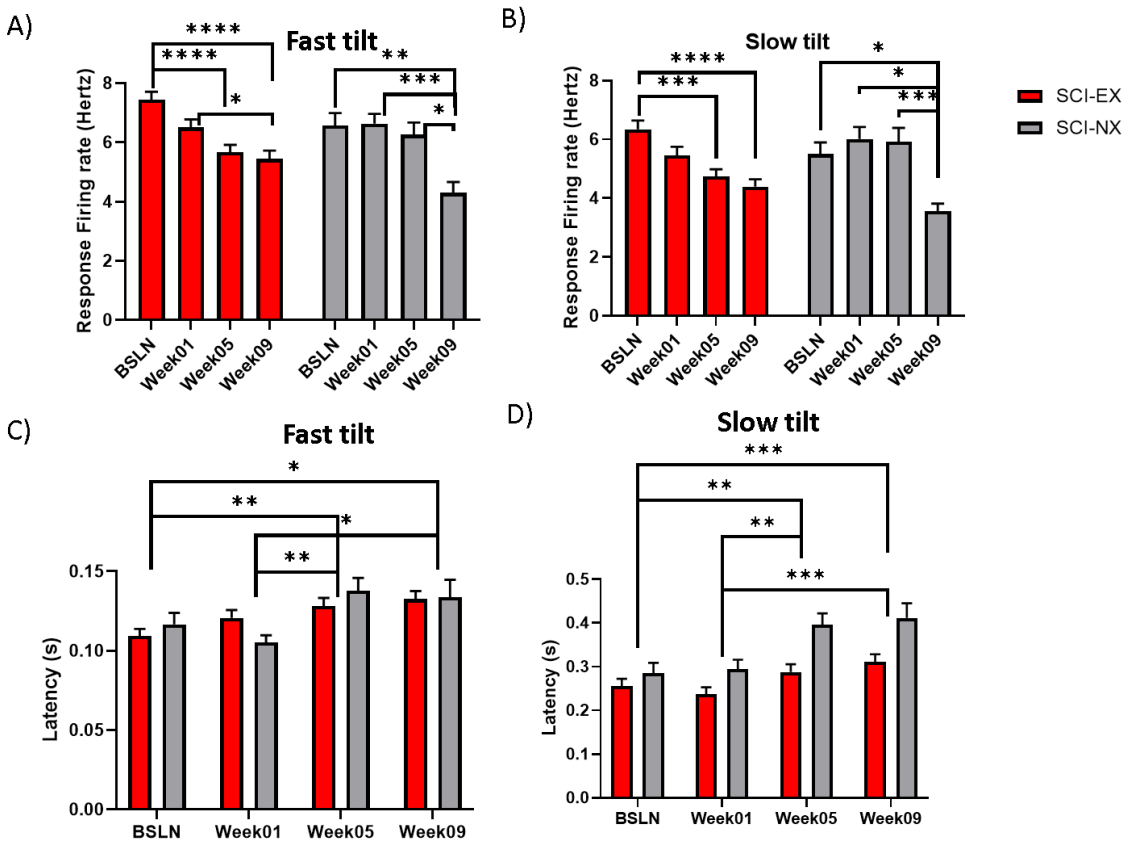

Figure 4. 4 Firing rate of neurons decrease while the latency onset increase after SCI A, B) The average response firing rate decreases after SCI in SCI-EX animals by week 5 and in SCI-NX animals by week 9 post injury for both slow and fast tilts. C, D) Latency onset of neuronal response increases after SCI, regardless of therapy for fast tilts, while the increase in the latency onset is attenuated by therapy for slow tilts. Statistical comparisons were done with 2-way ANOVA, all error bars represent mean +/- 1SEM.

Exercise therapy facilitates improvement in recovery of toe height after SCI accompanied by enhanced neuronal modulation during weight supported stepping on a treadmill.

Kinematic recordings and simultaneous neural data were acquired in animals as they took weight supported steps on a treadmill on SCI-EX (N=6) and SCI-NX (N= 4). Fifty percent of SCI-EX animals and 3/4 of SCI-NX animals were able to take at least take occasional weight supported steps by week 2 (BBB score >-=10). Hence, changes in toe-height during weight supported step cycles were quantified between SCI-EX and SCI-NX animals that were able take at least

occasional weight supported steps 2 weeks post injury without any vertical or lateral support. First, there were changes in toe height with time after injury *(2 Way ANOVA time: $F(2, 1664) = 20.90$, $p < 0.0001$)* and toe height was impacted by therapy *(2 Way ANOVA $F(1, 1664) = 13.15$, $p < 0.001$*) and a significant interaction effect ($F(2, 1664) = 13.62$, $p < 0.0001$)

In animals that were not given any therapy (SCI-NX), the toe height during weight supported stepping, did not change from Week 2 to week 5 (Tukey's multiple comparison, Padj = 0.15) while toe height increased significantly from week 2 to 5 during the early phase of treadmill training in SCI-EX animals (Tukey's multiple comparison, Padj <0.0001).

During the late phase of treadmill training (week5- week9), therapy animals maintained the increase in toe height with no differences between week 5 and week 9 post SCI (Tukey's multiple comparison, Padj = 0.10), while animals that did not receive any therapy significantly decreased their toe height from week 5 to 9 post injury (Tukey's multiple comparison, Padj <0.0001).

These results support evidence that exercise therapy enhances recovery of locomotion especially during the early phase of treadmill training while supporting maintenance in functional improvement during the late phase of treadmill training (Week 5 -week8) . The neuronal activity of single neurons in the reorganized cortex (LTM1, HLM1) were recorded, responsiveness of neurons (Phase modulated activity during step cycle) and depth of modulation of phase modulated cells were calculated at week 2, 5 and 9.

Surprisingly, neurons continue to modulate neuronal activity during step cycle after spinal cord injury during treadmill locomotion as early as week2 post SCI. In fact, the proportion of neurons that were phase modulated (Rayleigh's test, $p < 0.05$) remained consistent across weeks 2 -9 in both SCI-EX ($\chi^2(2, 512) = 2.797$, $p = 0.4570$) and SCI-NX animals ($\chi^2(2, 307) = 1.561$, $p = 0.45$).

However, the proportional of phase modulated cells were significantly higher in SCI-EX compared to SCI-NX animals at week 2 (SCI-EX: 59/172 (34%), SCI-NX: 16/106 (15%), Bon Ferroni-adjusted Fisher's exact test, $p_{adj} = 0.0015$) and week 5 (SCI-EX: 63/177 (36%), SCI-NX: 23/106 (22%), Bon Ferroni- adjusted Fisher's exact test, $p_{adj} = 0.048$) but not week 9 (SCI-EX: 45/163 (28%), SCI-NX: 17/95 (18%), Bon Ferroni- adjusted Fisher's exact test, $p_{adj} = 0.28$).

The change in the magnitude of firing rate (depth of modulation) during a step cycle was significantly higher in animals that received therapy across all weeks compared SCI-NX animals (2 way ANOVA Therapy: $F\ (1, 217) = 12.38, p < 0.001$), while there was no significant changes across time (2 way ANOVA Therapy: $F\ (1, 217) = 1.621, p = 0.2$) and no significant interaction (2 way ANOVA therapy*time: $F\ (2, 217) = 0.2381, p = 0.78$). These results taken together suggest that exercise therapy enhances both recovery of toe height and enhanced modulation of neuronal activity during treadmill locomotion especially during the early phase of treadmill training (week2 – week5).

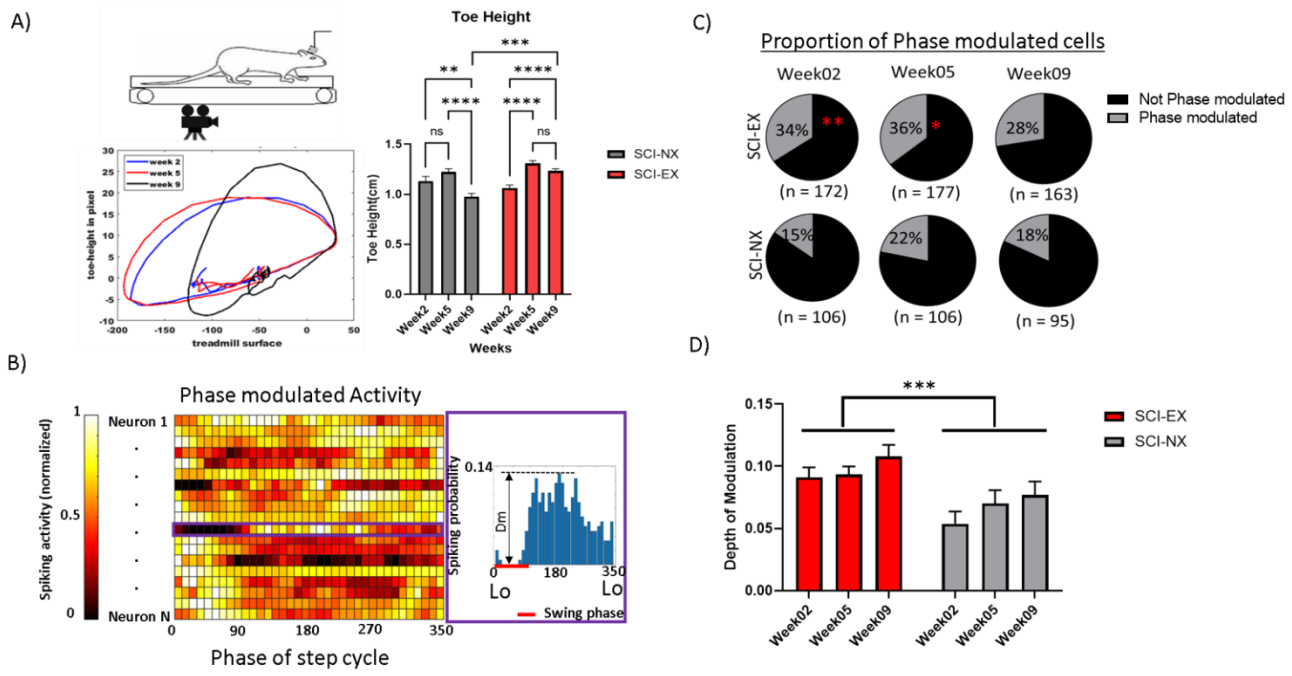

Figure 4. 5 Exercise therapy facilitates recovery of toe-height and enhanced neuronal modulation during treadmill locomotion A) Simultaneous kinematic recordings and neural activity recorded in SCI-EX (n = 6) and SCI-NX (n= 4) during unassisted treadmill locomotion. A) Hindlimb toe-height of weight supported steps was quantified in a subset of animals (SCI-NX = 3, SCI-EX =3) that could at least take occasional weight supported steps at week2. Exemplar Hindlimb toe height trajectories of an animal plotted across weeks; each weight supported step was considered an independent sample. Toe height improved in animals that undergo physical therapy (SCI-EX) especially during the early weeks of training. B) Examplar PSTH raster of phase modulated neuronal activity. The spiking probability of each neuron (y axis) to a particular phase of the step cycle (x axis) plotted. C) The proportion of phase modulated cells were significantly higher in the animals that received physical therapy week 2 and 5 post SCI compared to SCI-NX animals. Bon-ferroni adjusted Fisher's exact test used to compare difference between animal groups. D) Depth of modulation of phase modulated cells between SCI-EX and SCI NX (No of phase modulated cells: SCI-EX, SCI-NX) evaluated at week2 (59, 16), week5 (63, 23) and week 9 (45,17). Exercise therapy enhanced depth of modulation.

Discussion

Therapy altered postural control strategy during locomotion.

Animals that spontaneously recovered the ability to take weight-supported stepping increased their hindlimb base of support during locomotion, this is likely a strategy to compensate for postural instability such that the COP is always within the base of support during locomotion. This has been shown in a recent study in a cervical model of contusion injury (232). Animals that received the exercise therapy reduce their HL BOS during weight supported locomotion after spinal cord injury, indicating that exercise therapy altered postural control strategy during locomotion. Exercise therapy also improved recovery of toe height during the early phase of treadmill training. These findings re-enforce the idea that physical rehabilitation after SCI enhances the recovery of locomotion after SCI.

Altered Postural encoding after SCI and impact of therapy.

After SCI, neurons in the reorganized cortex (LTM1, HLM1) continued to encode for postural perturbation and weight supporting stepping during treadmill locomotion after SCI. However, the responsiveness was also reduced both in response to postural perturbation as well as during weight

supported stepping on treadmill. This could be due to a result in the disruption of somatosensory feedback from hindlimb. In the intact trunk system, somatosensory input to trunk M1 was dominated by hindlimb information (Refer chapter1).

Sensory integration from the visual system (144, 233), vestibular system (144, 234, 235) and somatosensory feedback (106, 226) from extremities, all play a role in postural control. However, in the absence of vision (144, 236) or vestibular input (144), postural control is driven by somatosensory feedback from the extremities (237). In fact, disruption of this somatosensory feedback due to spinal cord injury impaired ability to do postural corrections (156, 238). In the absence of hindlimb somatosensory feedback, the neurons LTM1 and HLM1 could likely receive input from above the level of the injury via proprioceptive feedback from upper trunk and forelimb.

After SCI, responsive neurons reduced their firing rate and increased their latency onset after injury. The neural encoding in reorganized cortex associated with tilt detection was also impaired.

Therapy interestingly prevented the loss of responsiveness of neurons to tilt, however it was not sufficient to ameliorate the loss in mutual information in the cortex regarding tilt detection. Exercise therapy through activity dependent plasticity could potentially improve somatosensory feedback to M1 by strengthening spared circuits above as well as below the level of lesion.

Therapy dependent reorganization of lower thoracic trunk M1 could also contribute to the maintenance of neuronal responsiveness to postural perturbation after SCI (Chapter 2)

Proportion of phase modulated cells and their depth of modulation was enhanced at week 2 and 5 post injury in animals that received therapy after SCI. Increase in the depth of modulation.

More work is needed to understand whether these changes in phase modulated activity leads to increase in neuronal encoding of weight supported stepping and the source of altered afferent

feedback to M1. Understanding changes in cellular plasticity with time after SCI and the impact of rehabilitation on these changes can lend insight into the improvement of brain-controlled neuromodulation therapies or BMI-FES systems targeted at restoring volitional locomotion and postural control.

Methods

Experimental design

A total of (SCI-EX =7) and (SCI-NX =7) female Sprague Dawley rats were chronically implanted with microwire arrays in the reorganized cortex spanning both lower thoracic trunk M1 and HLM1. Neuronal activity was recorded during tilt task (Refer chapter 1) along with BBB score (refer chapter 2) and catwalk pre-injury. Animals received a moderate contusion injury at T10 and started quadrupedal treadmill training starting after 1 week post injury (refer chapter 2) until 8 weeks post injury. Week1 recordings were carried out before the therapy onset. Kinematic and neural recordings were done in a subset of animals (SCI-EX =6, SCI-NX = 4) at weeks 2, 5 and 9 post spinal cord injury. All experiments were done in compliance with the UC Davis IACUC.

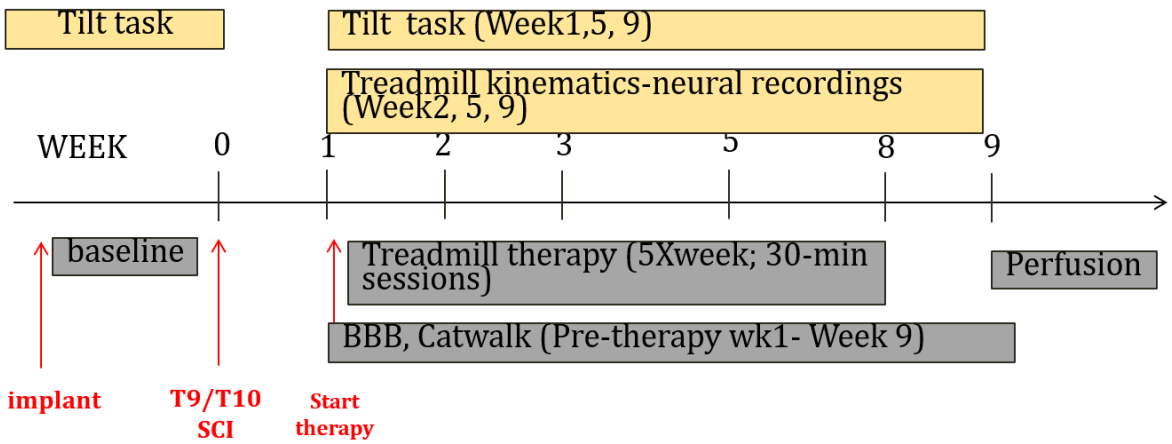

Figure 4. 6 Experimental design to assess functional relevance of sensorimotor integration.

Tilt task:

Animals were chronically implanted with chronic microwire arrays in regions of the putative trunk and hindlimb M1. Single neuron activity was evaluated in the reorganized cortex encompassing putative LTM1 and HLM1 region identified previously, in response to un-expected postural perturbation along the lateral plane as the animals actively maintained balance. The Neuronal activity in M1 in response to 2 varying tilt severity, a slow speed (: max speed: 26.2°/s; duration to final amplitude: 0.9 s) and a fast speed (max speed: 76.5°/s; duration to final amplitude: 0.5 s). The final angle for all tilt types had the same final amplitude of 16.5° (refer chapter 1).

Single neuron measures: Peristimulus time histograms were constructed around 1 second preceding start of tilt and the duration to reach final amplitude (0.5 seconds – Fast tilt, 0.9 seconds – slow tilt) with a bin size of 20ms. Responsiveness, firing rate and latency of single neurons quantified as measures of cellular plasticity. A neuron was considered responsive to a particular tilt if the neuronal activity in the response window exceeded background by 2 standard deviations from background (threshold) with an at-least 5 consecutive bins above threshold. Response clusters

were identified. A response cluster is defined as neuronal activity comprising of at least 5 consecutive bins above threshold, with a minimum bin gap of 2 consecutive bins below separating response clusters. For responsive neurons, first bin latency was defined as the first of the consecutive bins to exceed threshold, while last bin latency was last time bin beyond which there is at least 2 consecutive bins below threshold. Firing rate and latency evaluated for the first response cluster. Response duration is defined as the duration between in the first and last bin of first cluster. Response magnitude was defined as the total no. of spikes that occurred between the first and last bin latency. Response firing rate (in Hz) was estimated as the response magnitude divided by the respective response duration and represents the average firing rate of the cell in response to postural perturbation.

Information analysis: Information Analysis: Information was quantified using a PSTH-based method (126). In short, PSTHs were generated to find the average response profile (100 trials) of each neuron to each event. In a leave-on-out manner, individual trials were compared to the average response (generated without the single trial) and the difference between the single trial and the average profiles was calculated in a bin-bin comparison. The single trial was classified as either a particular tilt response or a background response by identifying the profile with the smallest difference from the single trial. Performance was expressed as the percentage of correctly classified trials. The information was calculated using Shannon's information formula, formally defined as:

$$I(s;r) = \sum_{s,r} P(r,s)\, log_2 \left[\frac{P(r,s)}{P(r)P(s)}\right] \quad \text{(Equation 1)}$$

Where P(r), P(s), and P(r,s) correspond to the probability of the tilt-perturbation response *r*, the tilt perturbation stimulus *s*, and their joint probability, respectively. *I(s;r)*, which is measured in bits, was calculated for each neuron using the actual and predicted tilt type confusion matrix generated when applying the classifier. Residual bias for *I(s;r)* was then estimated using a bootstrapping procedure by pairing the trial response and tilt types in a randomized order – effectively eliminating their associations. This bootstrapping procedure was performed 100 times, and the calculated bias was subtracted from *I(s;r)* such that 0 bits is chance. The corrected mutual information was calculated as the difference relative to residual bias and was used for further analysis only if corrected mutual information was greater than 0.

To establish the bin size that resulted in the maximal PSTH classifier performance, a range of bin sizes between 5ms and 500ms were considered. For tilt detection, the window of time required to reach final amplitude after tilt onset considered. Th optimal bin size was determined to be 50ms across animals, so this bin size was used for all information analyses.

Base of Support: The paw prints during walking can be recorded using were tracked with a high-speed camera as animals walked through a glass plate using the catwalk locomotion analysis system (Noldus Information Technology). Base of support (BOS) is defined as the distance between the two fore pawpads (FL BOS) or hindlimb (HL BOS). Animal maintains its balance during stance and in locomotion by maintaining the center of pressure of the body staying within its base of support. BOS was assessed in animals that were able to take weight supported steps after moderate contusion injury. BOS was evaluated at week 5 and week 9 post injury to understand the changes in behavioral adaptation as the animal balances itself and walks along a narrow glass way.

Kinematic analysis during unassisted weight supported stepping on treadmill:

Kinematic and neural data were collected at week2, 5, and 9 post spinal cord injury using plexon Data acquisition system (Cineplex). Cameras were setup on either side of the treadmill to capture the movement of all the four paws simultaneously, as the animal walked on the treadmill. Colored markers applied to toe of hind paws and forepaws. The cameras tracked cartesian co-ordinates of the markers at 80 frames per second to characterize weight supported stepping. Percentage of Weight supported stepping (%WSS) was quantified as the proportion of hindlimb steps that were weight supported throughout the entire step cycle defined by the forelimb Lift-off (100 forelimb step cycle). A step was considered to have weight support, if during a hind paw step, the abdomen, pelvis, and knee are completely off the treadmill belt, and the animal successfully transfers the load to the other weight bearing limb during a step cycle. MATLAB script was used to extract the toe position data, lift off times. Toe height calculated, for all weight supported steps. These measures are evaluated at weeks 2,5 and 9 after SCI in SCI-EX and SCI-NX animals. (2 Way ANOVA) comparisons are made to evaluate effect of time and the Therapy in the recovery of function after SCI.

Neural Data and analysis (Treadmill task)

Analog local field potential signals from the chronic micro wire arrays were filtered and amplified using multi-neuron acquisition processor (MNAP, Plexon, and Dallas, TX). Single neurons were discriminated online before each recording session. Neural recordings and Kinematic video recordings were done simultaneously such that the signals are synchronized between the 2 systems. PETH were constructed from the extracted lift off times for each of the paws (L-FL-LO, L-HL-LO, R-F-LO, R-HL-LO). Since the step cycle duration/ stride duration varies for each step, to

identify phase modulated activity, the response window is normalized to the respective stride duration. The cell's activity during the step cycle (L-Forelimb Lift off to subsequent L-forelimb Lift off) of each step cycle is analyzed. Like previous studies assessing phase modulated activity during locomotion (Beloozerova & Sirota, 1988; Drew & Doucet, 1991), rayliegh's test used to classify whether the cells are significantly phase modulated during step cycle ($p<0.05$). Depth of modulation (Dm) was calculated in phase modulated cells, defined as the difference between the peak firing rate and minimum firing rate within the step cycle. Proportion of phase modulated cells and their depth of modulation was evaluated in animals that received exercise therapy (SCI-EX) and non-therapy animals (SCI-NX).

Statistical comparisons for proportion of phase modulated cells were done within group (SCI-EX/NX) to understand changes with time (Week02, Week05, Week09) using independent chi square test. Bonferroni corrected Fisher's exact test were done to understand differences between pre-injury baseline and post injury time points.

Depth of modulation was evaluated for phase modulated cells and a 2-Way ANOVA test was done to understand the impact of therapy and time.

Discussion, Conclusion, and future directions

In Chapter 2, I investigated the organization of trunk M1 and sensorimotor integration in trunk M1 in intact animals and found that there is an extensive integration of hindlimb somatosensory input in both trunk S1 and M1. Within trunk M1, lower thoracic trunk M1 was identified and more specialized in postural encoding than upper trunk M1 region.

In Chapter 3, I investigated the network level plasticity changes between rehabilitation assisted recovery and animals that spontaneously recover using 2 contusion injury models with varying severity.

Rehabilitation dependent enhancement of spontaneous recovery of locomotion was associated with reorganization in putative LTM1, associated with re-establishing cortical control of lower thoracic trunk muscles below the injury level.

Rehabilitation independent spontaneous recovery to regain weight supported stepping was associated with expansion of trunk M1 into de-efferent HLM1.

In Chapter 4, I examined the changes in cellular neuroplasticity with time up to 9 weeks post SCI associated with neuronal encoding of posture and weight supported stepping on a treadmill. Exercise therapy prevented the loss of neuronal responsiveness to postural perturbations after SCI and the enhanced neuronal modulation during treadmill locomotion.

These results from this thesis points out the following take home message that strategy adopted by rehabilitation assisted plasticity relied on re-establishing control of trunk muscles of below the injury while animals that spontaneously recovered relied on establishing control of muscle at the level of injury. The results also suggest that LTM1 could be a good target for neuromodulation and BMI applications relevant for postural control. We still do not understand how the cortex is able to recruit trunk muscles below the injury. Trunk muscles have multisegmented innervation and could span the lesion site. Therapy could promote axonal sprouting of CST axons rostral to injury (11, 239) and trigger muscle responses below injury and indirectly recruit lower thoracic muscles via reflex chaining with mid thoracic muscles at the level of the injury. Another possibility could be that exercise therapy could promote CST sprouting in the cervical grey matter and contact long descending propriospinal neurons that can directly relay the information to areas below the level of injury. (184, 186, 240, 241). Recent studies also point out that activity dependent plasticity influences the propriospinal neurons and the maintenance of synaptic contacts

of axotomized CST with the propriospinal network at cervical level. Silencing the propriospinal pathway selectively with chemo genetic approaches also impeded spontaneous recovery (242).

Anatomical tracing studies can shed light on the mechanisms of cortical reorganization associated with recovery of function. The cortex continued to encode for changes in posture and during treadmill locomotion despite a spinal injury, that completely disrupted direct cortical control of hindlimb musculature. While the trunk biomechanically coupled upper and lower extremities, they could also serve as a sensory relay of proprioceptive information from regions below the level of the lesion. This Proprioceptive information from the trunk could explain the integration of somatosensory info from lower extremities in the cortex after spinal injury. Another possibility is the extensive integration of proprioceptive information from upper extremities and trunk in the cortex after spinal injury. Dissecting contribution of proprioceptive feedback by selectively silencing proprioceptive afferents of trunk with chemo genetic/ pharma logical approaches can also help understand the role of trunk sensory afferents in relaying information to the cortex. More work is needed to understand sensorimotor integration of trunk proprioceptive information after a spinal injury and whether enhanced somatosensory feedback via trunk could be beneficial to the recovery of volitional control of lower extremities. Recent work (243) has shown that paired corticospinal motor neuronal stimulation (PCMS) combined with physical rehabilitation can improve recovery of function. This recovery of function was mediated by corticospinal motor neuronal plasticity and improved outcomes persisted beyond the therapy period. A similar approach could be used by pairing the corticospinal input from the lower thoracic trunk motor cortex with somatosensory and proprioceptive input from lower trunk by means of neural stimulation. Understanding the trunk sensorimotor system and changes in the organization after injury can provide roadmaps to harness recovery of function after spinal cord injury.

Appendix

Supplementary information (Chapter 2)

Muscle synergy analysis of coactivation zones within trunk M1

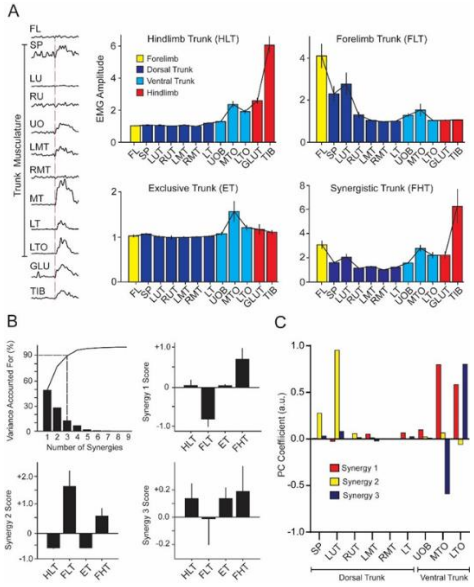

Supp Figure 2. 1 Muscle synergy analysis of the different coactivation zones in trunk M1. A) Average MEP amplitude within the different coactivation zones (HLT [N =174], FLT [N = 38], FHT [N = 85], and ET [N = 10]). EMG electrodes implanted along the trunk, forelimb, and hindlimb musculature (Top to bottom: Forelimb bicep [bicep], spinous trapezius [SP], left upper thoracic longissimus [LUT], right upper thoracic longissimus [RUT], upper external oblique [UOB], left mid thoracic longissimus [LMT], right mid thoracic longissimus [RMT], mid thoracic external oblique [MTO], lower thoracic longissimus [LT], lower thoracic external oblique [LTO], gluteus maximus [Glut], tibialis anterior [Tib]). B) PCA was performed to identify muscle synergies and their synergy scores were plotted. C) Synergy weights: Relative contribution of every trunk muscle towards the synergy was plotted. Three synergies were extracted that accounted for 90% of the cumulative variance in the data. Synergy 1 and synergy 3 represented ventral trunk musculature activation with the highest weights representing mid and lower thoracic muscles, synergy 2 represented dorsal trunk musculature activation with the highest weights representing the contralateral upper thoracic longissimus. The synergy scores were compared across coactivation zones to explain the role of the different muscle groups. For example, synergy 1 and synergy 2 explain the difference between FLT and HLT coactivation zones. Specifically, synergy 1 score of FLT was different from that of HLT by almost exclusive contribution of mid and lower thoracic ventral trunk musculature. Alternatively, the scores for synergy 2 were different between all coactivation zones, primarily through contribution of upper thoracic dorsal trunk musculature. Synergy 3 scores, whose predominate contribution was also from mid and lower thoracic ventral trunk, were not different between coactivation zones suggesting it might not be possible to explain differences between muscle contribution to exclusively trunk (ET) and contribution to coactivation zones.

Exemplar SEPs confirm stronger sensory integration between trunk and hindlimb vs. forelimb

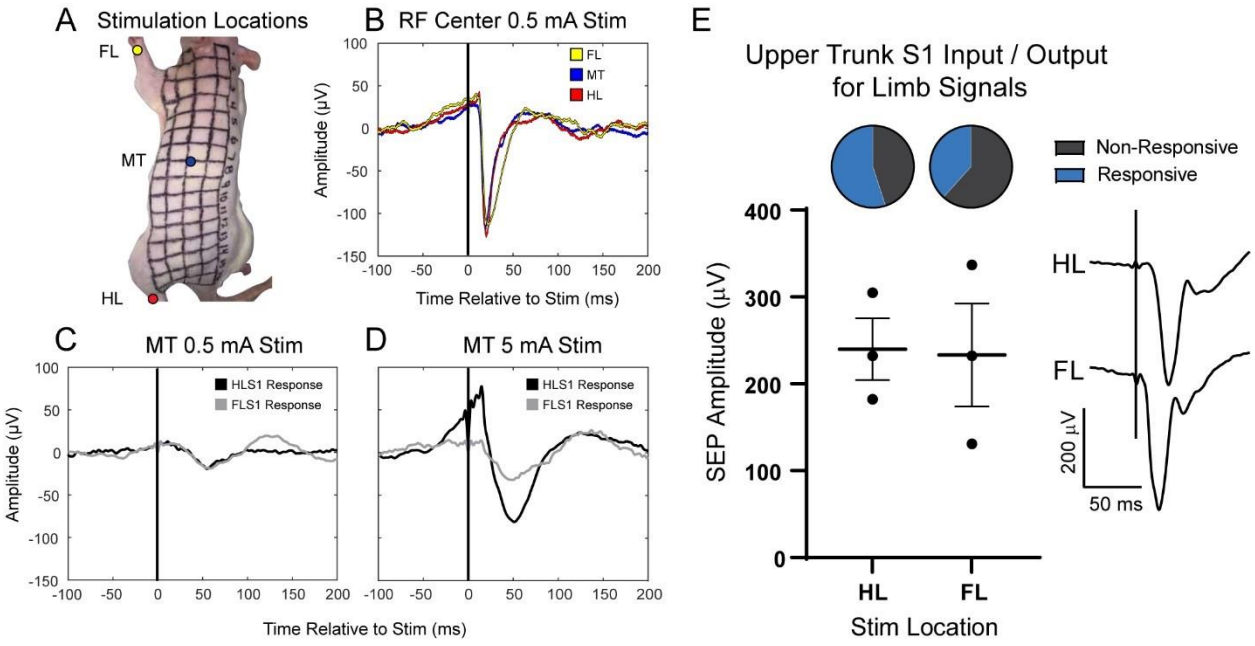

Supp Figure 2. 2: Exemplar SEPs confirm stronger sensory integration between trunk and hindlimb vs. forelimb. A) Photograph of an animal with the body grid, indicating the electrical stimulation locations (forelimb [FL], mid trunk [MT], hindlimb [HL]). The line running from the ear to tail next to the numbers 1-16 is along the midline of the dorsal trunk and the animal is lying partly on its side. B). Exemplar SEPs recorded in cortical receptive field centers from stimulation to the corresponding body location at 0.5 mA. Supporting results in Fig. 3A, these SEPs show that the electrical stimulation to FL, MT, and HL produce similar responses in each of these body locations' cortical receptive field centers, affirming that electrical stimulation can be used to compare SEPs between different cortical regions. C & D) Exemplar SEPs from HLS1 and FLS1 from stimulation to MT at 0.5 mA (C) and 5.0 mA (D), supporting results from Fig. 3B showing a larger overlap of trunk information in HLS1 compared to FLS1. E) Average SEP amplitudes recorded from upper TrS1 during 5.0 mA stimulation to FL (N = 3) and HL (N = 3). Example SEPs are shown on the right. No differences in average SEP amplitudes or proportion of responsive cells were found, suggesting that the proximity of body regions likely does not contribute to the increased responsiveness seen in TrS1 during hindlimb stimulation.

Trunk M1 receives hindlimb proprioceptive information from thalamus (Current source density analysis)

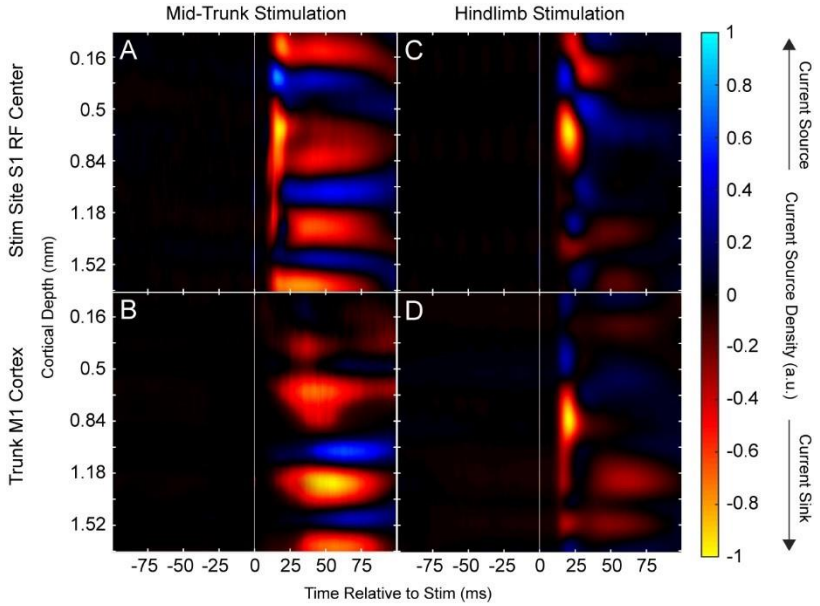

Supp Figure 2. 3 *Current source density analysis supports TrM1 receiving hindlimb proprioceptive information from the thalamus. A 16-channel laminar microelectrode array (A2X16, Neuronexus probe 100 µm interelectrode distance) was inserted perpendicularly to a depth of 1.60 mm and LFPs were recorded across the depth of the cortex. Current source density (CSD) provides spatiotemporal information (location, latency) of current sinks (yellow) and sources (blue) to confirm the position of the electrode. CSD was quantified as the second spatial derivative of SEP response, computed using the standard CSD method (Nicholson and Freeman 1975). Contour plots were generated with CSD toolbox (Pettersen et al. 2006). CSD profile was spatially filtered with a gaussian filter (SD = 0.1 mm). All CSD (measured in µA/mm^2) were normalized to the absolute maximum value of the CSD in response window of 100 ms from stimulus onset. Current sinks represent net inward transmembrane current, while current sources represent outward currents. Images were derived from laminar cortical LFP recordings in TrS1 (A) and TrM1 (B) during mid trunk stimulation (5.0 mA), as well as HLS1 (C) and TrM1 (D) during hindlimb stimulation (5.0 mA). Therefore, top panels A and C are the responses in S1 to stimulation of RF center. TrS1 in response to trunk stimulation (A) and HLS1 in response to hindlimb stimulation (C), both receive early current sinks in the granular layers, suggesting fast input directly from the thalamus. During trunk stimulation, TrM1 receives later current sinks in the infragranular layers, suggesting intracortical communication of sensory information from S1 to M1. Alternatively, TrM1 receives an early current sink during HL stimulation, suggesting early proprioceptive information ascending to M1 directly from the VPL of the thalamus.*

Bibliography

1. National Spinal Cord Injury Statistical Center, Facts and Figures at a Glance. Birmingham, AL: University of Alabama at Birmingham, 2020. *Natl. Spinal Cord Inj. Stat. Cent.* (2020).

2. G. Courtine, *et al.*, Recovery of supraspinal control of stepping via indirect propriospinal relay connections after spinal cord injury. *Nat Med* **14**, 69–74 (2008).

3. X. Wang, J. Hu, Y. She, G. M. Smith, X. M. Xu, Cortical PKC inhibition promotes axonal regeneration of the corticospinal tract and forelimb functional recovery after cervical dorsal spinal hemisection in adult rats. *Cereb Cortex* **24**, 3069–3079 (2014).

4. P. Lu, *et al.*, Motor axonal regeneration after partial and complete spinal cord transection. *J. Neurosci.* **32**, 8208–8218 (2012).

5. S. Wilson, *et al.*, The Hemisection Approach in Large Animal Models of Spinal Cord Injury: Overview of Methods and Applications. *J. Investig. Surg.* **33**, 240–251 (2020).

6. B. K. Kwon, T. R. Oxland, W. Tetzlaff, Animal models used in spinal cord regeneration research. *Spine (Phila. Pa. 1976).* **27**, 1504–1510 (2002).

7. T. Cheriyan, *et al.*, Spinal cord injury models: A review. *Spinal Cord* **52**, 588–595 (2014).

8. G. Foffani, J. Shumsky, E. B. Knudsen, P. D. Ganzer, K. A. Moxon, Interactive Effects between Exercise and Serotonergic Pharmacotherapy on Cortical Reorganization after Spinal Cord Injury. *Neurorehabil. Neural Repair* **30**, 479–489 (2016).

9. S. Giszter, M. R. Davies, A. Ramakrishnan, U. I. Udoekwere, W. J. Kargo, Trunk Sensorimotor Cortex Is Essential for Autonomous Weight-Supported Locomotion in Adult Rats Spinalized as P1/P2 Neonates. *J. Neurophysiol.* **100**, 839–851 (2008).

10. P. D. Ganzer, K. A. Moxon, E. B. Knudsen, J. S. Shumsky, Serotonergic pharmacotherapy promotes cortical reorganization after spinal cord injury. *Exp. Neurol.* **241**, 84–94 (2013).

11. A. Manohar, G. Foffani, P. D. Ganzer, J. R. Bethea, K. A. Moxon, Cortex-dependent recovery of unassisted hindlimb locomotion after complete spinal cord injury in adult rats. *Elife* **6**, 1–23 (2017).

12. J. Girgis, *et al.*, Reaching training in rats with spinal cord injury promotes plasticity and task specific recovery. *Brain* **130**, 2993–3003 (2007).

13. A. Singh, M. Murray, J. D. Houle, A training paradigm to enhance motor recovery in contused rats: Effects of staircase training. *Neurorehabil. Neural Repair* **25**, 24–34 (2011).

14. H. R. Sandrow-Feinberg, J. D. Houle, Exercise after spinal cord injury as an agent for neuroprotection, regeneration and rehabilitation. *Brain Res* **1619**, 12–21 (2015).

15. A. J. Peters, J. Lee, N. G. Hedrick, K. O'Neil, T. Komiyama, Reorganization of corticospinal output during motor learning. *Nat Neurosci* **advance on** (2017).

16. A. L. Behrman, E. M. Ardolino, S. J. Harkema, Activity-Based Therapy: From Basic Science to Clinical Application for Recovery After Spinal Cord Injury. *J. Neurol. Phys. Ther.* **41 Suppl 3**, S39–S45 (2017).

17. B. J. Hilton, *et al.*, Re-Establishment of Cortical Motor Output Maps and Spontaneous Functional Recovery via Spared Dorsolaterally Projecting Corticospinal Neurons after Dorsal Column Spinal Cord Injury in Adult Mice. *J. Neurosci.* **36**, 4080–4092 (2016).

18. L. Asboth, *et al.*, Cortico-reticulo-spinal circuit reorganization enables functional recovery after

severe spinal cord contusion. *Nat Neurosci* **21**, 576–588 (2018).

19. A. L. Behrman, *et al.*, Activity-Based Therapy Targeting Neuromuscular Capacity After Pediatric-Onset Spinal Cord Injury. *Top. Spinal Cord Inj. Rehabil.* **25**, 132–149 (2019).

20. S. F. Giszter, G. Hockensmith, A. Ramakrishnan, U. I. Udoekwere, How spinalized rats can walk: biomechanics, cortex, and hindlimb muscle scaling--implications for rehabilitation. *Ann N Y Acad Sci* **1198**, 279–293 (2010).

21. A. Bjerkefors, M. G. Carpenter, A. G. Cresswell, A. Thorstensson, Trunk muscle activation in a person with clinically complete thoracic spinal cord injury. *J Rehabil Med* **41**, 390–392 (2009).

22. C. S. Oza, S. F. Giszter, Trunk Robot Rehabilitation Training with Active Stepping Reorganizes and Enriches Trunk Motor Cortex Representations in Spinal Transected Rats. *J. Neurosci.* **35**, 7174–7189 (2015).

23. M. Rath, *et al.*, Trunk Stability Enabled by Noninvasive Spinal Electrical Stimulation after Spinal Cord Injury. *J. Neurotrauma* **35**, 2540–2553 (2018).

24. C. S. Oza, S. F. Giszter, Plasticity and alterations of trunk motor cortex following spinal cord injury and non-stepping robot and treadmill training. *Exp. Neurol.* **256**, 57–69 (2014).

25. N. A. Young, J. Vuong, C. Flynn, G. C. Teskey, Optimal parameters for microstimulation derived forelimb movement thresholds and motor maps in rats and mice. *J. Neurosci. Methods* **196**, 60–69 (2011).

26. M. S. A. Graziano, C. S. R. Taylor, T. Moore, Complex Movements Evoked by Microstimulation of Precentral Cortex. *Neuron* **34**, 841–851 (2002).

27. S. A. Overduin, A. d'Avella, J. M. Carmena, E. Bizzi, Muscle synergies evoked by microstimulation are preferentially encoded during behavior. *Front Comput Neurosci* **8**, 20 (2014).

28. D. Ramanathan, J. M. Conner, M. H. Tuszynski, A form of motor cortical plasticity that correlates with recovery of function after brain injury. *Proc Natl Acad Sci U S A* **103**, 11370–11375 (2006).

29. A. R. Brown, G. C. Teskey, Motor cortex is functionally organized as a set of spatially distinct representations for complex movements. *J Neurosci* **34**, 13574–13585 (2014).

30. P. L. Strick, Stimulating research on motor cortex. *Nat. Neurosci.* **5**, 714–715 (2002).

31. M. K. L. Baldwin, D. F. Cooke, L. Krubitzer, Intracortical Microstimulation Maps of Motor, Somatosensory, and Posterior Parietal Cortex in Tree Shrews (Tupaia belangeri) Reveal Complex Movement Representations. *Cereb. Cortex* **27**, 1439–1456 (2017).

32. A. C. Halley, M. K. L. Baldwin, D. F. Cooke, M. Englund, L. Krubitzer, Distributed Motor Control of Limb Movements in Rat Motor and Somatosensory Cortex: The Sensorimotor Amalgam Revisited. *Cereb. Cortex* **1**, 1–17 (2020).

33. M. Watson, M. Sawan, N. Dancause, The Duration of Motor Responses Evoked with Intracortical Microstimulation in Rats Is Primarily Modulated by Stimulus Amplitude and Train Duration. *PLoS One* **11**, e0159441 (2016).

34. P. D. Ganzer, A. Manohar, J. S. Shumsky, K. A. Moxon, Therapy induces widespread reorganization of motor cortex after complete spinal transection that supports motor recovery. *Exp. Neurol.* **279**, 1–12 (2016).

35. R. D. Hall, E. P. Lindholm, Organization of motor and somatosensory neocortex in the albino rat.

Brain Res. **66**, 23–38 (1974).

36. J. P. Donoghue, S. P. Wise, The motor cortex of the rat: cytoarchitecture and microstimulation mapping. *J Comp Neurol* **212**, 76–88 (1982).

37. P. D. Cheney, E. E. Fetz, Comparable patterns of muscle facilitation evoked by individual corticomotoneuronal (CM) cells and by single intracortical microstimuli in primates: Evidence for functional groups of CM cells. *J. Neurophysiol.* **53**, 786–804 (1985).

38. E. Beaumont, S. M. Onifer, W. R. Reed, D. S. K. Magnuson, Magnetically evoked inter-enlargement response: an assessment of ascending propriospinal fibers following spinal cord injury. *Exp. Neurol.* **201**, 428–440 (2006).

39. B. Nandakumar, G. H. Blumenthal, F. P. Pauzin, K. A. Moxon, Hindlimb Somatosensory Information Influences Trunk Sensory and Motor Cortices to Support Trunk Stabilization. *Cereb. Cortex* (2021) https:/doi.org/10.1093/cercor/bhab150.

40. T. Mao, *et al.*, Long-Range Neuronal Circuits Underlying the Interaction between Sensory and Motor Cortex. *Neuron* **72**, 111–123 (2011).

41. S. Rossignol, R. Dubuc, J.-P. Gossard, Dynamic sensorimotor interactions in locomotion. *Physiol. Rev.* **86**, 89–154 (2006).

42. S. Chakrabarti, M. Zhang, K. D. Alloway, MI neuronal responses to peripheral whisker stimulation: relationship to neuronal activity in si barrels and septa. *J. Neurophysiol.* **100**, 50–63 (2008).

43. T. Farkas, Z. Kis, J. Toldi, J. R. Wolff, Activation of the primary motor cortex by somatosensory stimulation in adult rats is mediated mainly by associational connections from the somatosensory cortex. *Neuroscience* **90**, 353–361 (1999).

44. I. Ferezou, *et al.*, Spatiotemporal Dynamics of Cortical Sensorimotor Integration in Behaving Mice. *Neuron* **56**, 907–923 (2007).

45. B. M. Hooks, *et al.*, Organization of cortical and thalamic input to pyramidal neurons in mouse motor cortex. *J. Neurosci.* **33**, 748–760 (2013).

46. J. B. Smith, K. D. Alloway, Rat whisker motor cortex is subdivided into sensory-input and motor-output areas. *Front. Neural Circuits* **7**, 4 (2013).

47. P. Megevand, *et al.*, Long-Term Plasticity in Mouse Sensorimotor Circuits after Rhythmic Whisker Stimulation. *J. Neurosci.* **29**, 5326–5335 (2009).

48. H. Asanuma, S. D. Stoney Jr., C. Abzug, Relationship between afferent input and motor outflow in cat motorsensory cortex. *J Neurophysiol* **31**, 670–681 (1968).

49. J. K. Chapin, Laminar differences in sizes, shapes, and response profiles of cutaneous receptive fields in the rat SI cortex. *Exp Brain Res* **62**, 549–559 (1986).

50. B. Tutunculer, G. Foffani, B. T. Himes, K. A. Moxon, Structure of the excitatory receptive fields of infragranular forelimb neurons in the rat primary somatosensory cortex responding to touch. *Cereb Cortex* **16**, 791–810 (2006).

51. M. L. Morales-Botello, J. Aguilar, G. Foffani, Imaging the Spatio-Temporal Dynamics of Supragranular Activity in the Rat Somatosensory Cortex in Response to Stimulation of the Paws. *PLoS One* **7**, e40174 (2012).

52. N. Kunori, I. Takashima, High-order motor cortex in rats receives somatosensory inputs from the primary motor cortex via cortico-cortical pathways. *Eur. J. Neurosci.* **44**, 2925–2934 (2016).

53. J. P. Donoghue, K. L. Kerman, F. F. Ebner, Evidence for two organizational plans within the somatic sensory-motor cortex of the rat. *J. Comp. Neurol.* **183**, 647–663 (1979).

54. H. Hummelsheim, M. Wiesendanger, Is the hindlimb representation of the rat's cortex a "sensorimotor amalgam"? *Brain Res.* **346**, 75–81 (1985).

55. A. Ghosh, *et al.*, Functional and anatomical reorganization of the sensory-motor cortex after incomplete spinal cord injury in adult rats. *J. Neurosci.* **29**, 12210–9 (2009).

56. T. Kao, J. S. Shumsky, M. Murray, K. a Moxon, Exercise induces cortical plasticity after neonatal spinal cord injury in the rat. *J. Neurosci.* **29**, 7549–57 (2009).

57. J. K. Chapin, C. S. Lin, Mapping the body representation in the SI cortex of anesthetized and awake rats. *J. Comp. Neurol.* **229**, 199–213 (1984).

58. C. Welker, Microelectrode delineation of fine grain somatotopic organization of SmI cerebral neocortex in albino rat. *Brain Res.* **26**, 259–275 (1971).

59. A. M. H. Seelke, J. C. Dooley, L. A. Krubitzer, The Emergence of Somatotopic Maps of the Body in S1 in Rats: The Correspondence Between Functional and Anatomical Organization. *PLoS One* **7**, e32322 (2012).

60. C. Xerri, J. Stern, M. Merzenich, Alterations of the cortical representation of the rat ventrum induced by nursing behavior. *J. Neurosci.* **14**, 1710–1721 (1994).

61. C. Lenschow, M. Brecht, Physiological and Anatomical Outputs of Rat Genital Cortex. *Cereb. Cortex* **28**, 1472–1486 (2018).

62. M. C. Lombard, B. S. Nashold, Denise Albe-Fessard, N. Salman, Deafferentation hypersensitivity in the rat after dorsal rhizotomy: A possible animal model of chronic pain. *Pain* **6**, 163–174 (1979).

63. Y. Takahashi, Y. Nakajima, T. Sakamoto, Dermatome mapping in the rat hindlimb by electrical stimulation of the spinal nerves. *Neurosci. Lett.* **168**, 85–88 (1994).

64. Y. Gioanni, M. Lamarche, A reappraisal of rat motor cortex organization by intracortical microstimulation. *Brain Res.* **344**, 49–61 (1985).

65. E. J. Neafsey, *et al.*, The organization of the rat motor cortex: A microstimulation mapping study. *Brain Res. Rev.* **11**, 77–96 (1986).

66. S. Tandon, N. Kambi, H. Mohammed, N. Jain, Complete reorganization of the motor cortex of adult rats following long-term spinal cord injuries. *Eur. J. Neurosci.* **38**, 2271–2279 (2013).

67. S. F. Giszter, W. J. Kargo, M. Davies, M. Shibayama, Fetal Transplants Rescue Axial Muscle Representations in M1 Cortex of Neonatally Transected Rats That Develop Weight Support. *J. Neurophysiol.* **80** (2017).

68. C. L. Smith, Sensory neurons supplying touch domes near the body midlines project bilaterally in the thoracic spinal cord of rats. *J. Comp. Neurol.* **245**, 541–552 (1986).

69. W. J. T. Wessels, H. K. P. Feirabend, E. Marani, Anatomy and Embryolo Review article The rostrocaudal organization in the dorsal root ganglia of the rat : a consequence of plexus formation ? *Anat. Embryol. (Berl).*, 1–11 (1994).

70. J. Hekmatpanah, Organization of tactile dermatomes, C1 through L4, in cat. *J Neurophysiol* **24**, 129–140 (1961).

71. R. A. Kuhn, Organization of tactile dermatomes in cat and monkey. *J Neurophysiol* **16**, 169–182 (1953).

72. E. J. Kirk, The dermatomes of the sheep. *J. Comp. Neurol.* **134**, 353–369 (1968).

73. E. J. Kirk, D. Denny-Brown, Functional variation in dermatomes in the macaque monkey following dorsal root lesions. *J. Comp. Neurol.* **139**, 307–320 (1970).

74. C. S. Sherrington, Experiments in examination of the peripheral distribution of the fibres of the posterior roots of some spinal nerves. *Proc. R. Soc. London* **52**, 333–337 (1892).

75. K. Itomi, R. Kakigi, K. Maeda, M. Hoshiyama, Dermatome versus homunculus; detailed topography of the primary somatosensory cortex following trunk stimulation. *Clin. Neurophysiol.* **111**, 405–412 (2000).

76. G. Foffani, J. K. Chapin, K. A. Moxon, Computational role of large receptive fields in the primary somatosensory cortex. *J Neurophysiol* **100**, 268–280 (2008).

77. S. B. Frost, *et al.*, Output properties of the cortical hindlimb motor area in spinal cord-injured rats. *J. Neurotrauma* **32**, 1666–1673 (2015).

78. M. G. Boyeson, D. M. Feeney, W. G. Dail, Cortical microstimulation thresholds adjacent to sensorimotor cortex injury. *J. Neurotrauma* **8**, 205–217 (1991).

79. A. Canedo, Primary Motor Cortex Influenceson the Descendingand Ascending Systems. **51** (1997).

80. T. Mao, *et al.*, Long-range neuronal circuits underlying the interaction between sensory and motor cortex. *Neuron* **72**, 111–123 (2011).

81. B. M. Hooks, Sensorimotor Convergence in Circuitry of the Motor Cortex. *Neuroscientist* **23**, 251–263 (2017).

82. J. T. Francis, S. Xu, J. K. Chapin, Proprioceptive and cutaneous representations in the rat ventral posterolateral thalamus. *J. Neurophysiol.* **99**, 2291–2304 (2008).

83. N. R. Bridges, M. Meyers, J. Garcia, P. A. Shewokis, K. A. Moxon, A rodent brain-machine interface paradigm to study the impact of paraplegia on BMI performance. *J. Neurosci. Methods* **306**, 103–114 (2018).

84. E. B. Knudsen, K. A. Moxon, Restoration of hindlimb movements after complete spinal cord injury using brain-controlled functional electrical stimulation. *Front. Neurosci.* **11**, 1–12 (2017).

85. E. A. Clement, *et al.*, Cyclic and sleep-like spontaneous alternations of brain state under urethane anaesthesia. *PLoS One* **3** (2008).

86. C. Xerri, J. M. Stern, M. M. Merzenich, Alterations of the cortical representation of the rat ventrum induced by nursing behavior. *J. Neurosci.* **14**, 1710–1721 (1994).

87. T. B. Leergaard, K. D. Alloway, J. J. Mutic, J. G. Bjaalie, Three-dimensional topography of corticopontine projections from rat barrel cortex: correlations with corticostriatal organization. *J. Neurosci.* **20**, 8474–84 (2000).

88. C. X. li, R. S. Waters, Organization of the Mouse Motor Cortex Studied by Retrograde Tracing

and Intracortical Microstimulation (ICMS) Mapping. *Can. J. Neurol. Sci. / J. Can. des Sci. Neurol.* **18**, 28–38 (1991).

89. D. F. Cooke, J. Padberg, T. Zahner, L. Krubitzer, The functional organization and cortical connections of motor cortex in squirrels. *Cereb. Cortex* **22**, 1959–1978 (2012).

90. I. Stepniewska, P.-C. Fang, J. H. Kaas, Microstimulation reveals specialized subregions for different complex movements in posterior parietal cortex of prosimian galagos. *Proc. Natl. Acad. Sci. U. S. A.* **102**, 4878–4883 (2005).

91. M. K. L. Baldwin, D. F. Cooke, A. B. Goldring, L. Krubitzer, Representations of Fine Digit Movements in Posterior and Anterior Parietal Cortex Revealed Using Long-Train Intracortical Microstimulation in Macaque Monkeys. *Cereb. Cortex* **28**, 4244–4263 (2018).

92. M. Lemieux, N. Josset, M. Roussel, S. Couraud, F. Bretzner, Speed-dependent modulation of the locomotor behavior in adult mice reveals attractor and transitional gaits. *Front. Neurosci.* **10** (2016).

93. H. Asanuma, D. Stoney, C. Abzug, Relationship Between Afferent Input and Cortex in Cat Motorsensory Trl io msec. *J Neurophysiol* (1968).

94. I. Rosén, H. Asanuma, Peripheral afferent inputs to the forelimb area of the monkey motor cortex: Input-output relations. *Exp. Brain Res.* **14**, 257–273 (1972).

95. S. P. Hicks, C. J. D'Amato, Motor-sensory cortex-corticospinal system and developing locomotion and placing in rats. *Am J Anat* **143**, 1–42 (1975).

96. E. Beaumont, *et al.*, Functional electrical stimulation post-spinal cord injury improves locomotion and increases afferent input into the central nervous system in rats. *J. Spinal Cord Med.* **37**, 93–100 (2014).

97. R. Olivares-Moreno, *et al.*, The rat corticospinal system is functionally and anatomically segregated. *Brain Struct. Funct.* **222**, 3945–3958 (2017).

98. E. E. Brink, J. I. Morrell, D. W. Pfaff, Localization of lumbar epaxial motoneurons in the rat. *Brain Res* **170**, 23–41 (1979).

99. C. Anders, *et al.*, Trunk muscle activation patterns during walking at different speeds. *J. Electromyogr. Kinesiol.* **17**, 245–252 (2007).

100. W. Song, I. Cajigas, E. N. Brown, S. F. Giszter, Adaptation to elastic loads and BMI robot controls during rat locomotion examined with point-process GLMs. *Front. Syst. Neurosci.* **9** (2015).

101. A. J. Murray, K. Croce, T. Belton, T. Akay, T. M. Jessell, Balance Control Mediated by Vestibular Circuits Directing Limb Extension or Antagonist Muscle Co-activation. *Cell Rep.* **22**, 1325–1338 (2018).

102. F. B. Horak, J. V. Jacobs, Cortical control of postural responses. *J. Neural Transm.* **114**, 1339–1348 (2007).

103. P. J. Whelan, The involvement of the motor cortex in postural control: A delicate balancing act. *J. Physiol.* **587**, 3753 (2009).

104. T. G. Deliagina, I. N. Beloozerova, P. V. Zelenin, G. N. Orlovsky, Spinal and supraspinal postural networks. *Brain Res. Rev.* **57**, 212–221 (2008).

105. A. Karayannidou, *et al.*, Activity of pyramidal tract neurons in the cat during standing and walking on an inclined plane. *J. Physiol.* (2009) https:/doi.org/10.1113/jphysiol.2009.170183.

106. T. G. Deliagina, *et al.*, Role of Different Sensory Inputs for Maintenance of Body Posture in Sitting Rat and Rabbit. *Motor Control* **4**, 439–452 (2016).

107. I. N. Beloozerova, M. G. Sirota, H. A. Swadlow, Activity of different classes of neurons of the motor cortex during locomotion. *J. Neurosci.* **23**, 1087–1097 (2003).

108. H. Tsao, M. P. Galea, P. W. Hodges, Reorganization of the motor cortex is associated with postural control deficits in recurrent low back pain. *Brain* **131**, 2161–2171 (2008).

109. P. W. Hodges, Changes in motor planning of feedforward postural responses of the trunk muscles in low back pain. *Exp Brain Res* **141**, 261–266 (2001).

110. H. Tsao, K. J. Tucker, P. W. Hodges, Changes in excitability of corticomotor inputs to the trunk muscles during experimentally-induced acute low back pain. *Neuroscience* **181**, 127–133 (2011).

111. V. R. Edgerton, *et al.*, Training locomotor networks. *Brain Res. Rev.* **57**, 241–254 (2008).

112. G. Taccola, D. Sayenko, P. Gad, Y. Gerasimenko, V. R. Edgerton, And yet it moves: Recovery of volitional control after spinal cord injury. *Prog. Neurobiol.* **160**, 64–81 (2018).

113. R. van den Brand, *et al.*, Restoring Voluntary Control of Locomotion after Paralyzing Spinal Cord Injury. *Science (80-.).* **336**, 1182–1185 (2012).

114. E. Formento, *et al.*, Electrical spinal cord stimulation must preserve proprioception to enable locomotion in humans with spinal cord injury. *Nat. Neurosci.* **21** (2018).

115. M. Bonizzato, *et al.*, Brain-controlled modulation of spinal circuits improves recovery from spinal cord injury. *Nat. Commun.* **9**, 1–14 (2018).

116. M. Capogrosso, *et al.*, A brain-spine interface alleviating gait deficits after spinal cord injury in primates. *Nature* **539**, 284–288 (2016).

117. S. Harkema, *et al.*, Effect of epidural stimulation of the lumbosacral spinal cord on voluntary movement, standing, and assisted stepping after motor complete paraplegia: A case study. *Lancet* **377**, 1938–1947 (2011).

118. E. Rejc, C. A. Angeli, D. Atkinson, S. J. Harkema, Motor recovery after activity-based training with spinal cord epidural stimulation in a chronic motor complete paraplegic. *Sci. Rep.* **7**, 1–12 (2017).

119. A. Takeoka, I. Vollenweider, G. Courtine, S. Arber, Muscle spindle feedback directs locomotor recovery and circuit reorganization after spinal cord injury. *Cell* **159**, 1626–1639 (2014).

120. M. L. Ingemanson, *et al.*, Somatosensory system integrity explains differences in treatment response after stroke. *Neurology*, 10.1212/WNL.0000000000007041 (2019).

121. G. H. Blumenthal, *et al.*, Modeling at-level allodynia after mid-thoracic contusion in the rat. *Eur. J. Pain* **n/a** (2020).

122. M. H. Friedberg, S. M. Lee, F. F. Ebner, Modulation of receptive field properties of thalamic somatosensory neurons by the depth of anesthesia. *J Neurophysiol* **81**, 2243–2252 (1999).

123. J. Lilja, *et al.*, Blood oxygenation level-dependent visualization of synaptic relay stations of sensory pathways along the neuroaxis in response to graded sensory stimulation of a limb. *J*

Neurosci **26**, 6330–6336 (2006).

124. J. G. Yagüe, D. Humanes-Valera, J. Aguilar, G. Foffani, Functional reorganization of the forepaw cortical representation immediately after thoracic spinal cord hemisection in rats. *Exp. Neurol.* **257**, 19–24 (2014).

125. D. Humanes-Valera, J. Aguilar, G. Foffani, Reorganization of the intact somatosensory cortex immediately after spinal cord injury. *PLoS One* **8**, e69655 (2013).

126. G. Foffani, K. A. Moxon, PSTH-based classification of sensory stimuli using ensembles of single neurons. *J Neurosci Methods* **135**, 107–120 (2004).

127. B. Tutunculer, G. Foffani, B. T. Himes, K. A. Moxon, Structure of the excitatory receptive fields of infragranular forelimb neurons in the rat primary somatosensory cortex responding to touch. *Cereb. Cortex* **16**, 791–810 (2006).

128. T. Kao, J. S. Shumsky, M. Murray, K. A. Moxon, Exercise induces cortical plasticity after neonatal spinal cord injury in the rat. *J. Neurosci.* **29**, 7549–7557 (2009).

129. S. Tandon, N. Kambi, N. Jain, Overlapping representations of the neck and whiskers in the rat motor cortex revealed by mapping at different anaesthetic depths. *Eur J Neurosci* **27**, 228–237 (2008).

130. E. J. Neafsey, *et al.*, The organization of the rat motor cortex: A microstimulation mapping study. *Brain Res. Rev.* **11**, 77–96 (1986).

131. D. M. Griffin, H. M. Hudson, A. Belhaj-Saif, P. D. Cheney, EMG activation patterns associated with high frequency, long-duration intracortical microstimulation of primary motor cortex. *J Neurosci* **34**, 1647–1656 (2014).

132. W. J. Kargo, D. A. Nitz, Early skill learning is expressed through selection and tuning of cortically represented muscle synergies. *J Neurosci* **23**, 11255–11269 (2003).

133. T. B. Leergaard, K. D. Alloway, J. J. Mutic, J. G. Bjaalie, Three-dimensional topography of corticopontine projections from rat barrel cortex: correlations with corticostriatal organization. *J Neurosci* **20**, 8474–8484 (2000).

134. A. Manohar, R. D. Flint, E. Knudsen, K. A. Moxon, Decoding hindlimb movement for a brain machine interface after a complete spinal transection. *PLoS One* **7**, e52173 (2012).

135. C. Liu, G. Foffani, A. Scaglione, J. Aguilar, K. A. Moxon, Adaptation of thalamic neurons provides information about the spatiotemporal context of stimulus history. *J. Neurosci.* **37**, 10012–10021 (2017).

136. J. M. Macpherson, D. W. Lywood, A. Van Eyken, A system for the analysis of posture and stance in quadrupeds. *J. Neurosci. Methods* (1987) https:/doi.org/10.1016/0165-0270(87)90040-9.

137. T. G. Deliagina, G. N. Orlovsky, Comparative neurobiology of postural control. *Curr. Opin. Neurobiol.* **12**, 652–657 (2002).

138. T. G. Deliagina, P. V. Zelenin, G. N. Orlovsky, Physiological and circuit mechanisms of postural control. *Curr. Opin. Neurobiol.* **22**, 646–652 (2012).

139. J. Massion, A. Alexandrov, A. Frolov, Why and how are posture and movement coordinated? *Prog. Brain Res.* **143**, 13–27 (2004).

140. C. S. Sherrington, Decerebrate Rigidity, and Reflex Coordination of Movements. *J. Physiol.*

(1898) https:/doi.org/10.1113/jphysiol.1898.sp000697.

141. T. G. Deliagina, M. G. Sirota, P. V. Zelenin, G. N. Orlovsky, I. N. Beloozerova, Interlimb postural coordination in the standing cat. *J. Physiol.* **573**, 211–224 (2006).

142. I. N. Beloozerova, *et al.*, Activity of different classes of neurons of the motor cortex during postural corrections. *J. Neurosci.* **23**, 7844–53 (2003).

143. P. J. Stapley, L. H. Ting, M. Hulliger, J. M. Macpherson, Automatic postural responses are delayed by pyridoxine-induced somatosensory loss. *J. Neurosci.* **22**, 5803–5807 (2002).

144. J. T. Inglis, J. M. Macpherson, Bilateral labyrinthectomy in the cat: effects on the postural response to translation. *J. Neurophysiol.* **73**, 1181–1191 (1995).

145. F. B. Horak, J. Kluzik, F. Hlavacka, Velocity dependence of vestibular information for postural control on tilting surfaces. *J. Neurophysiol.* (2016) https:/doi.org/10.1152/jn.00057.2016.

146. L. J. Hsu, P. V. Zelenin, G. N. Orlovsky, T. G. Deliagina, Effects of galvanic vestibular stimulation on postural limb reflexes and neurons of spinal postural network. *J. Neurophysiol.* **108**, 300–313 (2012).

147. P. V. Zelenin, V. F. Lyalka, L. J. Hsu, G. N. Orlovsky, T. G. Deliagina, Effects of reversible spinalization on individual spinal neurons. *J. Neurosci.* (2013) https:/doi.org/10.1523/JNEUROSCI.2394-13.2013.

148. P. J. Stapley, T. Drew, The pontomedullary reticular formation contributes to the compensatory postural responses observed following removal of the support surface in the standing cat. *J. Neurophysiol.* (2009) https:/doi.org/10.1152/jn.91013.2008.

149. Z. Afelt, Functional significance of ventral descending tracts of the spinal cord in the cat. *Acta Neurobiol. Exp. (Wars)*. (1974).

150. T. Bem, T. Górska, H. Majczyński, W. Zmysłowski, Different patterns of fore-hindlimb coordination during overground locomotion in cats with ventral and lateral spinal lesions. *Exp. Brain Res.* (1995) https:/doi.org/10.1007/BF00229856.

151. T. Gorska, T. Bem, H. Majczynski, Locomotion in cats with ventral spinal lesions: Support patterns and duration of support phases during unrestrained walking in *Acta Neurobiologiae Experimentalis*, (1990).

152. T. Górska, T. Bem, H. Majczyński, W. Zmysłowski, Unrestrained walking in cats with partial spinal lesions. *Brain Res. Bull.* (1993) https:/doi.org/10.1016/0361-9230(93)90183-C.

153. H. G. J. M. Kuypers, The Descending Pathways to the Spinal Cord, their Anatomy and Function. *Prog. Brain Res.* **11**, 178–202 (1964).

154. D. G. Lawrence, H. G. J. M. Kuypers, The functional organization of the motor system in the monkey: II. The effects of lesions of the descending brain-stem pathways. *Brain* (1968) https:/doi.org/10.1093/brain/91.1.15.

155. E. Brustein, S. Rossignol, Recovery of locomotion after ventral and ventrolateral spinal lesions in the cat. I. Deficits and adaptive mechanisms. *J. Neurophysiol.* (1998) https:/doi.org/10.1152/jn.1998.80.3.1245.

156. V. F. Lyalka, *et al.*, Impairment and Recovery of Postural Control in Rabbits With Spinal Cord Lesions. *J. Neurophysiol.* **94**, 3677–3690 (2005).

157. K. Matsuyama, T. Drew, Vestibulospinal and reticulospinal neuronal activity during locomotion in the intact cat. II. Walking on an inclined plane. *J. Neurophysiol.* (2000) https:/doi.org/10.1152/jn.2000.84.5.2257.

158. P. V. Zelenin, I. N. Beloozerova, M. G. Sirota, G. N. Orlovsky, T. G. Deliagina, Activity of red nucleus neurons in the cat during postural corrections. *J. Neurosci.* (2010) https:/doi.org/10.1523/JNEUROSCI.2991-10.2010.

159. A. Karayannidou, *et al.*, Influences of sensory input from the limbs on feline corticospinal neurons during postural responses. *J. Physiol.* **586**, 247–263 (2008).

160. T. G. Deliagina, I. N. Beloozerova, G. N. Orlovsky, P. V. Zelenin, Contribution of supraspinal systems to generation of automatic postural responses. *Front. Integr. Neurosci.* **8**, 1–20 (2014).

161. J. M. Macpherson, J. Fung, Weight support and balance during perturbed stance in the chronic spinal cat. *J. Neurophysiol.* **82**, 3066–3081 (1999).

162. H. Barbeau, S. Rossignol, Recovery of locomotion after chronic spinalization in the adult cat. *Brain Res.* **412**, 84–95 (1987).

163. J. M. Macpherson, J. Fung, Weight support and balance during perturbed stance in the chronic spinal cat. *J. Neurophysiol.* **82**, 3066–3081 (1999).

164. S. Rossignol, *et al.*, Locomotor capacities after complete and partial lesions of the spinal cord. *Acta Neurobiol. Exp. (Wars).* **56**, 449–463 (1996).

165. S. Rossignol, T. Drew, E. Brustein, W. Jiang, Locomotor performance and adaptation after partial or complete spinal cord lesions in the cat. **123** (1999).

166. C. A. Giuliani, J. L. Smith, Stepping behaviors in chronic spinal cats with one hindlimb deafferented. *J. Neurosci.* **7**, 2537–2546 (1987).

167. V. R. Edgerton, *et al.*, Edgerton_et_al-2001-The_Journal_of_Physiology. 15–22 (2001).

168. C. A. Pratt, J. Fung, J. M. Macpherson, Stance control in the chronic spinal cat. *J. Neurophysiol.* **71**, 1981–1985 (1994).

169. S. Grillner, M. L. Shik, On the Descending Control of the Lumbosacral Spinal Cord from the "Mesencephalic Locomotor Region." *Acta Physiol. Scand.* (1973) https:/doi.org/10.1111/j.1748-1716.1973.tb05396.x.

170. R. D. De Leon, J. A. Hodgson, R. R. Roy, V. R. Edgerton, Locomotor capacity attributable to step training versus spontaneous recovery after spinalization in adult cats. *J. Neurophysiol.* **79**, 1329–1340 (1998).

171. D. C. Dunbar, F. B. Horak, J. M. Macpherson, D. S. Rushmer, Neural control of quadrupedal and bipedal stance: Implications for the evolution of erect posture. *Am. J. Phys. Anthropol.* (1986) https:/doi.org/10.1002/ajpa.1330690111.

172. I. Lavrov, *et al.*, Plasticity of spinal cord reflexes after a complete transection in adult rats: relationship to stepping ability. *J. Neurophysiol.* **96**, 1699–710 (2006).

173. A. Valero-Cabré, K. Tsironis, E. Skouras, X. Navarro, W. F. Neiss, Peripheral and Spinal Motor Reorganization after Nerve Injury and Repair. *J. Neurotrauma* (2004) https:/doi.org/10.1089/089771504772695986.

174. S. Mori, Integration of posture and locomotion in acute decerebrate cats and in awake, freely

moving cats. *Prog. Neurobiol.* (1987) https:/doi.org/10.1016/0301-0082(87)90010-4.

175. P. E. Musienko, P. V. Zelenin, G. N. Orlovsky, T. G. Deliagina, Facilitation of Postural Limb Reflexes With Epidural Stimulation in Spinal Rabbits. *J. Neurophysiol.* **103**, 1080–1092 (2009).

176. O. Raineteau, M. E. Schwab, Plasticity of motor systems after incomplete spinal cord injury. *Nat Rev Neurosci* **2**, 263–273 (2001).

177. Y. Nishimura, *et al.*, Time-dependent central compensatory mechanisms of finger dexterity after spinal cord injury. *Science (80-.).* **318**, 1150–1155 (2007).

178. R. Rasmussen, E. M. Carlsen, Spontaneous functional recovery from incomplete spinal cord injury. *J. Neurosci.* **36**, 8535–8537 (2016).

179. C. Heng, R. D. de Leon, Treadmill training enhances the recovery of normal stepping patterns in spinal cord contused rats. *Exp. Neurol.* **216**, 139–147 (2009).

180. C. R. Battistuzzo, R. J. Callister, R. Callister, M. P. Galea, A systematic review of exercise training to promote locomotor recovery in animal models of spinal cord injury. *J Neurotrauma* **29**, 1600–1613 (2012).

181. K. Loy, F. M. Bareyre, Rehabilitation following spinal cord injury: How animal models can help our understanding of exercise-induced neuroplasticity. *Neural Regen. Res.* **14**, 405–412 (2019).

182. V. R. Edgerton, *et al.*, Use-dependent plasticity in spinal stepping and standing. *Adv. Neurol.* **72**, 233–247 (1997).

183. V. Dietz, R. Müller, G. Colombo, Locomotor activity in spinal man: Significance of afferent input from joint and load receptors. *Brain* **125**, 2626–2634 (2002).

184. F. M. Bareyre, *et al.*, The injured spinal cord spontaneously forms a new intraspinal circuit in adult rats. *Nat Neurosci* **7**, 269–277 (2004).

185. J. V Lynskey, A. Belanger, R. Jung, Activity-dependent plasticity in spinal cord injury. *J. Rehabil. Res. Dev.* **45**, 229–240 (2008).

186. K. Loy, *et al.*, Enhanced Voluntary Exercise Improves Functional Recovery following Spinal Cord Injury by Impacting the Local Neuroglial Injury Response and Supporting the Rewiring of Supraspinal Circuits. *J. Neurotrauma* **35**, 2904–2915 (2018).

187. N. L. U. van Meeteren, R. Eggers, A. J. Lankhorst, W. H. Gispen, F. P. T. Hamers, Locomotor Recovery after Spinal Cord Contusion Injury in Rats Is Improved by Spontaneous Exercise. *J. Neurotrauma* **20**, 1029–1037 (2003).

188. J. E. Stevens, *et al.*, Changes in soleus muscle function and fiber morphology with one week of locomotor training in spinal cord contusion injured rats. *J. Neurotrauma* **23**, 1671–1681 (2006).

189. A. K. Brown, S. A. Woller, G. Moreno, J. W. Grau, M. A. Hook, Exercise therapy and recovery after SCI: evidence that shows early intervention improves recovery of function. *Spinal Cord* **49**, 623 (2011).

190. B. Nandakumar, G. H. Blumenthal, F. P. Pauzin, K. A. Moxon, Trunk sensory and motor cortex is preferentially integrated with hindlimb sensory information that supports trunk stabilization. *bioRxiv*, 2020.08.31.272583 (2020).

191. S. B. Frost, *et al.*, Output Properties of the Cortical Hindlimb Motor Area in Spinal Cord-Injured Rats. *J Neurotrauma* (2015) https:/doi.org/10.1089/neu.2015.3961.

192. H. A. Petrosyan, V. Alessi, S. A. Sisto, M. Kaufman, V. L. Arvanian, Transcranial magnetic stimulation (TMS) responses elicited in hindlimb muscles as an assessment of synaptic plasticity in spino-muscular circuitry after chronic spinal cord injury. *Neurosci. Lett.* **642**, 37–42 (2017).

193. J. A. Gruner, C. K. Wade, G. Menna, B. T. Stokes, Myoelectric evoked potentials versus locomotor recovery in chronic spinal cord injured rats. *J Neurotrauma* **10**, 327–347 (1993).

194. K. Fouad, V. Pedersen, M. E. Schwab, C. Brösamle, Cervical sprouting of corticospinal fibers after thoracic spinal cord injury accompanies shifts in evoked motor responses. *Curr. Biol.* **11**, 1766–1770 (2001).

195. A. Ghosh, *et al.*, Rewiring of hindlimb corticospinal neurons after spinal cord injury. *Nat Neurosci* **13**, 97–104 (2010).

196. A. J. Del-Ama, Á. Gil-Agudo, J. L. Pons, J. C. Moreno, Hybrid FES-robot cooperative control of ambulatory gait rehabilitation exoskeleton. *J. Neuroeng. Rehabil.* **11**, 1–15 (2014).

197. S. F. Giszter, M. R. Davies, V. Graziani, Motor strategies used by rats spinalized at birth to maintain stance in response to imposed perturbations. *J Neurophysiol* **97**, 2663–2675 (2007).

198. S. F. Giszter, M. R. Davies, V. Graziani, *Coordination strategies for limb forces during weight-bearing locomotion in normal rats, and in rats spinalized as neonates* (2008).

199. D. J. Stelzner, W. B. Ershler, E. D. Weber, Effects of spinal transection in neonatal and weanling rats: Survival of function. *Exp. Neurol.* **46**, 156–177 (1975).

200. D. Kim, M. Murray, K. J. Simansky, The Serotonergic 5-HT2C Agonist m-Chlorophenylpiperazine Increases Weight-Supported Locomotion without Development of Tolerance in Rats with Spinal Transections. *Exp. Neurol.* **169**, 496–500 (2001).

201. J. P. Cummings, D. R. Bernstein, D. J. Stelzner, Further evidence that sparing of function after spinal cord transection in the neonatal rat is not due to axonal generation or regeneration. *Exp. Neurol.* **74**, 615–620 (1981).

202. N. J. K. Tillakaratne, *et al.*, Functional recovery of stepping in rats after a complete neonatal spinal cord transection is not due to regrowth across the lesion site. *Neuroscience* **166**, 23–33 (2010).

203. T. Kao, J. S. Shumsky, E. B. Knudsen, M. Murray, K. A. Moxon, Functional role of exercise-induced cortical organization of sensorimotor cortex after spinal transection. *J. Neurophysiol.* **106**, 2662–2674 (2011).

204. K. A. Moxon, A. Oliviero, J. Aguilar, G. Foffani, Cortical reorganization after spinal cord injury: Always for good? *Neuroscience* **283**, 78–94 (2014).

205. U. I. Udoekwere, C. S. Oza, S. F. Giszter, Teaching adult rats spinalized as neonates to walk using trunk robotic rehabilitation: Elements of success, failure, and dependence. *J. Neurosci.* **36**, 8341–8355 (2016).

206. K. Matsuyama, *et al.*, Locomotor role of the corticoreticular-reticulospinal-spinal interneuronal system. *Prog. Brain Res.* **143**, 239–249 (2004).

207. M. Ballermann, K. Fouad, Spontaneous locomotor recovery in spinal cord injured rats is accompanied by anatomical plasticity of reticulospinal fibers. *Eur. J. Neurosci.* **23**, 1988–1996 (2006).

208. P. D. Ganzer, *et al.*, Awake behaving electrophysiological correlates of forelimb hyperreflexia, weakness and disrupted muscular synchronization following cervical spinal cord injury in the rat.

Behav. Brain Res. **307**, 100–111 (2016).

209. M. Bonizzato, *et al.*, Multi-pronged neuromodulation intervention engages the residual motor circuitry to facilitate walking in a rat model of spinal cord injury. *Nat. Commun.* **12**, 1–14 (2021).

210. M. Martinez, J. M. Brezun, Y. Zennou-Azogui, N. Baril, C. Xerri, Sensorimotor training promotes functional recovery and somatosensory cortical map reactivation following cervical spinal cord injury. *Eur. J. Neurosci.* **30**, 2356–2367 (2009).

211. L. Asboth, *et al.*, Cortico–reticulo–spinal circuit reorganization enables functional recovery after severe spinal cord contusion. *Nat. Neurosci.* **21**, 1–13 (2018).

212. M. T. Jurkiewicz, D. J. Mikulis, W. E. McIlroy, M. G. Fehlings, M. C. Verrier, Sensorimotor cortical plasticity during recovery following spinal cord injury: a longitudinal fMRI study. *Neurorehabil. Neural Repair* **21**, 527–538 (2007).

213. M. Oudega, M. A. Perez, Corticospinal reorganization after spinal cord injury. *J. Physiol.* **590**, 3647–3663 (2012).

214. N. Weidner, A. Ner, N. Salimi, M. H. Tuszynski, Spontaneous corticospinal axonal plasticity and functional recovery after adult central nervous system injury. *Proc. Natl. Acad. Sci. U. S. A.* **98**, 3513–3518 (2001).

215. E. S. Rosenzweig, *et al.*, Extensive spontaneous plasticity of corticospinal projections after primate spinal cord injury. *Nat. Neurosci.* **13**, 1505–1512 (2010).

216. M. Hayashibe, *et al.*, Locomotor improvement of spinal cord-injured rats through treadmill training by forced plantar placement of hind paws. *Spinal Cord* **54**, 521–529 (2016).

217. P. Musienko, *et al.*, Controlling Specific Locomotor Behaviors through Multidimensional Monoaminergic Modulation of Spinal Circuitries. *J. Neurosci.* **31**, 9264–9278 (2011).

218. D. Kim, *et al.*, Direct Agonists for Serotonin Receptors Enhance Locomotor Function in Rats that Received Neural Transplants after Neonatal Spinal Transection. *J. Neurosci.* **19**, 6213–6224 (1999).

219. J. A. Nessler, *et al.*, Hindlimb loading determines stepping quantity and quality following spinal cord transection. *Brain Res.* **1050**, 180–189 (2005).

220. D. M. BASSO, M. S. BEATTIE, J. C. BRESNAHAN, A Sensitive and Reliable Locomotor Rating Scale for Open Field Testing in Rats. *J. Neurotrauma* (1995) https:/doi.org/10.1089/neu.1995.12.1.

221. C. A. Schneider, W. S. Rasband, K. W. Eliceiri, NIH Image to ImageJ: 25 years of image analysis. *Nat. Methods* **9**, 671–675 (2012).

222. S. Mori, INTEGRATION OF POSTURE AND LOCOMOTION IN ACUTE DECEREBRATE CATS AND IN AWAKE , FREELY MOVING CATS To initiate and terminate locomotor movements both in the biped and in the quadruped , a smooth transition from and to standing is necessary , standing being. **28**, 161–195 (1987).

223. P. E. Musienko, P. V. Zelenin, V. F. Lyalka, G. N. Orlovsky, T. G. Deliagina, Postural performance in decerebrated rabbit. *Behav. Brain Res.* **190**, 124–134 (2008).

224. I. N. Beloozerova, *et al.*, Activity of Different Classes of Neurons of the Motor Cortex during Postural Corrections. *J. Neurosci.* **23**, 7844–7853 (2018).

225. W. Song, A. Ramakrishnan, U. I. Udoekwere, S. F. Giszter, Multiple types of movement-related information encoded in hindlimb/trunk cortex in rats and potentially available for brain-machine interface controls. *IEEE Trans. Biomed. Eng.* **56**, 2712–2716 (2009).

226. I. N. Beloozerova, *et al.*, Postural Control in the Rabbit Maintaining Balance on the Tilting Platform. *J. Neurophysiol.* **90**, 3783–3793 (2006).

227. R. M. Ichiyama, *et al.*, Step Training Reinforces Specific Spinal Locomotor Circuitry in Adult Spinal Rats. **28**, 7370–7375 (2008).

228. Y. P. Gerasimenko, *et al.*, Spinal cord reflexes induced by epidural spinal cord stimulation in normal awake rats. **157**, 253–263 (2006).

229. F. Bretzner, T. Drew, Contribution of the motor cortex to the structure and the timing of hindlimb locomotion in the cat: a microstimulation study. *J Neurophysiol* **94**, 657–672 (2005).

230. D. M. Armstrong, Supraspinal contributions to the initiation and control of locomotion in the cat. *Prog. Neurobiol.* **26**, 273–361 (1986).

231. J. DiGiovanna, *et al.*, Engagement of the Rat Hindlimb Motor Cortex across Natural Locomotor Behaviors. *J. Neurosci.* **36**, 10440–10455 (2016).

232. G. Zheng, *et al.*, The CatWalk XT® Gait Analysis Is Closely Correlated with Tissue Damage after Cervical Spinal Cord Injury in Rats. *Appl. Sci.* **11** (2021).

233. V. Krishnan, A. S. Aruin, Postural control in response to a perturbation: role of vision and additional support. *Exp. brain Res.* **212**, 385–397 (2011).

234. S. Liu, J. D. Dickman, D. E. Angelaki, Response dynamics and tilt versus translation discrimination in parietoinsular vestibular cortex. *Cereb. Cortex* **21**, 563–573 (2011).

235. G. A. Bush, A. A. Perachio, D. E. Angelaki, Encoding of head acceleration in vestibular neurons. I. Spatiotemporal response properties to linear acceleration. *J. Neurophysiol.* **69**, 2039–2055 (1993).

236. A. Shumway-Cook, F. B. Horak, Assessing the Influence of Sensory Interaction on Balance: Suggestion from the Field. *Phys. Ther.* **66**, 1548–1550 (1986).

237. P. Musienko, *et al.*, Somatosensory control of balance during locomotion in decerebrated cat. *J. Neurophysiol.* **107**, 2072–2082 (2012).

238. V. F. Lyalka, G. N. Orlovsky, T. G. Deliagina, Impairment of Postural Control in Rabbits With Extensive Spinal Lesions. 1932–1940 (2019).

239. Y. Goldshmit, N. Lythgo, M. P. Galea, A. M. Turnley, Treadmill Training after Spinal Cord Hemisection in Mice Promotes Axonal Sprouting and Synapse Formation and Improves Motor Recovery. *J. Neurotrauma* **25**, 449–465 (2008).

240. A. C. Conta Steencken, D. J. Stelzner, Loss of propriospinal neurons after spinal contusion injury as assessed by retrograde labeling. *Neuroscience* **170**, 971–980 (2010).

241. P. K. Shah, *et al.*, Use of quadrupedal step training to re-engage spinal interneuronal networks and improve locomotor function after spinal cord injury. *Brain* **136**, 3362–3377 (2013).

242. P. M. Bradley, *et al.*, Corticospinal circuit remodeling after central nervous system injury is dependent on neuronal activity. *J. Exp. Med.* **216**, 2503–2514 (2019).

243. H. J. Jo, M. A. Perez, Corticospinal-motor neuronal plasticity promotes exercise-mediated recovery in humans with spinal cord injury. *Brain* **143**, 1368–1382 (2020).